DNA-linked inhibitor antibody assay (DIANA) as a new method for screening influenza neuraminidase inhibitors

Milan Kožíšek[1*], Václav Navrátil[1], Kateřina Rojíková[1], Jana Pokorná[1], Carlos Berenguer Albiñana[1,2], Petr Pachl[1], Jitka Zemanová[1], Aleš Machara[1,2], Pavel Šácha[1], Jason Hudlický[2], Ivana Císařová[3], Pavlína Řezáčová[1,4], Jan Konvalinka[1,5*]

[1]Institute of Organic Chemistry and Biochemistry of the Czech Academy of Sciences, Czech Republic, Gilead Sciences and IOCB Research Center, Flemingovo n. 2, 16610 Prague 6, Czech Republic; [2]Department of Organic Chemistry, Faculty of Science, Charles University, Hlavova 8, 12800 Prague 2, Czech Republic; [3]Department of Inorganic Chemistry, Faculty of Science, Charles University, Hlavova 8, Prague 2, 12843, Czech Republic; [4]Institute of Molecular Genetics of the Academy of Sciences of the Czech Republic, Vídeňská 1083, 14000 Prague 4, Czech Republic; [5]Department of Biochemistry, Faculty of Science, Charles University, Hlavova 8, 12800 Prague 2, Czech Republic

*Corresponding authors:
Milan Kožíšek and Jan Konvalinka
fax : +420 220 183 578; tel : +420 220 183 218
e-mails : milan.kozisek@uochb.cas.cz, konval@uochb.cas.cz

ABSTRACT

Influenza neuraminidase is responsible for the escape of new viral particles from the infected cell surface. Several neuraminidase inhibitors are used clinically to treat patients or stockpiled for emergencies. However, the increasing development of viral resistance against approved inhibitors has underscored the need for development of new antivirals effective against resistant influenza strains. A facile, sensitive, and inexpensive screening method would help achieve this goal.

Recently, we described a multiwell plate-based DNA-linked inhibitor antibody assay (DIANA). This highly sensitive method can quantify femtomolar concentrations of enzymes. DIANA also has been applied to high-throughput enzyme inhibitor screening, allowing evaluation of inhibition constants from a single inhibitor concentration.

Here, we report the design, synthesis, and structural characterization of a tamiphosphor derivative linked to a reporter DNA oligonucleotide for the development of a DIANA-type assay to screen potential influenza neuraminidase inhibitors. The neuraminidase is first captured by an immobilized antibody, and the test compound competes for binding to the enzyme with the oligo-linked detection probe, which is then quantified by qPCR. We validated this novel assay by comparing it with the standard fluorometric assay and demonstrated its usefulness for sensitive neuraminidase detection as well as high-throughput screening of potential new neuraminidase inhibitors.

Abbreviations

AU, asymmetric unit; CCP4, Collaborative Computational Project Number 4; CuAAC, copper(I)-catalyzed azide alkyne cycloaddition; PDBCO, dibenzocyclooctyne group; DCM, dichloromethane; DIANA, DNA-linked inhibitor antibody assay; DIPEA, N,N-diisopropylethylamine; DMAP, 4-dimethylaminopyridine; DMS, dimethyl sulfate; DMSO, dimethyl sulfoxide; ELISA, enzyme-linked immunosorbent assay; FDA, Food and Drug Administration; HEPES, 4-(2-hydroxyethyl)-1-piperazineethanesulfonic acid; HOTT, N,N,N',N'-tetramethyl-S-(1-oxido-2-pyridyl)thiuronium hexafluorophosphate; HPLC, high-performance liquid chromatography; K_d, dissociation constant; K_i, inhibition constant; LC-MS, liquid chromatography-mass spectrometry; 4-MUNANA, 2′-(4-methylumbelliferyl)-α-D-N-acetylneuraminic acid; NA, neuraminidase; NHS, N-hydroxysuccinimide; PDB, Protein Data Bank; PEG, polyethylene glycol; qPCR, quantitative polymerase chain reaction; RMSD, root-mean-square deviation; SPAAC, strain-promoted alkyne-azide cycloaddition; TBS, Tris-buffered saline; TBTU, N,N,N′,N′-tetramethyl-O-(benzotriazol-1-yl)uronium tetrafluoroborate; TFA, trifluoroacetic acid; THF, tetrahydrofuran; Tris, tris(hydroxymethyl)aminomethane; TMF, tamiphosphor.

INTRODUCTION

Influenza virus causes severe respiratory infections associated with significant morbidity and mortality. Worldwide, annual influenza epidemics result in three to five million cases of severe acute viral infection, and roughly 290,000 to 650,000 deaths (1). Several influenza pandemics have occurred in the last century, each caused by a new strain of the virus in humans. Two types of influenza antivirals, which target different steps in the viral lifecycle, have been approved by the Food and Drug Administration (FDA). The first type blocks the viral ion channel formed by the M2 protein, preventing the virus from infecting the cell. However, use of M2 inhibitors leads to rapid development of drug resistance, and these drugs are no longer routinely used. The second type inhibits neuraminidase (NA).

NA is an influenza virus membrane glycoprotein that is essential for release of new virions from an infected cell. NA inhibitors are the first line treatment for patients in need of anti-influenza drug therapy. Nevertheless, the increasing development of viral resistance against approved NA inhibitors has underscored the need for new anti-influenza drugs active against resistant viral strains and different NA subtypes. While several methods for NA inhibitor characterization based on enzymatic activity measurements have been described, most of them are time-consuming, sensitive to interference, and expensive (2-5).

Recently, our group developed a multiwell plate-based DNA-linked inhibitor antibody assay (DIANA) as a simple and reliable technique for enzyme detection and screening of small-molecule inhibitors (6). First, the target enzyme is captured by an antibody immobilized on the well. The enzyme then binds a detection probe consisting of a DNA oligonucleotide covalently linked to a known competitive inhibitor. The bound probe is measured by quantitative PCR (qPCR, Figure 1A). DIANA showed a several-order-of-magnitude higher sensitivity toward a model enzyme when compared to sandwich ELISA and enabled detection of target enzymes in complex biological matrices. DIANA also has been used to screen inhibitors of two clinically relevant enzymes: glutamate carboxypeptidase II and carbonic anhydrase IX (6). The assay enables inhibition constants (K_i) to be calculated directly from single-well measurements.

Here, we propose DIANA as a new reliable and rapid method for screening influenza NA inhibitors. We report preparation of an active-site-directed detection probe, and structurally characterize the interactions of the inhibitor incorporated in the probe with recombinant NA. Additionally, we compare inhibition constants for various compounds tested by DIANA with results from the standard fluorometric assay.

EXPERIMENTAL

Cloning, expression, and purification of recombinant NA2009$_{wt}$

DNA encoding the neuraminidase ectodomain (residues 82 to 469) from the A/California/07/2009 (H1N1) influenza virus was prepared by GenScript USA Inc. (Genbank Source Sequence CY121682). DNA was inserted into the pMT/BiP/V5-HisA vector (Invitrogen) with an N-terminal tag containing two Strep-tags, a FLAG-tag and a thrombin cleavage site. This construct was used to transfect *Drosophila* Schneider S2 cells (Invitrogen), and large-scale expression was performed as previously described (7). Recombinant neuraminidase expressed into the cell culture medium was subsequently purified using one-step purification on Strep-Tactin agarose resin (IBA GmbH) (8, 9). First, Strep-Tactin resin was equilibrated in buffer W (100 mM Tris-HCl, pH 8.0, 150 mM NaCl), and medium with added BioLock biotin blocking solution (IBA GmbH) was applied. The matrix with bound tagged protein was thoroughly washed with buffer W, and elution was performed with 10 mM desthiobiotin in buffer W. The resin was regenerated with buffer W containing 1 mM 2-(4-hydroxyphenylazo)benzoic acid (Sigma-Aldrich) and stored at 4 ˚C for later use. The purification process was monitored by SDS PAGE and Western blot using murine monoclonal Anti-FLAG M2-peroxidase antibody clone M2 (Sigma-Aldrich). The N-terminal tag was removed by cleavage with thrombin protease immobilized on agarose beads (Sigma-Aldrich).

Synthesis of inhibitors

The compounds presented here were either prepared by the same procedures described previously (10) (compounds **2**-**7**) or as outlined in Figures 2 and 3. For preparation of ω-hexylazido tamiphosphor **1,** we used our previously described approach to a key Barton ester based on a modified version of Gunasekera's procedure (Figure 2). Briefly, the phosphonate salt of ethyl oseltamivir carboxylate was free-based with aqueous bicarbonate and Boc-protected to provide **12**. The ethyl ester moiety was hydrolyzed, and acid **13** was treated with HOTT (*N*,*N*,*N'*,*N'*-tetramethyl-*S*-(1-oxido-2-pyridyl)thiuronium hexafluorophosphate) reagent to yield the key Barton thioester. Upon irradiation with a flood lamp in a solution of bromotrichloromethane, bromide **14** was obtained. Palladium-catalyzed Hirao coupling of **14** with dimethyl phosphite afforded dimethyl phosphonate **15** in very good yield. The dimethyl ester was subjected to selective mono-O-demethylation with sodium hydroxide, yielding intermediate **16**. Surprisingly, alkylation of **16** at 60 °C furnished alkylated product **17**, which lacks the methyl ester moiety. Apparently, under these conditions, the desired alkylation was

followed with demethylation mediated by halide ions (11). This serendipitous finding led to a shortcut in the synthesis of ω-hexylazido tamiphosphor that resulted not only in omission of the problematic second O-demethylation by thiophenolate but also improvement of overall yield. The last step of the reaction sequence was Boc deprotection with trifluoroacetic acid (TFA). Compound **2** was prepared by the same procedure and was isolated as a mixture of diastereomeric monoalkyl esters because the phosphorus atom is an additional stereogenic center. As expected, we were not able to observe separation of these diastereomers on analytical HPLC, and thus the material was used as such.

Oseltamivir derivatives with an alkyl moiety at the C-5 amino functionality were also prepared from oseltamivir phosphonate. In this case, the starting compound was treated with ethyl 2-bromopropionate to yield a mixture of diastereomers **18** and **19**. After separation followed by saponification and Boc deprotection with TFA (Figure 3), diastereomers **8** and **9** were produced in 38% and 34% yield, respectively. To determine the absolute configuration of the introduced polar moiety, we performed crystallization attempts in different solvent systems. However, our attempts to obtain a monocrystal of **19** suitable for X-ray analysis failed, and we decided to introduce 4-nitrobenzoyl moiety to the structure of **19** to facilitate crystallization.

Diastereomer **19** was treated with 4-nitrobenzoyl chloride in the presence of triethylamine. Crystallization of the resulting derivative **20** eventually yielded a suitable monocrystal, the X-ray structure of which is shown in Figure S1. This structural information allowed us to assign an (*R*) configuration to the newly formed stereocenter in **20**. We surmise that the stereogenic center in **9** has the same configuration since it is not altered by *N*-acylation.

Alkylation of the same starting material with dimethyl maleate produced a diastereomeric mixture of triester **21** in good yield (Figure 3). Cleavage of alkylesters followed by preparative HPLC resulted in **10**, which was used as a mixture of diastereomers. Amide **11** has an intentionally impaired basic functionality at C-5. All potent NA inhibitors possess either basic amino or guanidino functionalities at C-5, as their interaction with three acidic residues of NA contributes significantly to strong inhibitor-NA binding. Therefore, the binding affinity of **11**, which has a non-basic moiety at C-5, should be greatly diminished. This compound was prepared to demonstrate the viability of DIANA assay on a broader range of K_i values. An acetate was introduced by standard amide coupling mediated with TBTU, yielding ethyl ester **22**, which was subsequently hydrolyzed to give sialylmimetic **11** in 65% overall yield.

Preparation of DIANA detection probe

The detection probe was prepared by copper-free click-chemistry (12). The probe consists of an oligonucleotide of sequence 5′-CCT GCC AGT TGA GCA TTT TTA TCT GCC ACC TTC TCC ACC AGA CAA AAG CTG GAA A-3′ with the terminal 3′- phosphate moiety modified by an 6-amino-2-(hydroxymethyl)hexyl group (Generi-Biotech, OPC purification). The modified oligonucleotide was reacted with NHS-DBCO (dibenzocyclooctyne-*N*-hydroxysuccinimidyl ester, Sigma Aldrich) in a 1:50 ratio. The product (designated as DNA_DBCO) was conjugated with a NA inhibitor containing an azido group (**1**). The conjugation was performed at a 1:10 ratio of DNA_DBCO conjugate to **1**. The DNA conjugates were purified from the unconjugated small molecule by ultrafiltration with a 10 kDa cutoff and then analyzed by LC-MS.

Determination of inhibition constants (K_i) by fluorometric assay

Enzyme inhibition constants (K_i) were determined in 0.1 M MES, pH 6.15, 150 mM NaCl and 10 mM $CaCl_2$ at 37 °C by fluorometric assay using 2′-(4-methylumbelliferyl)-α-D-N-acetylneuraminic acid (4-MUNANA, Sigma-Aldrich) as a substrate (2). Substrate cleavage was monitored with an Infinite M1000 fluorescence reader (TECAN) using an excitation wavelength of 355 nm and an emission wavelength of 450 nm.

Each 40 µl reaction contained 17 nM (34 ng) $NA2009_{wt}$ and 500 µM 4-MUNANA. The reactions were performed for 20 min at 37 ˚C in black fluorescence 96-well plates and terminated by addition of 40 µl of 1 M sodium carbonate. Inhibition constants were determined by measuring the reduction in fluorescence of the product 4-MU in the presence of different inhibitor concentrations. The data were analyzed using the equation for competitive inhibition according to Williams and Morrison or Dixon analysis when the K_i value was expected to be above 100 nM (13, 14).

General DIANA protocol

The protocol described as “general assay conditions” by Navrátil et al. (6) was used with the following modifications. A sheep antibody against NA of influenza A virus H1N1 (cat. no. AF4858, R&D systems) was used as the capture antibody and was immobilized onto the plate by applying 5 µl antibody solution (10 ng/µl in TBS: 20 mM Tris-HCl, 150 mM NaCl) to the bottom of the wells. Then, the immobilized antibody was blocked with casein blocker and incubated overnight, followed by washing using a microplate washer (405™ Microplate Washer LS, BioTek). Next, 2 ng NA in 5 µl Q1 buffer (20 mM Tris-HCl, 150 mM NaCl, 0.1% (w/v) Tween 20, 5 mM $CaCl_2$) was applied to the bottom of the wells and incubated for 2 h,

followed by another wash in the microplate washer. Afterward, 5 µl of detection probe at a concentration of 200 pM diluted in Q2 buffer (20 mM Tris-HCl, 150 mM NaCl, 0.1% (w/v) Tween 20, 5 mM $CaCl_2$, 0.0055% (w/v) casein) mixed in a 9:1 ratio with inhibitor dissolved in 100% DMSO was applied to the bottom of the wells (final concentration of 10% DMSO) and incubated for 1 h. The plate was again washed in the microplate washer to remove unbound probe. Finally, the amount of bound probe was determined by qPCR as described (6).

Determination of inhibition constants by DIANA

Inhibitors were tested at concentrations ranging from 10 nM to 10 µM for tight-binding inhibitors and 316 nM to 316 µM for weak inhibitors. The model for determination of K_i in the presence of detection probe with serial dilutions of inhibitor was described previously (6). K_i was determined as follows: the ΔC_q values for each inhibitor were obtained as the difference in C_q between the well(s) incubated with inhibitor and the mean of wells without inhibitor (typically 12 wells per experiment). The K_i values of the inhibitors were computed from their ΔC_q values and concentration of inhibitor according to the formula $K_i = (2^{-\Delta Cq} / (1 - 2^{-\Delta Cq})) \times I_{tot} / (1 + (P_{tot} / K_d))$, where the I_{tot} is the total inhibitor concentration, P_{tot} is the total concentration of the probe (200 pM) and K_d is the dissociation constant of the probe determined by incubating serial dilutions of the probe with a constant amount of enzyme (K_d = 3.9 nM). The final K_i value for each inhibitor was calculated as the average of K_i values determined from each inhibitor concentration and corresponding C_q.

Protein crystallography

Enzyme-inhibitor complexes for crystallization were prepared by mixing $NA2009_{wt}$ in 5 mM Tris-HCl, pH 8.0, with **1** and **3**. Mixtures were concentrated by ultrafiltration to a final concentration of 8 mg/ml (3-fold molar excess of inhibitor in the mixture). Crystals were grown using the hanging-drop vapor diffusion method at 19 ºC. Drops consisted of 1 µl NA-inhibitor complex and 1 µl reservoir solution. The reservoir solutions for $NA2009_{wt}$-**1** and $NA2009_{wt}$-**3** were 100 mM HEPES, pH 7.5, 10% PEG 8000 and 100 mM HEPES, pH 7.0, 8% PEG 8000, respectively. All crystals were transferred into a cryoprotectant consisting of reservoir solution supplemented with 20% (v/v) ethylene glycol and flash-cooled in liquid nitrogen.

Data collection and structure determination

Diffraction data were collected at 100K on BL14.1 at the BESSY II electron storage ring operated by the Helmholtz-Zentrum Berlin MX14.1 of BESSY, Berlin, Germany (15). The

dataset was processed using XDSAPP (16). The crystal parameters and data collection statistics are listed in Table 1. The structure was determined by molecular replacement with the program Molrep (17) using the crystal structure of $NA2009_{wt}$ complexed with tamiphosphor (10). Model refinement was performed using the program REFMAC 5.7.0032 (18) from the CCP4 package (19) in combination with manual adjustments in Coot software (20). Compounds were modeled after complete refinement of the protein chains and solvent model. The Molprobity server (21) was used to evaluate the final model quality. The final refinement statistics are summarized in Table 1. The structures were analyzed using the programs lsqkab (superpose) (22), baverage, and contact from the CCP4 package (19).

PDB accession codes

Atomic coordinates and structure factors have been deposited in the PDB database under accession codes 6G01 and 6G02.

RESULTS

Design of the detection probe

The FDA-approved drug oseltamivir carboxylate is the most widely used NA inhibitor, and we aimed to prepare our detection probe by linking this compound or a derivative to a DNA oligonucleotide. First, we sought to determine an appropriate way to link the oligonucleotide with the inhibitor without compromising inhibitor binding to NA. The main features of oseltamivir carboxylate that mimic the sialic acid substrate of influenza NA are as follows: (i) a negatively charged carboxylate at C-1 interacting with three arginine residues (also known as the arginine triad conserved in sialidases), (ii) a C-3 pentyloxy moiety accommodated in the hydrophobic pocket, (iii) the C-4 acetamide and basic amino group at carbon C-5 that interact with an aspartic acid and two glutamic acids. According to the crystal structure of NA in complex with oseltamivir (PDB 3TI6) (23), the C-1 carboxylate group is suitable site for attachment of a linker. However, a negative charge at C-1 is indispensable for inhibitor tight binding, as demonstrated on a series of oseltamivir derivatives substituted at the carboxylate moiety and a series of phospha-congeners (tamiphosphor derivatives) (24-26). As attachment of a linker to the carboxylate moiety *via* an ester bond would lead to loss of the negative charge, we used an oseltamivir derivative with a negatively charged C-1 phosphonate group, which maintains its negative charge after linker.

In 2009, Streicher and co-workers demonstrated that replacement of the C-1 carboxylate with a monoalkyl phosphonate moiety does not diminish inhibitory activity (27, 28). This so-called tamiphosphor binds NA with similar potency as oseltamivir carboxylate, as we recently confirmed by protein microcalorimetry (10). Moreover, the same group in 2011 demonstrated immobilization/conjugation of the ω-azidohexyl ester of tamiphosphor by CuAAC click chemistry. Subsequently, conjugates of this modified tamiphosphor with biotin and fluorescein were designed for fluorometric detection and quantification of influenza viruses. Both conjugates displayed selective, high-affinity binding to influenza NA and showed promise for development of various diagnostic tools for biological research (29, 30). Together, these findings indicate that monoalkylated tamiphosphor derivatives are suitable sialylmimetics. Moreover, the phosphonate functionality is well-suited chemical handle for further modification to develop tethered and very potent NA inhibitors.

Construction of DIANA detection probes requires a linker of appropriate length equipped with bioorthogonal functional groups. In this particular case, ligation of the

sialylmimetic inhibitor to the oligonucleotide was performed by strain-promoted alkyne-azide cycloaddition (SPAAC). Tamiphosphor was modified with a clickable ω-azidoalkyl moiety (yielding **1**) suitable for conjugation to a DNA oligonucleotide equipped with a dibenzocyclooctyne moiety, and the probe was prepared by click-chemistry (Figure 1B) (12). The quality and quantity of the probe were monitored by LC-MS.

To determine the effect of linker attachment to tamiphosphor on enzyme binding, we determined the inhibition potencies of **1**, oseltamivir carboxylate (**4**), and tamiphosphor (**2**) using a standard kinetic assay. All three compounds bound NA with comparable affinity (K_i values of 24 nM, 24 nM and 26 nM, respectively), supporting use of a tamiphosphor-oligonucleotide conjugate as a DIANA detection probe (Figure 1B).

X-ray structures of neuraminidase in complex with tamiphosphor derivatives

We recently reported the structure of tamiphosphor in complex with NA at 1.8 Å resolution (10). The structure revealed that the O3 atom of the phosphonate functionality is oriented out of the active site and does not engage in direct interactions with protein residues (10). This observation led us to prepare a modified inhibitor for the DIANA detection probe by substituting one hydroxyl in tamiphosphor with a large linker connected to an oligonucleotide.

To analyze the binding of tamiphosphor derivatives to NA, we solved X-ray crystal structures of complexes of **1** (ω-azidoalkyl ester) and **3** (methyl ester) with NA (strain $NA2009_{wt}$) at high resolution. These structures revealed that the compounds bind into the active site with a pose very similar to that of tamiphosphor (10) (Figure 4A, B). The RMSD values for superposition of tamiphosphor with the corresponding atoms in **1** and **3** were 0.22 Å. The methyl ester of **3** was modeled into well-defined electron density map in a position pointing out of the active site (Figure 4A). Most of the atoms of **1** could be traced in the electron density map, with the exception of the three terminal nitrogen atoms of the tamiphosphor extension. The azide group does not interact with the protein and is fully exposed to the solvent, and thus its electron density map was of lower quality. Of the linker atoms, only C24 appears to interact with NA. This atom is within van der Waals distance (3.7 - 4.0 Å) of residues Pro431 and Ile149 (Figure 4C). This interaction may explain the slight improvement in K_i value observed for **1** (24 nM) compared to **3** (39 nM) (Table 2). The RMSD value for superposition of the corresponding atoms of **1** and **3** was 0.15 Å.

Development of DIANA for neuraminidase inhibitor screening

We captured recombinant NA with an immobilized polyclonal anti-NA antibody and detected it with the DNA probe based on **1** (Figure 1). Using this set-up, potential inhibitors can be screened by incubating the test compounds with the captured enzyme in the presence of the probe. The amount of bound probe is quantifiable by qPCR, and the inhibitory potency of the compounds can be calculated from the difference in qPCR cycle number between wells incubated with and without the test compound (ΔC_q) (6).

We found that it is important to include Ca^{2+} in the assay buffer, as Ca^{2+} is essential for NA activity and stabilization of the active site (31, 32). Because small-molecule libraries are typically dissolved in DMSO, we also tested the influence of including up to 10% DMSO in the assay and found no significant effect.

Using serial dilutions of NA and the probe, we determined optimal working concentrations of 2 ng NA and 200 pM probe per well. These concentrations led to a signal-to-background ratio of approximately 7 qPCR cycles (over 2 orders of magnitude) and a Z′-score of approximately 0.83 (average value calculated from several experiments with known inhibitors). According to JH Zhang *et al.* (1999), a Z′-score between 0.5 and 1.0 is indicative of an excellent assay for high-throughput screening (33).

We next assessed whether we could use this novel assay to determine the K_i value from a single inhibitor concentration. We determined inhibition constants from single-well measurements, as described in Materials and Methods, with serial dilutions of tamiphosphor. The resulting K_i values were constant within the range of the assay (i.e., over tamiphosphor concentrations spanning 43 nM to 12 μM; see Figure 5A). The average calculated K_i was 52 ± 9 nM, in good agreement with the value of 26 ± 4 nM obtained from standard enzyme kinetics. We conclude that DIANA is suitable for accurate K_i determinations from single-well measurements.

Comparison of DIANA with standard enzymatic assay

To compare the ability of DIANA and a standard enzymatic assay to determine inhibition constants of novel compounds, we prepared a series of eleven modified oseltamivir and tamiphosphor derivatives with various inhibition potencies. Compounds **2**-**4**, known inhibitors of NA with nanomolar K_i values, served as standards for validation of the assay for tight-binding inhibitors. Compounds **5**, an ethyl ester prodrug of oseltamivir phosphate, and **10**-**11** represent inhibitors with several-order-of-magnitude lower inhibition potency and were chosen to demonstrate the ability of the assay to identify and characterize weakly binding

compounds. Guanidylated compounds **6** and **7** also have been described previously, with contradictory data on their inhibitory activity compared to oseltamivir (10, 34, 35). In addition to these known inhibitors, we prepared and tested three new compounds that feature stereogenic centers adjacent to the former C-5 amino functionality. Compounds **8** and **9** are diastereomers, allowing us to validate the assay on two very structurally similar inhibitors.

We first used an established fluorometric assay to determine the inhibition constants of all compounds (see Table 2). This analysis was performed at pH 6.15, which is optimal for $NA2009_{wt}$ activity and is necessary to achieve a sufficient signal-to-background ratio, using the fluorescent substrate 4-MUNANA.(2, 36) The K_i values of **1-11** ranged from 20 nM to 40 μM. As expected, **1-4** exhibited the highest potency. Oseltamivir ethylester (**5**) was a roughly 100-fold inhibitor than oseltamivir carboxylate (**4**), which corroborates the necessity of a negatively charged moiety in the C-1 position. Interestingly, substitution of the basic amine moiety with the basic and bulkier guanidium group led to a several-fold decrease in potency (**6** and **7**). On the other hand, the effect of modifying the C-5 amino group with a propanoate moiety was dependent on the configuration of the stereogenic center: the S-configuration in **8** led to inhibitory potency comparable to that of oseltamivir carboxylate, whereas the R-configuration in **9** led to an approximately 10-fold decrease in potency. These results also indicate that an acidic substituent is tolerated at the C-5 position. Finally, **10** and **11** showed the lowest inhibitory activity of all compounds, with binding constants in the micromolar range.

We next evaluated the inhibition constants of all 11 compounds using DIANA. Because there was no requirement for acidic pH, this assay was performed in at physiological pH (pH 7.4). We tested serial dilutions of each inhibitor (7 concentrations spanning a three-order-of-magnitude range) in duplicate in two independent experiments and calculated K_i values as the average K_i determined from each well. However, only wells with C_q-values at least 2 cycles lower than the background C_q and at least 1 cycle higher than C_q in wells incubated without inhibitor were considered for K_i determination (note that cycle number is indirectly proportional to the logarithm of the probe concentration, i.e., the higher the probe concentration, the lower the cycle number). These cutoff values were applied to avoid potential errors in K_i values caused by considering C_q values near the limits of the assay window. Indeed, we found that the K_i values for individual compounds were constant over the concentrations tested (Table 2).

DISCUSSION

We previously described DIANA as an ultrasensitive tool with a large dynamic range for determination of enzyme inhibition constants (6). Here, we adapted the protocol for evaluation of NA inhibitors. In our setup, NA was captured by an immobilized antibody, and tested compounds competed with an active-site-directed detection probe, which was then quantified by qPCR (Figure 1A). The detection probe was prepared by linking a tamiphosphor derivative **1** to a reporter DNA oligonucleotide (Figure 1B). The crystal structure of complex of ω-azidoalkylester of tamiphosphor (compound **1**) with NA2009wt revealed that modification of the phosphate moiety of tamiphosphor does not affect its interactions with active site residues. The esterification results in very minor interactions with residues at the edge of the active site of the enzyme, and the terminal azide group is fully exposed to solvent and thus available for further modifications. We thus concluded that modification of the azide group with a DNA oligonucleotide in the DIANA probe will not significantly affect binding of **1** to the NA2009wt active site.

We then characterized and validated the assay setup using oseltamivir carboxylate as a reference inhibitor. We synthesized a series of novel oseltamivir derivatives and showed that DIANA faithfully reproduced the structure-activity relationship of the series determined by standard kinetic assay (Figure 5B). The absolute K_i values obtained by DIANA are, however, on average roughly 4-fold higher than those obtained by standard kinetics (ranging from equivalent to 12-fold higher). The most pronounced differences were observed for inhibitors containing substituents targeting 150-loop identified as very dynamic part of NA sensitive to protonation (37). These inconsistencies may thus result from the different protonation of the enzyme under different conditions used for individual methods, such as use of different pH and buffers. The advantage of DIANA assay is that it uses the experimental conditions that are similar to the physiological ones while the kinetic assay has to be performed in artificial conditions needed for efficient cleavage of the substrate.

In order to analyze whether our method is suitable for the testing of inhibitors of known resistant mutants of NA, we determined *Ki* values of the compound **1** with the wild-type NA and resistant variants containing oseltamivir major resistance mutations H275Y and H275Y/I223V . K_i values for these mutants were 1700- and 11100-fold higher than for the wt NA, respectively (data not shown). Due to these unfavourable binding characteristics of compound **1**, the DNA-probe would not be suitable for sensitive DIANA testing with resistant NA mutants.

In conclusion, our results demonstrate that DIANA is useful for determining inhibition constants of wt NA inhibitors and consumes only a small amount of enzyme (the kinetic assay consumes an amount more than ten-fold higher of NA per measurement). Moreover, the multi-well plate format, the possibility to determine inhibition potency from a single point measurement, and the possibility to use up to 10% DMSO make this assay a promising choice for screening small-molecule libraries for new influenza NA inhibitors.

Supplementary Material

Figure showing crystal structure of compound **20**, experimental details and spectra of prepared compounds.

Acknowledgments

The authors wish to thank Jana Starková and Iva Flaisigová for technical assistance and Hillary Hoffman for proofreading of the manuscript. Diffraction data were collected on BL14.1 at the BESSY II electron storage ring operated by the Helmholtz-Zentrum Berlin.

Declaration of interest

The Authors declare that there are no competing interests associated with this manuscript.

Funding information

This work was supported by the project InterBioMed LO1302 from the Ministry of Education of the Czech Republic.

Author contribution statement

MK - conceived idea, designed and performed experiments, analyzed results, wrote the paper and communicated; **VN** - designed experiments and wrote the paper; **KR** - performed experiments and analyzed data; **JP** - analyzed and validated data; **CBA** - designed and performed experiments; **PP** - analyzed and validated data; **JZ** - designed and performed experiments; **AM** - designed experiments; **PŠ** – designed experiments; **JH** - performed experiments; **IC** - performed experiments; **PŘ** - analyzed data, visualized results, and wrote the paper; **JK** - supervised the studies and revised the paper

REFERENCES

1. Iuliano AD, Roguski KM, Chang HH, Muscatello DJ, Palekar R, Tempia S, et al. Estimates of global seasonal influenza-associated respiratory mortality: a modelling study. Lancet. 2017.
2. Potier M, Mameli L, Belisle M, Dallaire L, Melancon SB. Fluorometric assay of neuraminidase with a sodium (4-methylumbelliferyl-alpha-D-N-acetylneuraminate) substrate. Anal Biochem. 1979;94(2):287-96.
3. Li AF, Wang WH, Xu WF, Gong JZ. A microplate-based screening assay for neuraminidase inhibitors. Drug Discov Ther. 2009;3(6):260-5.
4. Marjuki H, Mishin VP, Sleeman K, Okomo-Adhiambo M, Sheu TG, Guo L, et al. Bioluminescence-based neuraminidase inhibition assay for monitoring influenza virus drug susceptibility in clinical specimens. Antimicrob Agents Chemother. 2013;57(11):5209-15.
5. Okomo-Adhiambo M, Sheu TG, Gubareva LV. Assays for monitoring susceptibility of influenza viruses to neuraminidase inhibitors. Influenza Other Respir Viruses. 2013;7 Suppl 1:44-9.
6. Navratil V, Schimer J, Tykvart J, Knedlik T, Vik V, Majer P, et al. DNA-linked Inhibitor Antibody Assay (DIANA) for sensitive and selective enzyme detection and inhibitor screening. Nucleic Acids Res. 2017;45(2):e10.
7. Barinka C, Rinnova M, Sacha P, Rojas C, Majer P, Slusher BS, et al. Substrate specificity, inhibition and enzymological analysis of recombinant human glutamate carboxypeptidase II. J Neurochem. 2002;80(3):477-87.
8. Schmidt TG, Skerra A. The Strep-tag system for one-step purification and high-affinity detection or capturing of proteins. Nat Protoc. 2007;2(6):1528-35.
9. Schmidt TGM, Batz L, Bonet L, Carl U, Holzapfel G, Kiem K, et al. Development of the Twin-Strep-tag (R) and its application for purification of recombinant proteins from cell culture supernatants. Protein Expres Purif. 2013;92(1):54-61.
10. Albinana CB, Machara A, Rezacova P, Pachl P, Konvalinka J, Kozisek M. Kinetic, thermodynamic and structural analysis of tamiphosphor binding to neuraminidase of H1N1 (2009) pandemic influenza. European Journal of Medicinal Chemistry. 2016;121:100-9.
11. Boutevin B, Hervaud Y, Jeanmaire T, Boulahna A, Elasri M. Monodealkylation des esters phosphoniques synthese de monosels et de monoacides phosphoniques. Phosphorus, Sulfur, and Silicon and the Related Elements. 2001;174(1):1-14.
12. Baskin JM, Prescher JA, Laughlin ST, Agard NJ, Chang PV, Miller IA, et al. Copper-free click chemistry for dynamic in vivo imaging. Proc Natl Acad Sci U S A. 2007;104(43):16793-7.
13. Williams JW, Morrison JF. The kinetics of reversible tight-binding inhibition. Methods Enzymol. 1979;63:437-67.
14. Dixon M. The determination of enzyme inhibitor constants. Biochem J. 1953;55(1):170-1.
15. Mueller U, Forster R, Hellmig M, Huschmann FU, Kastner A, Malecki P, et al. The macromolecular crystallography beamlines at BESSY II of the Helmholtz-Zentrum Berlin: Current status and perspectives. Eur Phys J Plus. 2015;130(7).
16. Krug M, Weiss MS, Heinemann U, Mueller U. XDSAPP: a graphical user interface for the convenient processing of diffraction data using XDS. Journal of Applied Crystallography. 2012;45:568-72.
17. Vagin A, Teplyakov A. An approach to multi-copy search in molecular replacement. Acta Crystallogr D Biol Crystallogr. 2000;56(Pt 12):1622-4.

18. Murshudov GN, Vagin AA, Dodson EJ. Refinement of macromolecular structures by the maximum-likelihood method. Acta Crystallogr D Biol Crystallogr. 1997;53(Pt 3):240-55.
19. Collaborative Computational Project N. The CCP4 suite: programs for protein crystallography. Acta Crystallogr D Biol Crystallogr. 1994;50(Pt 5):760-3.
20. Emsley P, Cowtan K. Coot: model-building tools for molecular graphics. Acta Crystallogr D Biol Crystallogr. 2004;60(Pt 12 Pt 1):2126-32.
21. Lovell SC, Davis IW, Arendall WB, 3rd, de Bakker PI, Word JM, Prisant MG, et al. Structure validation by Calpha geometry: phi,psi and Cbeta deviation. Proteins. 2003;50(3):437-50.
22. Krissinel E, Henrick K. Secondary-structure matching (SSM), a new tool for fast protein structure alignment in three dimensions. Acta Crystallographica Section D-Biological Crystallography. 2004;60:2256-68.
23. Vavricka CJ, Li Q, Wu Y, Qi J, Wang M, Liu Y, et al. Structural and functional analysis of laninamivir and its octanoate prodrug reveals group specific mechanisms for influenza NA inhibition. PLoS Pathog. 2011;7(10):e1002249.
24. Chen CL, Lin TC, Wang SY, Shie JJ, Tsai KC, Cheng YSE, et al. Tamiphosphor monoesters as effective anti-influenza agents. European Journal of Medicinal Chemistry. 2014;81:106-18.
25. Lew W, Chen XW, Kim CU. Discovery and development of GS 4104 (oseltamivir): An orally active influenza neuraminidase inhibitor. Current Medicinal Chemistry. 2000;7(6):663-72.
26. Shie JJ, Fang JM, Wang SY, Tsai KC, Cheng YSE, Yang AS, et al. Synthesis of Tamiflu and its phosphonate congeners possessing potent anti-influenza activity. Journal of the American Chemical Society. 2007;129(39):11892-+.
27. Carbain B, Martin SR, Collins PJ, Hitchcock PB, Streicher H. Galactose-conjugates of the oseltamivir pharmacophore-new tools for the characterization of influenza virus neuraminidases. Organic & Biomolecular Chemistry. 2009;7(12):2570-5.
28. Carbain B, Collins PJ, Callum L, Martin SR, Hay AJ, McCauley J, et al. Efficient Synthesis of Highly Active Phospha-Isosteres of the Influenza Neuraminidase Inhibitor Oseltamivir. Chemmedchem. 2009;4(3):335-7.
29. Stanley M, Martin SR, Birge M, Carbain B, Streicher H. Biotin-, fluorescein- and 'clickable' conjugates of phospha-oseltamivir as probes for the influenza virus which utilize selective binding to the neuraminidase. Organic & Biomolecular Chemistry. 2011;9(16):5625-9.
30. Streicher H, Martin SR, Coombs PJ, McCauley J, Neill-Hall D, Stanley M. A phospha-oseltamivir-biotin conjugate as a strong and selective adhesive for the influenza virus. Bioorganic & Medicinal Chemistry Letters. 2014;24(7):1805-7.
31. Chong AK, Pegg MS, von Itzstein M. Influenza virus sialidase: effect of calcium on steady-state kinetic parameters. Biochim Biophys Acta. 1991;1077(1):65-71.
32. Burmeister WP, Cusack S, Ruigrok RW. Calcium is needed for the thermostability of influenza B virus neuraminidase. J Gen Virol. 1994;75 (Pt 2):381-8.
33. Zhang JH, Chung TDY, Oldenburg KR. A simple statistical parameter for use in evaluation and validation of high throughput screening assays. J Biomol Screen. 1999;4(2):67-73.
34. Hilfinger J, Shen W. Neuraminidase inhibitors. Google Patents; 2011.
35. Mooney CA, Johnson SA, 't Hart P, van Ufford LQ, de Haan CAM, Moret EE, et al. Oseltamivir Analogues Bearing N-Substituted Guanidines as Potent Neuraminidase Inhibitorsdx. Journal of Medicinal Chemistry. 2014;57(7):3154-60.

36. Xu R, Zhu X, McBride R, Nycholat CM, Yu W, Paulson JC, et al. Functional balance of the hemagglutinin and neuraminidase activities accompanies the emergence of the 2009 H1N1 influenza pandemic. J Virol. 2012;86(17):9221-32.
37. Wu Y, Qin G, Gao F, Liu Y, Vavricka CJ, Qi J, et al. Induced opening of influenza virus neuraminidase N2 150-loop suggests an important role in inhibitor binding. Sci Rep. 2013;3:1551.
38. Brunger AT. Free R-Value - a Novel Statistical Quantity for Assessing the Accuracy of Crystal-Structures. Nature. 1992;355(6359):472-5.
39. Chen VB, Arendall WB, Headd JJ, Keedy DA, Immormino RM, Kapral GJ, et al. MolProbity: all-atom structure validation for macromolecular crystallography. Acta Crystallographica Section D-Biological Crystallography. 2010;66:12-21.

Table 1: Crystal data and diffraction data collection and refinement statistics.

	NA2009wt/compound 3	**NA2009wt/compound 1**
PDB code	6G01	6G02
Data collection statistics		
Space group	$C222_1$	$P4$
Cell parameters (Å; °)	118.88 137.64 118.81 90 90 90	114.89 114.89 63.93 90 90 90
Number of molecules in AU	2	2
Wavelength (Å)	0.9184	0.9184
Resolution (Å)	44.89-1.61 (1.71-1.61)	42.72-1.86 (1.97-1.86)
Number of unique reflections	121,339 (19,127)	70,090 (11,223)
Redundancy	3.12 (2.79)	3.75 (3.58)
Completeness (%)	98.2 (96.4)	99.8 (99.6)
R_{meas}[a]	0.095 (0.645)	0.136 (0.738)
Average I/σ(I)	10.29 (1.88)	9.24 (1.86)
$CC_{1/2}$ (%)	99.7 (75.8)	99.4 (61.4)
Wilson B ($Å^2$)	22.3	24.1
Refinement statistics		
Resolution range (Å)	44.89-1.61 (1.656-1.614)	42.71-1.84 (1.891-1.84)
No. of reflections in working set	119,520 (8,443)	70,147 (5,127)
No. of reflections in test set	1,821 (129)	1,799 (131)
R value (%)[b]	17.8 (31.7)	15.3 (27.9)

R_{free} value (%)[c]	20.5 (30.3)	19.7 (28.9)
RMSD bond length (Å)	0.014	0.015
RMSD angle (°)	1.637	1.670
Number of atoms in AU	7,153	6,995
Number of protein atoms in AU	6056	6006
Number of water molecules in AU	825	809
Mean B value protein/waters/compounds ($Å^2$)	17.7/28.7/14.8	20.0/31.0/22.6
Ramachandran plot statistics[d]		
Residues in favored regions (%)	96.4	96.1
Residues in allowed regions (%)	3.6	3.9

The data in parentheses refer to the highest-resolution shell.

[a] $R_{meas} = \Sigma_{hkl}(n/(n-1))^{1/2}\Sigma_i|I_i^n(hkl) - \langle I(hkl)\rangle|/\Sigma_{hkl}\Sigma_i I_i(hkl)$, where the $I_i(hkl)$ is an individual intensity of the ith observation of reflection hkl and $\langle I(hkl)\rangle$ is the average intensity of reflection hkl with summation over all data.

[b] R-value = $||F_o| - |F_c||/|F_o|$, where F_o and F_c are the observed and calculated structure factors, respectively.

[c] R_{free} is equivalent to R-value but is calculated for 5 % of the reflections chosen at random and omitted from the refinement process (38).

[d] as determined by Molprobity (39).

Table 2. Inhibition constants determined by standard kinetic assay and DIANA. The chemical formulas of the inhibitors are also shown. The "fold K_i" parameter represents the ratio K_i (DIANA, pH 7.4)/K_i (kinetic assay, pH 6.15). Substitutions of the moieties in oseltamivir carboxylate (**4**) are highlighted in blue. The K_i values for both assays were calculated from two independent experiments.

Compound	*Chemical formula*	*K_i (kinetic assay) (pH 6.15) [nM]*	*K_i (DIANA) (pH 7.4) [nM]*	*fold K_i*
1	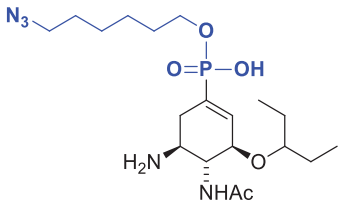	24 ± 5	33 ± 8	1.4
2	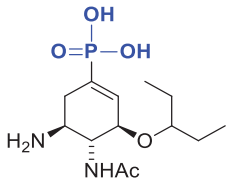	26 ± 4	52 ± 9	2.0
3	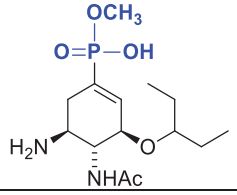	39 ± 1	100 ± 20	2.6
4	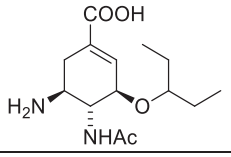	24 ± 4	31 ± 6	1.3
5	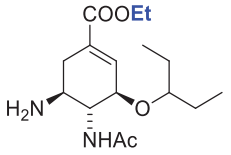	2 100 ± 200	2 000 ± 500	1.0
6	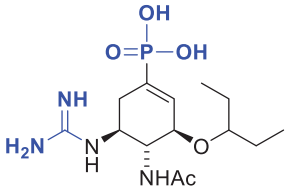	140 ± 30	570 ± 180	4.1
7	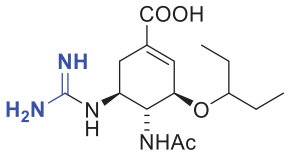	46 ± 12	570 ± 200	12
8	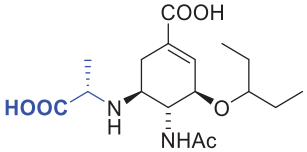	15 ± 2	170 ± 60	11

9	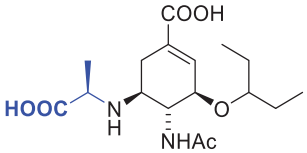	250 ± 40	960 ± 260	3.8
10	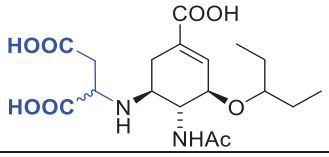	13 000 ± 1 000	16 000 ± 5 000	1.3
11	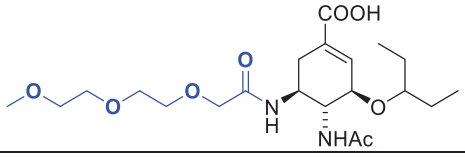	43 000 ± 11 000	210 000 ± 110 000	5

FIGURE LEGENDS

Figure 1. (A) Schematic representation of evaluation of neuraminidase inhibitors using DIANA. The detection probe binds to the active site of neuraminidase captured on the well by an immobilized anti-NA antibody. The amount of bound detection probe is determined by qPCR. The inhibition potency of the tested compound can be determined from the difference in the amount of bound probe after incubation of neuraminidase in the presence and absence of the compound. **(B)** Preparation of a covalent conjugate consisting of a reporter DNA oligonucleotide and a neuraminidase inhibitor (compound **1**) used as a DIANA detection probe. Only one regioisomer of SPAAC product is shown.

Figure 2. Synthesis of ω-azidohexyl tamiphosphor derivative **1**. The following reagents and conditions were used: (a) $NaHCO_3/H_2O$; (b) Boc_2O, Et_3N, 98%; (c) 0.5 M NaOH, 1,4-dioxane, 95%; (d) *S*-(1-oxido-2-pyridyl)-*N*,*N*,*N*′,*N*′-tetramethylthiuronium hexafluorophosphate, Et_3N, DMAP, THF; (e) bromotrichloromethane, DCM, hv, 78%; (f) dimethyl phosphite, tetrakis(triphenylphosphine)palladium, Et_3N, toluene, 86%; (g) 1-azido-6-bromohexane, NaI, DIPEA, DMF, 60 °C, 56%; (h) trifluoroacetic acid.

Figure 3. Synthesis of oseltamivir derivatives. The following reagents and conditions were used: (a) Ethyl 2-bromopropionate, $NaHCO_3$; b) 0.5 M NaOH, 1,4-dioxane; (c) 4-nitrobenzoyl chloride, Et_3N; (d) i. $NaHCO_3$, ii. dimethyl maleate; (e) 2-[2-(2-methoxyethoxy)ethoxy]acetic acid, TBTU, Et_3N, DMF.

Figure 4. Crystal structure of $NA2009_{wt}$ in complex with **3** (**A**) and **1** (**B**). Compounds are represented as sticks with carbon atoms colored yellow (**3**) or maroon (**1**), oxygen atoms red, nitrogen atoms blue, and phosphorus atoms orange. The tamiphosphor molecule from the previously reported structure (10) is overlaid and colored black. The protein is shown in green with residues forming polar interactions highlighted as sticks. The $2F_O$-F_C electron density maps are contoured at 1.0 σ. In panel B, van der Waals interactions are represented by dashed lines. (**C)** Overlay of **1** and **3**. The protein is represented by its solvent accessible surface (gray), and Pro431 and Ile149 are highlighted in green.

Figure 5. A) Determination of inhibition constants from a single inhibitor concentration by DIANA: serially diluted tamiphosphor (TMF, x-axis) was tested using DIANA, and K_i values were calculated from each data point (y-axis). The dashed horizontal line shows the average K_i calculated as the mean of K_i values determined from concentrations of tamiphosphor in the 43 nM to 12 μM range. Error bars indicate standard error of mean from two independent experiments. Both axes are shown as log-scales. **B)** Plot of K_i values of 11 neuraminidase inhibitors determined either by kinetic measurement (fluorometric assay; x-axis) or by DIANA (y-axis). Error bars indicate standard error of mean from two independent experiments. Both axes are shown as log-scales. The diagonal solid line represents a 1:1 ratio of values from both methods. The dashed line is the linear regression of the K_i values determined by both methods (K_i values determined by DIANA were on average 4-fold higher than those determined by kinetic assay).

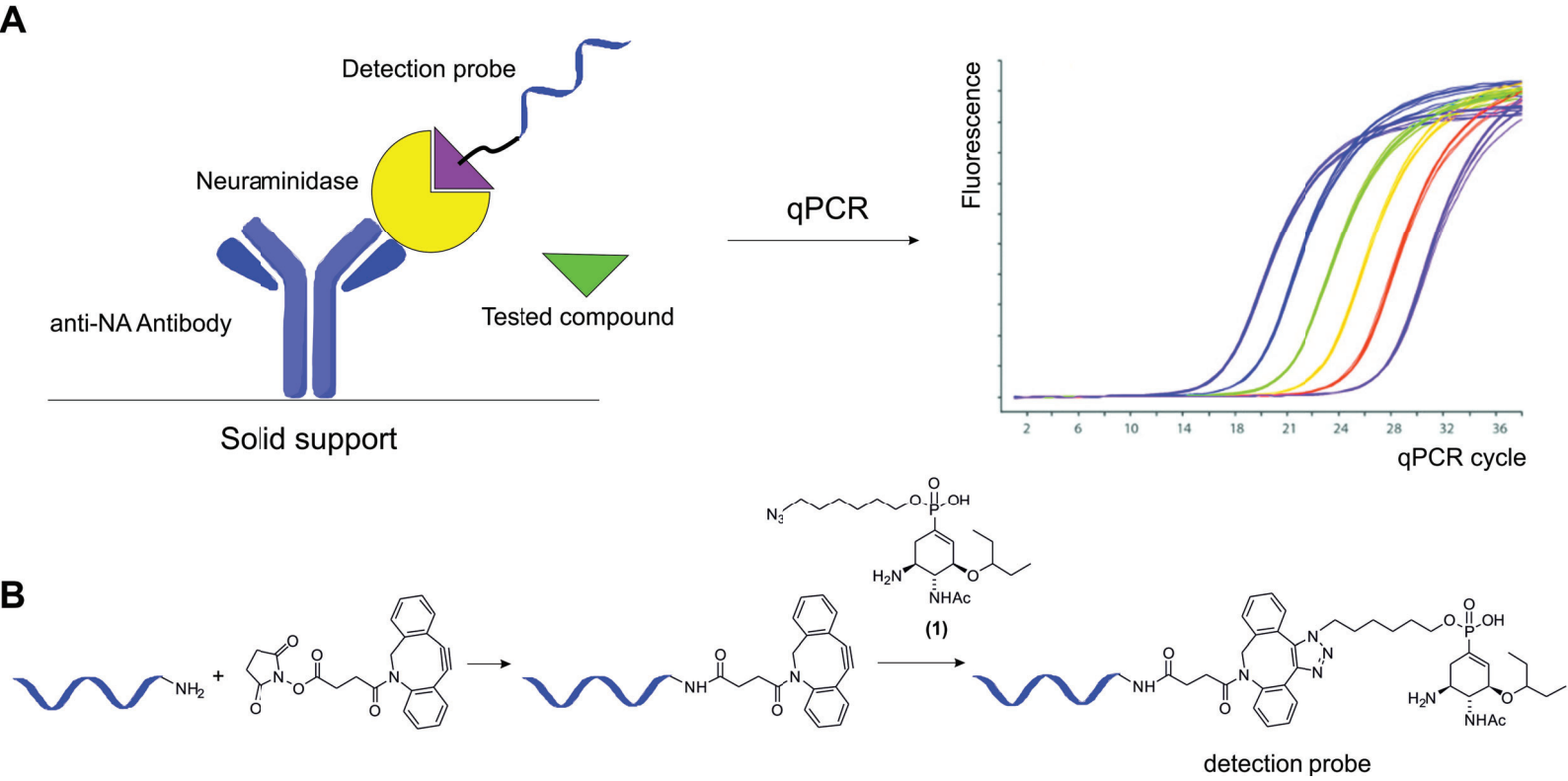
A
Detection probe
Neuraminidase
anti-NA Antibody
Tested compound
Solid support
qPCR
Fluorescence
2
6
10
14
18
21
24
28
32
36
qPCR cycle

B
NH2
+
NH
N
O
(1)
detection probe

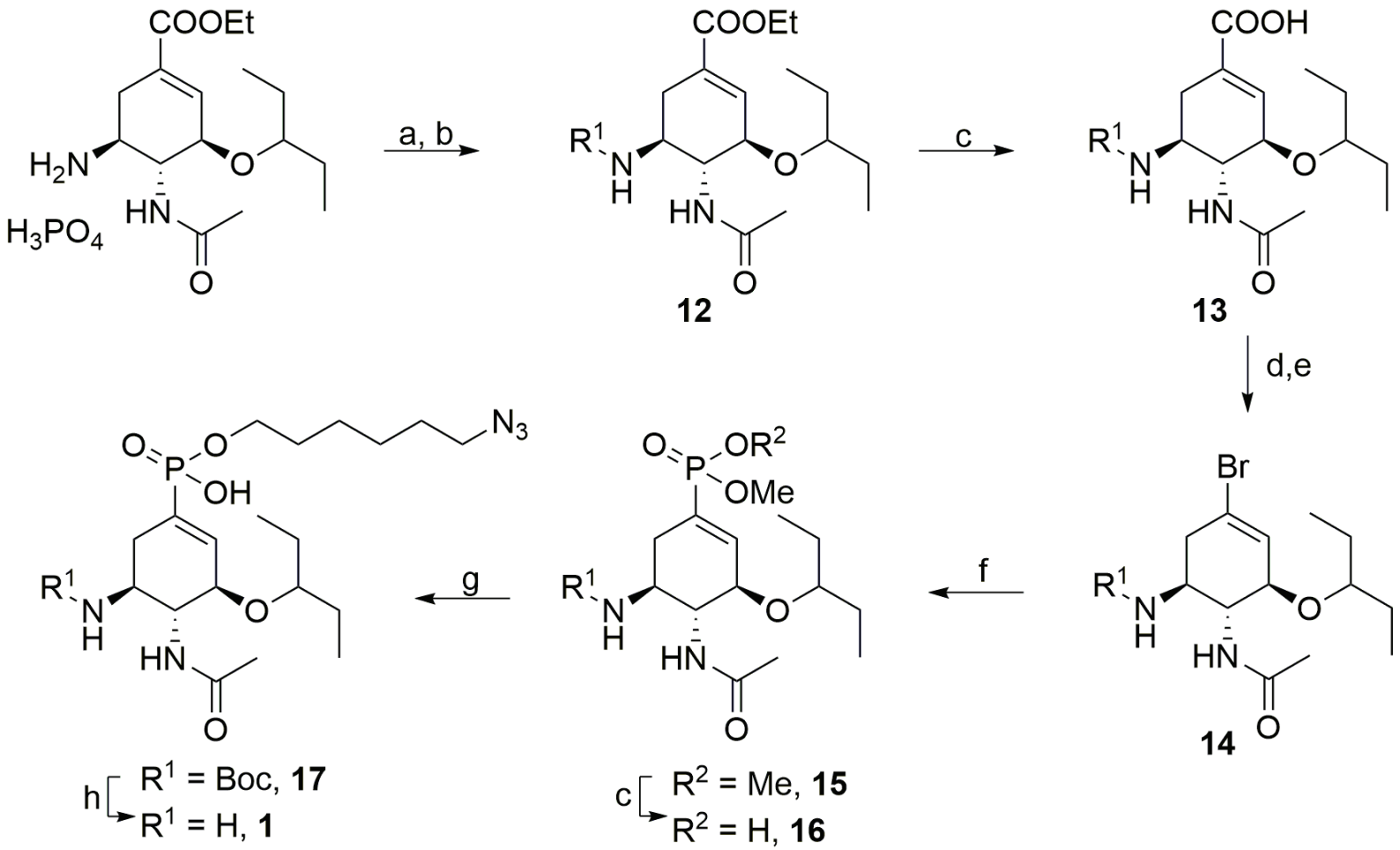
COOEt
H_2N
O
HN
O
H_3PO_4
a, b
R^1
N
H
COOEt
O
HN
O
12
c
COOH
R^1
N
H
O
HN
O
13
d,e
Br
R^1
N
H
O
HN
O
14
f
O
P
OR^2
OMe
R^1
N
H
O
HN
O
g
O
P
O
N_3
OH
R^1
N
H
O
HN
O
h
R^1 = Boc, 17
R^1 = H, 1
c
R^2 = Me, 15
R^2 = H, 16

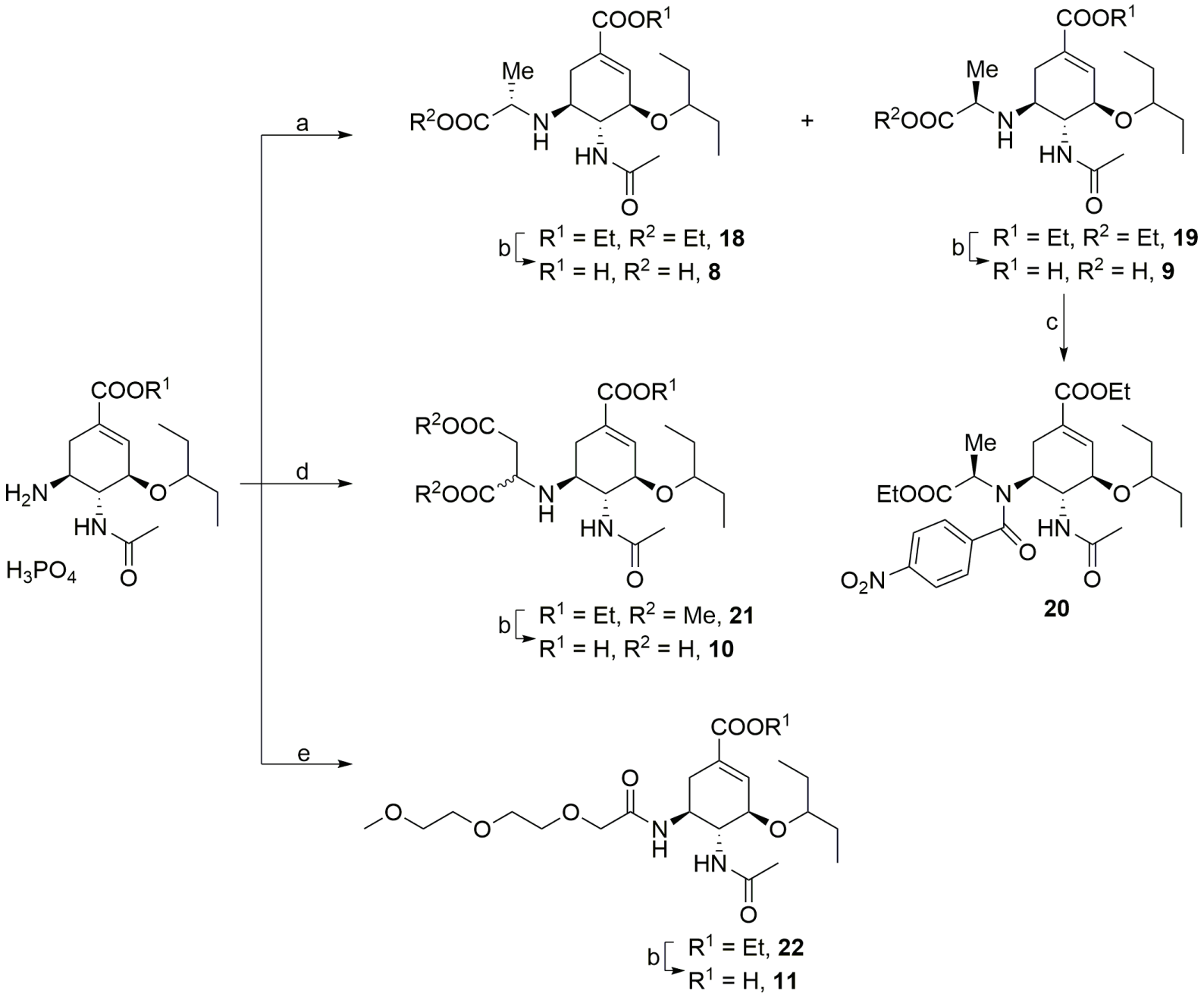
COOR1
Me
R2OOC
N
H
O
HN
O
a
+
b
R1 = Et, R2 = Et, 18
R1 = H, R2 = H, 8
R1 = Et, R2 = Et, 19
R1 = H, R2 = H, 9
c
COOEt
EtOOC
O2N
20
H2N
H3PO4
d
R2OOC
R1 = Et, R2 = Me, 21
R1 = H, R2 = H, 10
e
R1 = Et, 22
R1 = H, 11

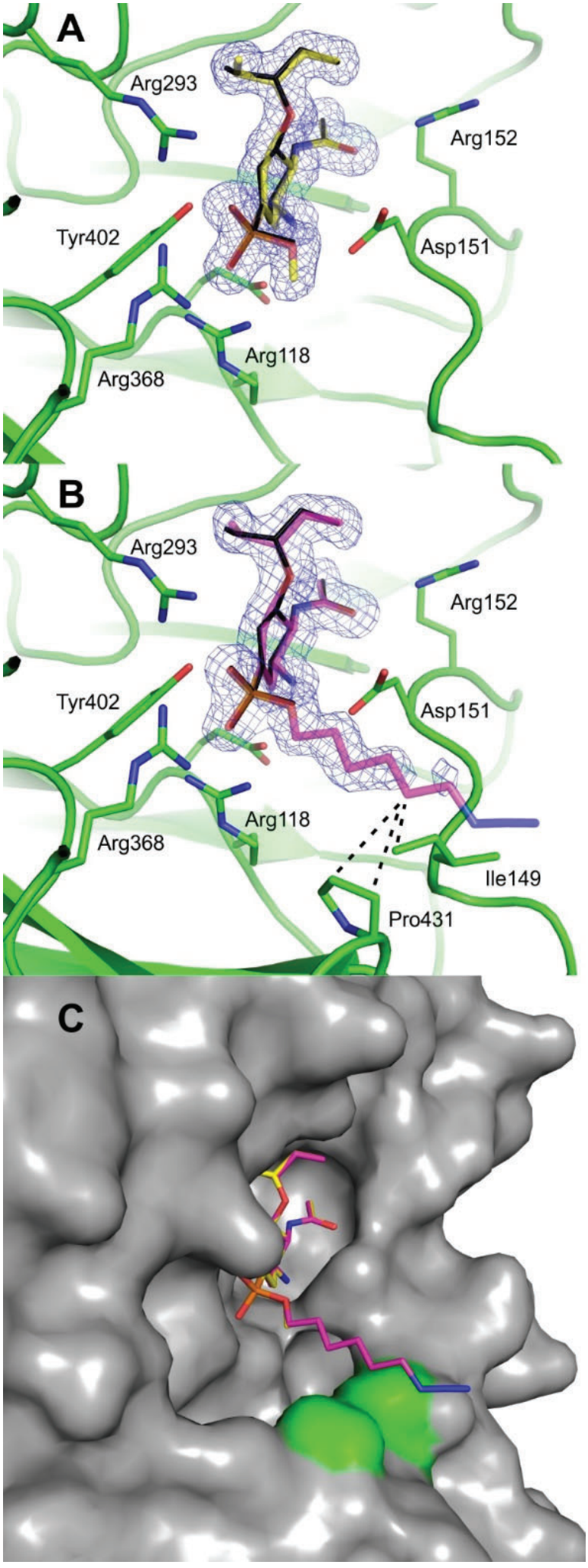
A
Arg293
Arg152
Tyr402
Asp151
Arg118
Arg368
B
Arg293
Arg152
Tyr402
Asp151
Arg118
Arg368
Ile149
Pro431
C

A

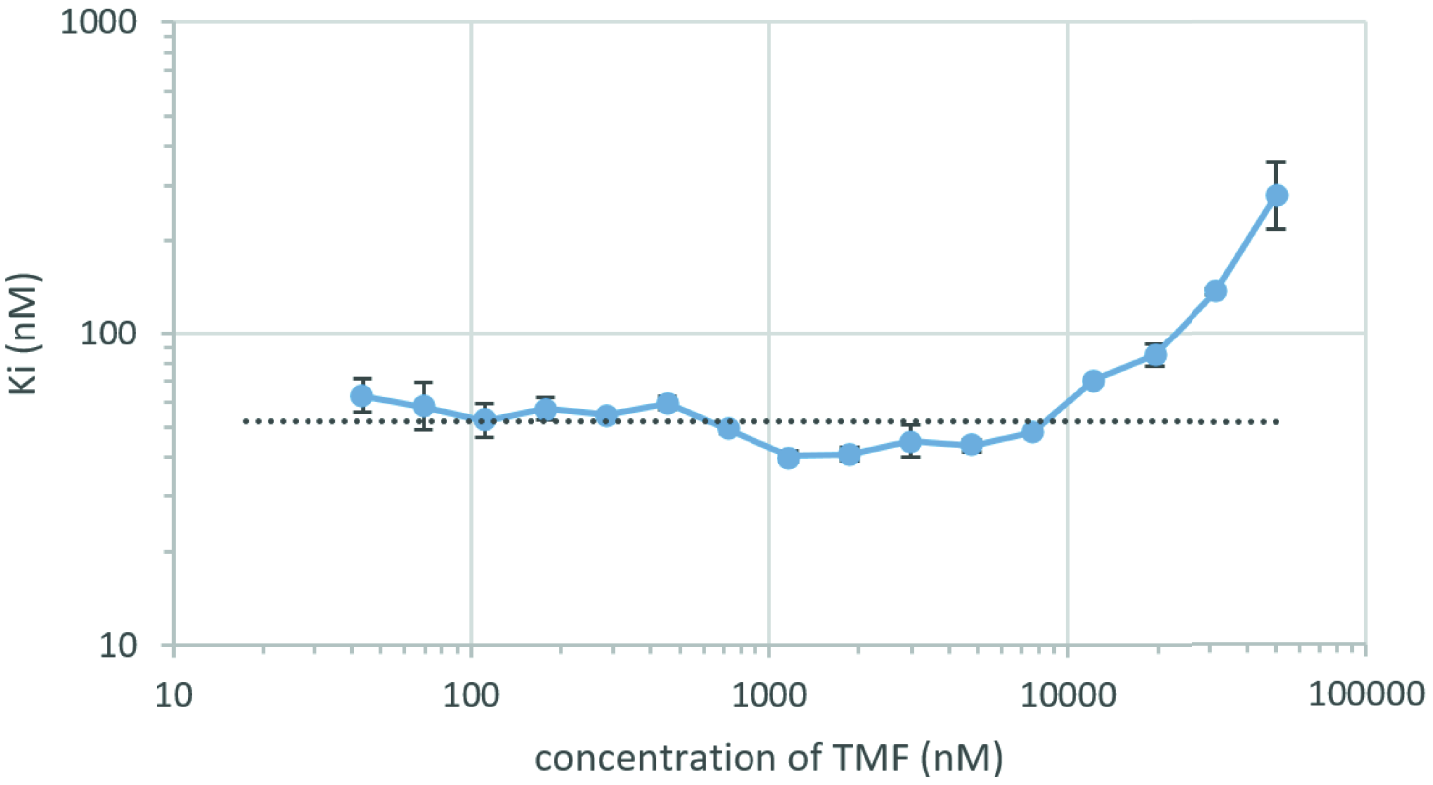
1000
100
10
Ki (nM)
10
100
1000
10000
100000
concentration of TMF (nM)

B

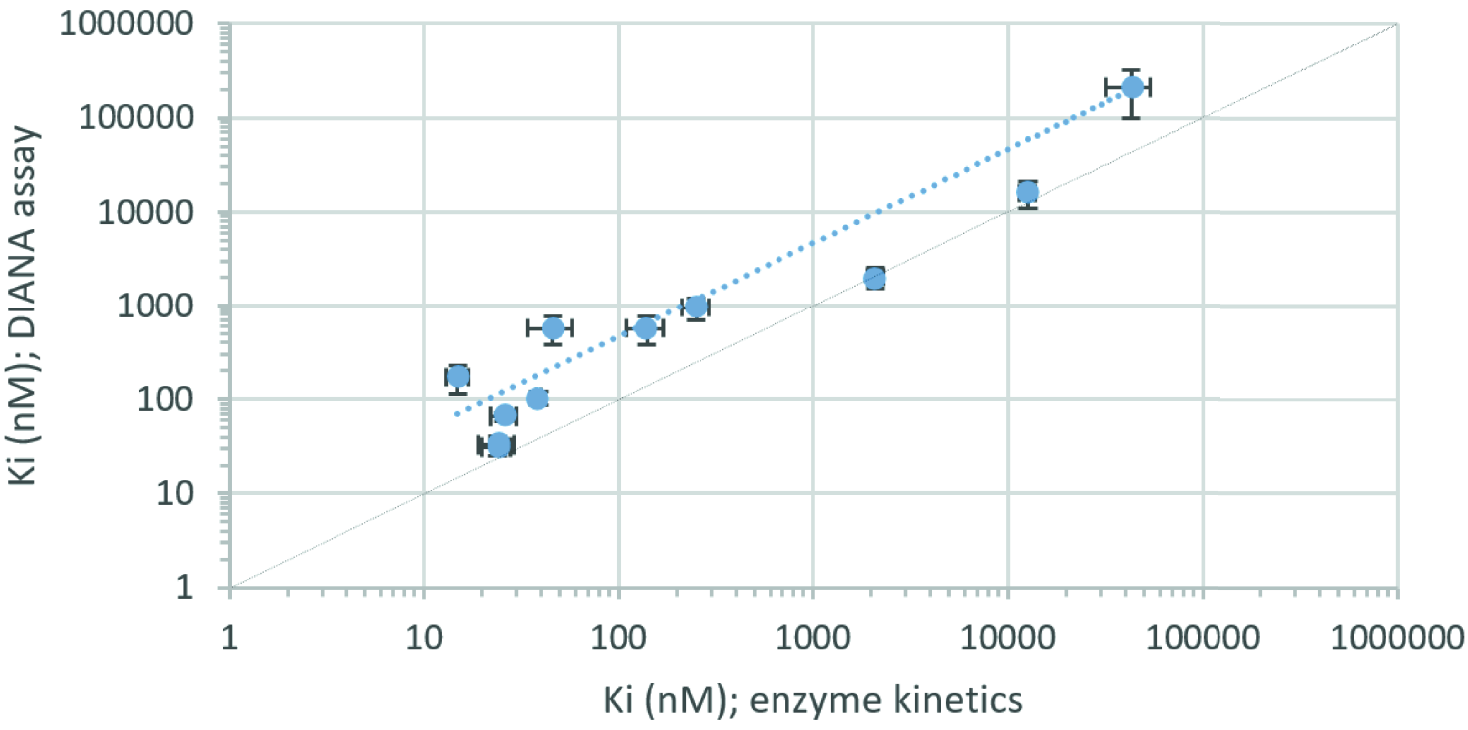
1000000
100000
10000
1000
100
10
1
Ki (nM); DIANA assay
1
10
100
1000
10000
100000
1000000
Ki (nM); enzyme kinetics

Supplementary Material

for the article

DNA-linked inhibitor antibody assay (DIANA) as a new method for screening influenza neuraminidase inhibitors

Milan Kožíšek[1*], Václav Navrátil[1], Kateřina Rojíková[1], Jana Pokorná[1], Carlos Berenguer Albiñana[1,2], Petr Pachl[1], Jitka Zemanová[1], Aleš Machara[1,2], Pavel Šácha[1], Jason Hudlický[2], Ivana Císařová[3], Pavlína Řezáčová[1,4], Jan Konvalinka[1,5*]

[1]Institute of Organic Chemistry and Biochemistry of the Czech Academy of Sciences, Czech Republic, Gilead Sciences and IOCB Research Center, Flemingovo n. 2, 166 10 Prague 6, Czech Republic; [2]Department of Organic Chemistry, Faculty of Science, Charles University, Hlavova 8, 128 00 Prague 2, Czech Republic; [3]Department of Inorganic Chemistry, Faculty of Science, Charles University, Hlavova 8, Prague, 128 43, Czech Republic; [4]Institute of Molecular Genetics of the Academy of Sciences of the Czech Republic, Vídeňská 1083, 140 00 Prague 4, Czech Republic; [5]Department of Biochemistry, Faculty of Science, Charles University, Hlavova 8, 128 00 Prague 2, Czech Republic

*Corresponding authors:

Milan Kožíšek or Jan Konvalinka, Institute of Organic Chemistry and Biochemistry of the Czech Academy of Sciences, Czech Republic, Gilead Sciences and IOCB Research Center, Flemingovo n. 2, 166 10 Prague 6, Czech Republic

Fax : +420 220 183 578; Tel : +420 220 183 218; e-mails : milan.kozisek@uochb.cas.cz, konval@uochb.cas.cz

Contents:

Figure S1. Crystal structure of compound 20. Chiral center is depicted in yellow color.

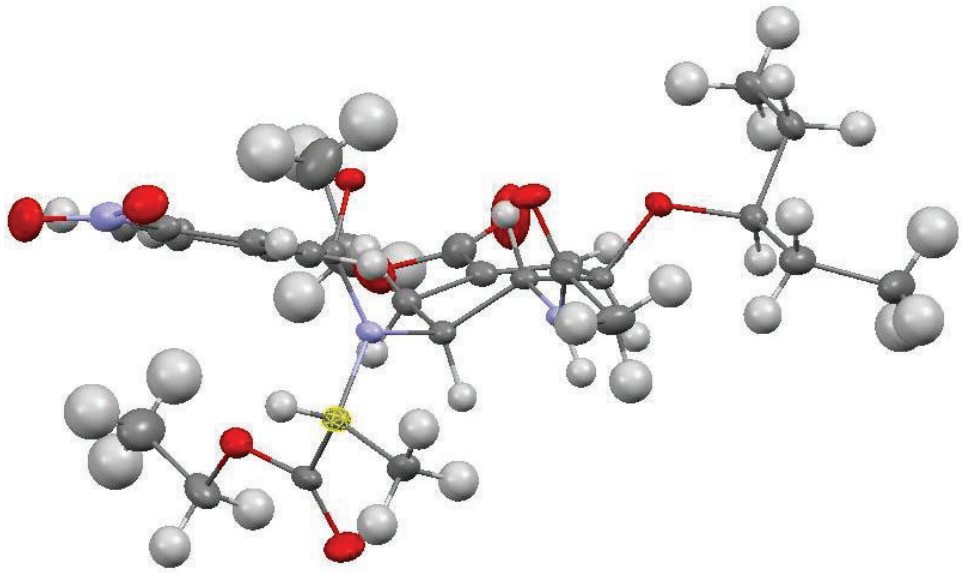

Crystallographic data for **20** were collected on Nonius KappaCCD diffractometer equipped with Bruker APEX-II CCD detector by monochromatized MoKα radiation (λ = 0.71073 Å) at a temperature of 150(2) K. The structure was solved by direct methods (SHELXT) and refined by full matrix least squares based on F^2 (SHELXL-2018). The absorption correction was carried on using multi-scan method. The hydrogen atoms were found on difference Fourier map and were recalculated into idealized positions. All hydrogen atoms were refined as fixed (riding model) with assigned temperature factors $H_{iso}(H)$ = 1.2 U_{eq}(pivot atom) or 1.5 U_{eq} for methyl moiety. The absolute configuration was assigned along known chirality on carbon.

Crystal data for **20**: $C_{28}H_{39}N_3O_9$, M_r = 561.62; Tetragonal, $P4_12_12$ (No. 92), a = 17.9556 (10) Å, c = 18.6157 (11) Å, V = 6001.8 (8) Å^3 , Z = 8, D_x = 1.243 Mg m^{-3}, colourless prism 0.35 × 0.26 × 0.21 mm, multi-scan absorption correction (μ = 0.09 mm^{-1}) T_{min} = 0.76, T_{max} = 0.98; a total of 28913 measured reflections (θ_{max}= 25.7˚), from which 5697 were unique (R_{int} = 0.048) and 4288 observed according to the $I > 2\sigma(I)$ criterion. The refinement converged (Δ/σ_{max}= 0.001) to R = 0.042 for observed reflections and $wR(F^2)$ = 0.109, GOF = 1.01 for 367 parameters

and all 5697 reflections. The final difference Fourier map displayed no peaks of chemical significance, ($\Delta\rho_{max}$ = 0.21, $\Delta\rho_{min}$ = -0.21 e.Å^{-3}). Absolute structure parameter -0.3 (5).

The crystallographic data have been deposited at the Cambridge Crystallographic Data Centre with CCDC 1832673. Copies of the data can be obtained, free of charge by application to the Cambridge Crystallographic Data Centre, 12 Union Road, Cambridge CB2 1EZ, UK, (fax: +44-(0)1223-336033 or e-mail: deposit@ccdc.cam.ac.uk).

Experimental procedures

General: Unless otherwise noted, all reactions were carried out under argon in oven-dried glassware. The solvents used for reactions were freshly distilled from the appropriate drying agent and were transferred under argon: THF (Na/benzophenone); toluene (Na); DCM (CaH_2). Chromatography was performed either using classical methods or using HPFC Biotage Isolera One system, using Fluka silica gel 60 (0.040 - 0.063mm) or Merck silica gel 60 RP-18 F_{254} – coated aluminium sheets. The spots were detected both in UV and by the solution of $Ce(SO_4)_2 \cdot 4H_2O$ (1%) and $H_3P(Mo_3O_{10})_4$ (2%) in 10% sulfuric acid (10%). All starting materials were used as received (Sigma Aldrich, Alfa Aesar, Strem Chemicals, TCI), unless otherwise indicated. Oseltamivir phosphate was purchased from Santiago. All tested inhibitors were purified using preparative HPLC of Jasco brand (flow rate 10 mL/min; gradient 2-100 % ACN in 50 minutes), with column Waters SunFire C18 OBD Prep Column, 5 μm, 19 x 150 mm. The purity of compounds was tested on analytical Jasco PU-1580 HPLC (flow rate 1 mL/min, invariable gradient 2-100 % ACN in 30 minutes) with column Watrex C18 Analytical Column, 5 μm, 250x5 mm. The final inhibitors were all >95 % purity. The ^{1}H-NMR spectra were measured at 400.13 or 600.13 MHz, the ^{13}C-NMR spectra at 100.61 or 150.90 MHz in $CDCl_3$ or $(CD_3)_2SO$, with tetramethylsilane or residual solvent peaks as an internal standard. The chemical shifts are given in δ-scale, coupling constants J are given in Hz. The EI mass spectra were determined at an ionizing voltage of 70 eV, the m/z values are given alone with their relative intensities (%). The ESI mass spectra were recorded using ZQ micromass mass spectrometer (Waters) equipped with an ESCi multimode ion source and controlled by MassLynx software. Methanol was used as solvent.

(6-Azidohexyl) (3*R*,4*R*,5*S*)-4-acetylamino-5-amino-3-(1-ethylpropoxy)-1-cyclohexene-1-phosphonic acid (1)

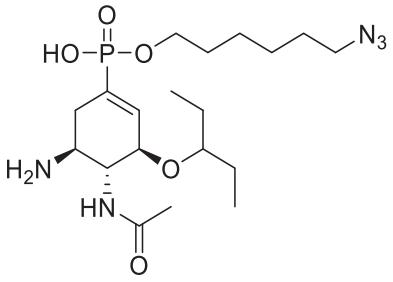

(6-azidohexyl) (3*R*,4*R*,5*S*)-4-acetylamino-5-[(*tert*-butoxycarbonyl)-amino]-3-(1-ethylpropoxy)-1-cyclohexene-1-phosphonic acid **17** was dissolved in trifluoroacetic acid (3 mL) and stirred for 2 h at room temperature. The solution was dried under reduced pressure and the resulting residue was purified by preparative HPLC to afford the deprotected phosphonic acid **1**.

^{1}H NMR (500 MHz, Methanol-*d4*) δ 6.42 (dd, *J* = 19.4, 1.0 Hz, 1H), 4.14 – 4.06 (m, 1H), 3.95 (dd, *J* = 11.2, 8.3 Hz, 1H), 3.83 (q, *J* = 6.5 Hz, 2H), 3.50 – 3.36 (m, 2H), 3.31 – 3.23 (m, 2H), 2.82 – 2.69 (m, 1H), 2.39 (ddd, *J* = 17.0, 10.1, 2.9 Hz, 1H), 2.03 (s, 3H), 1.69 – 1.56 (m, 4H), 1.55 – 1.46 (m, 4H), 1.45 – 1.37 (m, 4H), 0.91 (dt, *J* = 15.0, 7.4 Hz, 6H). ^{13}C NMR (126 MHz, Methanol-*d4*) δ 174.7, 137.1, 131.6 (d, *J* = 175.9 Hz), 83.4, 76.3 (d, *J* = 18.9 Hz), 65.7 (d, *J* = 5.4 Hz), 54.6, 52.4, 51.4, 31.8 (d, *J* = 6.8 Hz), 30.4 (d, *J* = 10.4 Hz), 29.9, 27.5, 27.3, 26.6, 26.5, 23.1, 9.9, 9.6. ^{31}P NMR (162 MHz, Methanol-*d4*) δ 13.01. HR-ESI-MS calculated for $C_{19}H_{35}O_5N_5P$ = 444.2381, found 444.2373.

(3*R*,4*R*,5*S*)-4-Acetamido-5-amino-3-(1-ethylpropoxy)-1-cyclohexene-1-phosphonate (2)

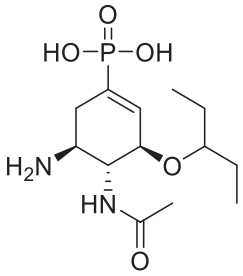

Bromotrimethylsilane (0.41 mL, 3.18 mmol) and 2,6-lutidine (0.44 mL, 3.81 mmol) were added to a solution of the Boc-protected phosphonic acid **16** (0.14 g, 0.318 mmol) in DCM (10 mL) and the reaction was allowed to stir for 9 h at room temperature. The solvent was evaporated and TFA (50% in water, 10 mL) was added. Then the reaction was allowed to stir for 1 h and the solvent was evaporated under reduced pressure. The residue was purified by preparative HPLC.

All spectral properties matched literature values[15]. HR-ESI-MS calculated for $C_{13}H_{25}O_5N_2NaP$ $(M+Na)^+$ 343.1393, found 343.1395.

Methyl (3*R*,4*R*,5*S*)-4-acetamido-5-amino-3-(1-ethylpropoxy)-1-cyclohexene-1-phosphonate (3)

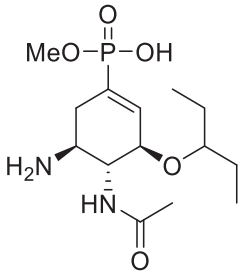

The phosphonic acid **16** (0.05 g, 1.14 mmol) was stirred with trifluoroacetic acid (50% in water, 4 mL) at room temperature for 1 h. The solution was evaporated under reduced pressure and later residue was purified by preparative HPLC to furnish the title compound **3** (0.02 g, 43% yield).

^{1}H NMR (600 MHz, D_2O) δ 6.38 (d, *J* = 19.4 Hz, 1H), 4.28 (d, *J* = 7.5 Hz, 1H), 4.14 – 4.01 (m, 1H), 3.65 – 3.55 (m, 2H), 3.53 (d, *J* = 10.8 Hz, 3H), 2.82 – 2.72 (m, 1H), 2.49 – 2.40 (m, 1H), 2.09 (s, 3H), 1.60 – 1.45 (m, 4H), 0.90 (t, *J* = 7.2 Hz, 3H), 0.85 (t, *J* = 7.2 Hz, 3H). ^{13}C NMR (151 MHz, D_2O) δ 175.8, 137.9 (d, *J* = 6.8 Hz), 129.7 (d, *J* = 174.4 Hz), 84.9, 76.5 (d, *J* = 19.4 Hz), 53.5, 52.5 (d, *J* = 5.1 Hz), 50.3 (d, *J* = 14.1 Hz), 29.8 (d, *J* = 11.0 Hz), 26.1, 25.8, 22.9, 9.2, 9,1. HR-ESI-MS calculated for $C_{14}H_{28}O_5N_2P$ $(M+H)^+$ 335.1730, found 335.1732.

Oseltamivir carboxylate (4)

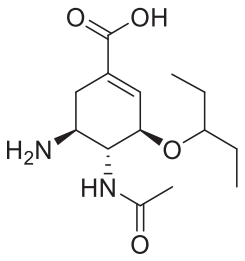

An aqueous solution of NaOH (0.5 M; 1.9 mL) was added dropwise to a stirred solution of oseltamivir phosphate **5** (0.2 g, 0.48 mmol) in 1,4-dioxane (1.9 mL). The reaction was stirred for 24 h at room temperature. The pH was adjusted to neutral by addition of Amberlite IR 120 hydrogen form. After removal of Amberlite by filtration, the filtrate was concentrated under reduced pressure and the formed residue was purified by preparative HPLC to furnish the free base derivative **4** (0.12 g, 88% yield).

^{1}H NMR (400 MHz, MeOD) δ 6.64 (s, 1H), 4.11 (d, *J* = 8.5 Hz, 1H), 3.83 (dd, *J* = 11.4, 8.7 Hz, 1H), 3.40 (td, *J* = 10.8, 5.5 Hz, 1H), 3.34 – 3.22 (m, 1H), 3.16 (dt, *J* = 3.3, 1.6 Hz, 1H), 2.80 (dd, *J* = 17.3, 5.1 Hz, 1H), 2.38 – 2.18 (m, 1H), 1.91 (s, 3H), 1.47 – 1.28 (m, 4H), 0.75 (dt, *J* = 12.6, 7.4 Hz, 6H). ^{13}C NMR (101 MHz, MeOD) δ 174.9, 169.6, 138.4, 129.8, 83.7, 76.0, 54.5, 50.5, 30.0, 27.2, 26.6, 23.4, 9.8, 9.6. HR-ESI-MS calculated for $C_{14}H_{23}O_4N_2$ ($M\text{-}H^+$) 283.1663, found 283.1656.

Ethyl (3*R*,4*R*,5*S*)-4-acetamido-5-amino-3-(1-ethylpropoxy)-1-cyclohexene-1-carboxylate (5)

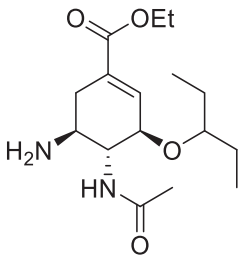

To a solution of oseltamivir phosphate (1.0 g, 2.43 mmol) in water (30 mL) was added a saturated solution of sodium bicarbonate (10 mL). The reaction mixture was stirred for 5 min at room temperature. The mixture was extracted with DCM/MeOH mixture (3:1; 4x10 mL). The combined organic phase was washed with brine, dried over anhydrous Na_2SO_4 and concentrated under reduced pressure to furnish the free base of oseltamivir (0.75 g, 98% yield). The product **5** was used without further purification.

^{1}H NMR (300 MHz, $CDCl_3$) δ 6.78 (t, *J* = 2.1 Hz, 1H), 6.26 (d, *J* = 8.3 Hz, 1H), 4.34 – 4.10 (m, 3H), 3.55 (dt, *J* = 10.3, 8.4 Hz, 1H), 3.37 (dd, *J* = 17.7, 12.0 Hz, 1H), 3.26 – 3.08 (m, 1H), 2.76 (dd, *J* = 17.7, 5.1 Hz, 1H), 2.26 – 2.08 (m, 1H), 2.04 (s, 3H), 1.58 (s, 2H), 1.55 – 1.44 (m, 4H),

1.29 (t, *J* = 7.1 Hz, 3H), 0.90 (td, *J* = 7.4, 3.8 Hz, 6H). ^{13}C NMR (75 MHz, $CDCl_3$) δ 171.1, 166.4, 137.8, 129.5, 81.7, 77.6, 77.2, 76.7, 75.0., 60.8, 58.9, 49.3, 33.7, 26.2, 25.7, 23.6, 14.2, 9.6, 9.3. HR-ESI-MS calculated for $C_{16}H_{29}O_4N_2$ (M+H)+ 313.2122, found 313.2122.

(3*R*,4*R*,5*S*)-4-Acetamido-5-guanidino-3-(1-ethylpropoxy)-1-cyclohexene-1-phosphonate (6)

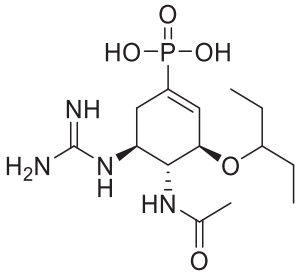

Neat bromotrimethylsilane (1.49 g, 9.68 mmol) was added to a solution of the phosphonate (0.07 g, 0.121 mmol) in DCM (5 mL) at 0 °C and the reaction was allowed to stir for 24 h at room temperature. The solvent was evaporated under reduced pressure; the remaining residue was quenched with water (4 mL) and then the mixture was stirred for 2 h. The solution was evaporated to dryness and later was purified by preparative HPLC to afford the free guanidine **6** (0.09 g, 21% yield).

^{1}H NMR (400 MHz, D_2O) δ 6.31 (d, *J* = 19.8 Hz, 1H), 4.26 (d, *J* = 8.5 Hz, 1H), 4.01 – 3.88 (m, 1H), 3.80 (td, *J* = 10.4, 5.2 Hz, 1H), 3.60 – 3.47 (m, 1H), 2.85 – 2.66 (m, 1H), 2.46 – 2.31 (m, 1H), 2.04 (s, 3H), 1.65 – 1.50 (m, 3H), 1.45 (dt, *J* = 14.4, 7.2 Hz, 1H), 0.87 (dt, *J* = 19.5, 7.4 Hz, 6H). ^{13}C NMR (151 MHz, H_2O+D_2O+*tert*-butyl alcohol) δ 175.3, 157.6, 157.5, 135.3, 135.3, 134.0, 132.8, 85.0, 77.0, 76.9, 70.5 (C), 55.9, 55.9, 51.8, 51.7, 31.5, 31.4, 30.2 (CH_3), 26.3, 26.0, 22.7, 22.6, 9.3, 9.2. ^{31}P NMR (162 MHz, D_2O) δ 11.13. All spectral properties matched literature values [2]. HR-ESI-MS calculated for $C_{14}H_{28}O_5N_4P$ $(M+H)^+$ 363.1792, found 363.1794.

(3*R*,4*R*,5*S*)-4-Acetamido-5-guanidino-3-(1-ethylpropoxy)-1-cyclohexene-1-carboxylic acid (7)

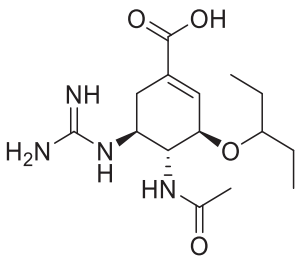

(3*R*,4*R*,5*S*)-4-Acetamido-5-[N^2,N^3-bis(*tert*-butoxycarbonyl)guanidino]-3-(1-ethylpropoxy)-1-cyclohexene-1-carboxylic acid (0.07 g, 0.13 mmol) was stirred with trifluoroacetic acid (50% in water, 5 mL) at room temperature for 1 h. The solution was evaporated under reduced pressure and purified by preparative HPLC to furnish the guanidine derivative **7** (0.02 g, 43%).

^{1}H NMR (400 MHz, Methanol-*d4*) δ 7.28 (d, *J* = 9.0 Hz, 1H), 6.79 (s, 1H), 4.15 (dd, *J* = 5.3, 2.1 Hz, 1H), 3.93 – 3.73 (m, 2H), 3.42 – 3.31 (m, 1H), 2.77 (dd, *J* = 17.6, 5.0 Hz, 1H), 2.37 – 2.20 (m, 1H), 1.94 (s, 3H), 1.48 (tdd, *J* = 12.9, 6.2, 4.5 Hz, 4H), 0.86 (dt, *J* = 12.8, 7.4 Hz, 6H). ^{13}C NMR (101 MHz, Methanol-*d4*) δ 174.2, 169.0, 158.6, 138.8, 129.8, 83.8, 76.1, 55.8, 51.7, 31.3, 27.2, 26.8, 22.8, 9.8, 9.7. All spectral properties matched literature values [3]. HR-ESI-MS calculated for $C_{15}H_{27}O_4N_4$ $(M+H)^+$ 327.2027, found 327.2028.

(3*R*,4*R*,5*S*)-4-Acetamido-5-{[(*S*)-1-carboxyethyl]amino}-3-(1-ethylpropoxy)-1-cyclohexene-1-carboxylic acid (8)

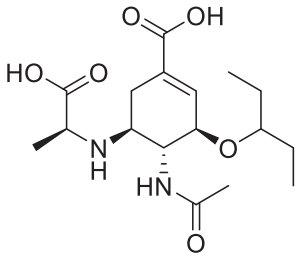

A solution of aqueous NaOH (1 mL, 0.5 M) was added dropwise to a solution of the A diastereomer (*S*) **18** (0.025 g, 0.06 mmol) in THF (1 mL) and the reaction mixture was stirred overnight at room temperature. The pH was adjusted to neutral by addition of Amberlite IR 120 hydrogen form. Amberlite was filtered off and the filtrate was concentrated under reduced pressure. The residue was purified by preparative HPLC.

^{1}H NMR (401 MHz, Methanol-*d4*) δ 6.90 (d, *J* = 1.4 Hz, 1H), 4.26 – 4.11 (m, 2H), 3.77 (dd, *J* = 13.9, 7.1 Hz, 1H), 3.64 – 3.58 (m, 1H), 3.48 – 3.39 (m, 1H), 2.99 – 2.90 (m, 1H), 2.67 – 2.55 (m, 1H), 2.04 (s, 3H), 1.64 – 1.42 (m, 7H), 0.99 – 0.84 (m, 6H). ^{13}C NMR (101 MHz, Methanol-*d4*) δ 174.7, 173.8, 168.7, 137.7, 129.3, 83.6, 75.2, 57.3, 55.1, 53.2, 27.7, 27.1, 26.6, 23.1, 15.9, 9.9, 9.5. HR-ESI-MS calculated for $C_{17}H_{28}N_2O_6Na$ $(M+Na)^+$ 379.1840, found 379.1839.

(3*R*,4*R*,5*S*)-4-Acetamido-5-{[(*R*)-1-carboxyethyl]amino}-3-(1-ethylpropoxy)-1-cyclohexene-1-carboxylic acid (9)

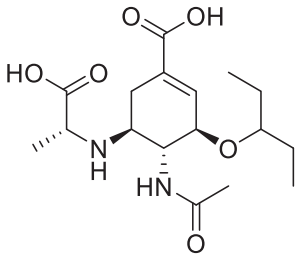

A solution of aqueous NaOH (2 mL, 0.5 M) was added dropwise to a solution of the diastereomer B (*R*) **19** (0.05 g, 0.12 mmol) in THF (2 mL) and the reaction mixture was stirred overnight at room temperature. The pH was adjusted to neutral by addition of Amberlite IR 120 hydrogen form. Amberlite was filtered off and the filtrate was concentrated under reduced pressure. The residue was purified by preparative HPLC.

^{1}H NMR (401 MHz, Methanol-*d4*) δ 6.92 – 6.80 (m, 1H), 4.21 – 4.05 (m, 2H), 3.82 (q, *J* = 7.2 Hz, 1H), 3.52 – 3.39 (m, 2H), 3.08 – 2.95 (m, 1H), 2.52 – 2.39 (m, 1H), 2.09 (s, 3H), 1.59 – 1.47 (m, 7H), 0.91 (dt, *J* = 11.2, 7.4 Hz, 6H). ^{13}C NMR (101 MHz, Methanol-*d4*) δ 175.1, 173.6, 168.5, 138.8, 128.7, 83.9, 76.1, 57.3, 57.2, 53.5, 27.8, 27.2, 26.6, 23.2, 16.9, 9.8, 9.6. HR-ESI-MS calculated for $C_{17}H_{28}N_2O_6Na$ $(M+Na)^+$ 379.1840, found 379.1839.

((1*S*,5*R*,6*R*)-6-Acetamido-3-carboxy-5-(pentan-3-yloxy)cyclohex-3-en-1-yl)aspartic acid (10)

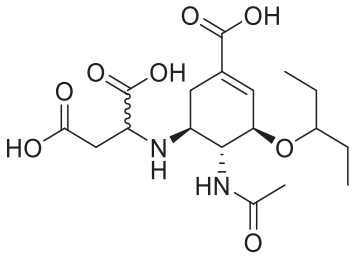

An aqueous solution of NaOH (0.5 M; 7.2 mL) was added dropwise to a stirred solution of the ester **21** (0.09 g, 0.19 mmol) in THF (3 mL). The reaction was stirred for 24 h at room temperature. The pH was adjusted to neutral by addition of Amberlite IR 120 hydrogen form. Amberlite was filtered off, the filtrate was concentrated under reduced pressure and purified by flash chromatography (DCM/MeOH 80:20) to furnish the free carboxylic acid derivative **10** (0.053 g, 70%).

^{1}H NMR (401 MHz, Methanol-*d4*) δ 6.87 (t, *J* = 1.2 Hz, 1H), 4.28 (dd, *J* = 8.1, 2.0 Hz, 1H), 4.07 (dd, *J* = 10.7, 8.1 Hz, 1H), 3.99 (t, *J* = 5.1 Hz, 1H), 3.67 (td, *J* = 10.2, 5.6 Hz, 1H), 3.48 – 3.39 (m, 1H), 3.05 – 2.91 (m, 3H), 2.62 – 2.52 (m, 1H), 2.04 (s, 3H), 1.60 – 1.49 (m, 4H), 0.92 (dt, *J* = 10.4, 7.4 Hz, 6H). ^{13}C NMR (101 MHz, Methanol-*d4*) for the major diastereomer δ 175.4, 175.0, 172.1, 168.7, 138.4, 129.1, 83.6, 75.3, 58.0, 55.5, 54.1, 33.6, 28.0, 27.2, 26.6, 23.2, 9.9, 9.5. ^{13}C NMR (101 MHz, Methanol-*d4*) for the minor diastereomer δ 175.4, 175.0, 173.9, 168.7, 138.9, 129.0, 83.9, 76.3, 57.8, 55.5, 53.9, 35.9, 28.0, 27.2, 26.7, 23.2, 9.8, 9.6. HR-ESI-MS calculated for $C_{18}H_{27}N_2O_8$ $(M-H)^-$ 399.1769, found 399.1773.

(3*R*,4*R*,5*S*)-4-Acetamido-5-{2-[2-(2-methoxyethoxy)ethoxy]acetamido}-3-(1-ethylpropoxy)-1-cyclohexene-1-carboxylic acid (11)

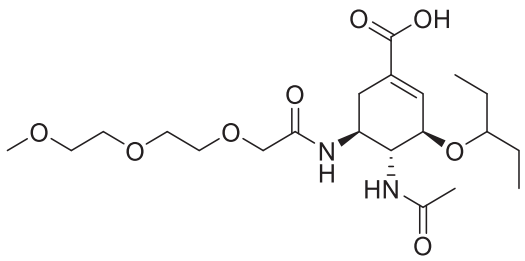

An aqueous solution of NaOH (0.5 M; 0.88 mL) was added dropwise to a stirred solution of the ethyl ester **22** (0.104 g, 0.22 mmol) in 1,4-dioxane (0.88 mL). The reaction was stirred for 24 h at room temperature. The pH was adjusted to neutral by addition of Amberlite IR 120 hydrogen form. Amberlite was filtered off, rinsed with MeOH several times and the filtrate was then concentrated under reduced pressure. The residue was purified by flash chromatography (DCM/MeOH 80:20) to furnish the free carboxylic acid derivative **11** (0.069 g, 70% yield).

^{1}H NMR (401 MHz, $CDCl_3$) δ 7.73 (d, *J* = 9.2 Hz, 1H), 6.92 (dt, *J* = 9.1, 4.6 Hz, 1H), 6.85 (d, *J* = 2.5 Hz, 1H), 5.74 (bs, 1H), 4.24 – 4.16 (m, 1H), 4.15 – 4.10 (m, 1H), 4.07 – 4.00 (m, 1H), 3.71 – 3.61 (m, 8H), 3.59 – 3.53 (m, 2H), 3.40 – 3.31 (m, 1H), 3.36 (s, 3H), 2.71 (dd, *J* = 18.0, 5.2 Hz, 1H), 2.47 – 2.32 (m, 1H), 1.95 (d, *J* = 1.7 Hz, 3H), 1.59 – 1.40 (m, 4H), 0.87 (m, 6H). ^{13}C NMR (101 MHz, $CDCl_3$) δ 177.1, 176.7, 174.0, 144.6, 134.5, 87.9, 81.2, 77.3, 76.5, 76.1, 75.9, 64.5, 60.1, 56.0, 53.2, 35.9, 31.8, 31.1, 28.6, 15.2, 14.7. HR-ESI-MS calculated for $C_{21}H_{36}O_8N_2$ $(M+Na)^+$ 467.2364, found 467.2363.

Ethyl (3*R*,4*R*,5*S*)-4-acetamido-5-[(tert-butoxycarbonyl)-amino]-3-(1-ethylpropoxy)-1-cyclohexene-1-carboxylate (12)

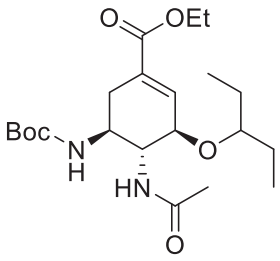

To a solution of oseltamivir free base **5** (0.38 g, 1.21 mmol) in DCM (3 mL) was added triethylamine (0.61 g, 6.08 mmol) followed by addition of di-*tert*-butyl dicarbonate (0.53 g, 2.42 mmol) and then the reaction mixture was stirred for 4 h at room temperature. The mixture was diluted with water (10 mL) and then extracted with DCM (3x10 mL). The combined organic phase was washed with brine, dried over $MgSO_4$ and concentrated under reduced pressure. The residue was purified by flash column chromatography (eluent DCM to DCM/MeOH, 20:1) to afford the protected amine **12** (0.49 g, 98% yield) as a white solid.

^{1}H NMR (300 MHz, $CDCl_3$) δ 6.78 (s, 1H), 5.80 (d, *J* = 8.2 Hz, 1H), 5.11 (d, *J* = 9.0 Hz, 1H), 4.20 (q, *J* = 7.1 Hz, 2H), 4.13 – 4.00 (m, 1H), 3.97 (s, 1H), 3.79 (dd, *J* = 9.7, 5.1 Hz, 1H), 3.52 – 3.28 (m, 1H), 2.74 (dd, *J* = 18.1, 4.9 Hz, 1H), 2.29 (dd, *J* = 17.7, 9.6 Hz, 1H), 1.98 (s, 3H), 1.51 (dd, *J* = 5.5, 4.1 Hz, 4H), 1.42 (s, 9H), 1.28 (t, *J* = 7.1 Hz, 3H), 0.88 (dd, *J* = 13.6, 7.3 Hz, 6H). ^{13}C NMR (75 MHz, $CDCl_3$) δ 170.9, 166.1, 156.4, 137.7, 129.5, 82.3, 79.8, 76.0, 61.1, 54.5, 49.2, 31.1, 28.5, 26.3, 25.8, 23.5, 14.3, 9.6, 9.4. HR-ESI-MS calculated for $C_{21}H_{37}O_6N_2$ $(M+H)^+$ 413.2646, found 413.2648.

(3*R*,4*R*,5*S*)-4-Acetamido-5-[(tert-butoxycarbonyl)-amino]-3-(1-ethylpropoxy)-1-cyclohexene-1-carboxylic acid (13)

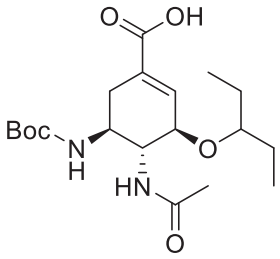

An aqueous solution of NaOH (0.5 M; 8.7 mL) was added dropwise to a stirred solution of the ester **12** (0.9 g, 2.18 mmol) in 1,4-dioxane (8.7 mL). The reaction mixture was stirred for 24 h at room temperature. The pH was adjusted to neutral by addition of Amberlite IR 120 hydrogen form. Amberlite was removed by filtration and the filtrate was concentrated under reduced pressure. The residue was purified by flash column chromatography (eluent DCM/MeOH gradient 10:1 to 10:3) to furnish the free acid **13** (1.28 g, 95% yield) as a white solid.

^{1}H NMR (300 MHz, $CDCl_3$) δ 6.81 (s, 1H), 6.69 (s, 1H), 5.72 (d, *J* = 9.3 Hz, 1H), 4.02 (d, *J* = 6.8 Hz, 2H), 3.75 (dd, *J* = 13.1, 8.4 Hz, 1H), 3.39 – 3.26 (m, 1H), 2.70 (dd, *J* = 17.5, 5.0 Hz, 1H), 2.25 (dd, *J* = 17.7, 11.1 Hz, 1H), 1.99 (s, 3H), 1.49 (dd, *J* = 14.0, 6.7 Hz, 4H), 1.41 (s, 9H), 0.86 (dd, *J* = 16.5, 7.4 Hz, 6H). ^{13}C NMR (75 MHz, $CDCl_3$) δ 171.5, 169.1, 156.9, 139.2, 129.2, 82.3, 79.8, 76.2, 55.2, 49.6, 31.0, 28.5, 26.3, 25.7, 23.4, 9.8, 9.2. HR-ESI-MS calculated for $C_{19}H_{33}O_6N_2$ $(M+H)^+$ 385.2333, found 385.2335.

(3*R*,4*R*,5*S*)-4-Acetamido-5-[(*tert*-butoxycarbonyl)-amino]-3-(1-ethylpropoxy)-1-bromocyclohexene (14)

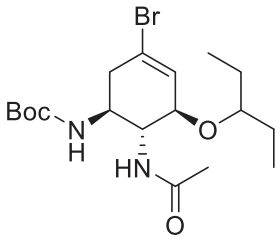

S-(1-Oxido-2-pyridyl)-*N,N,N′,N′*-tetramethylthiuronium hexafluorophosphate (0.26 g, 0.70 mmol) was added to a solution of the free acid **13** (0.21 g, 0.54 mmol), triethylamine (0.22 mL, 1.61 mmol) and 4-(dimethylamino)pyridine (0.007 g, 0.054 mmol) in dry THF (4 mL). The reaction was stirred in the dark for 40 min at room temperature. The solvent was removed by evaporation under reduced pressure. The remaining green oil was dissolved in DCM (2 mL) and bromotrichloromethane (2 mL). The formed solution was irradiated (refluxed) with a flood lamp for 90 min. The mixture was concentrated and purified by flash column chromatography (eluent Toluene/EtOAc gradient 2:1 to 1:1) to afford the vinyl bromide **14** (0.18 g, 78% yield).

TLC (Toluene/EtOAc 1:1) R_f = 0.45. ^{1}H NMR (300 MHz, $CDCl_3$) δ 6.07 (s, 1H), 5.52 (d, *J* = 9.4 Hz, 1H), 5.35 (d, *J* = 9.0 Hz, 1H), 4.09 (dd, *J* = 9.1, 6.8 Hz, 1H), 3.88 (dd, *J* = 7.9, 5.5 Hz, 1H), 3.83 (s, 1H), 3.39 – 3.25 (m, 1H), 2.68 (m, *J* = 26.0, 18.0, 6.8 Hz, 2H), 1.99 (s, 3H), 1.59 (s, 1H), 1.49 (dd, *J* = 7.3, 6.0 Hz, 3H), 1.42 (s, 9H), 0.88 (t, *J* = 7.4 Hz, 6H). ^{13}C NMR (75 MHz, $CDCl_3$) δ 171.5, 156.9, 129.2, 121.2, 82.3, 79.8, 76.2, 55.2, 50.9, 49.6, 28.5, 26.3, 25.7, 23.4, 9.7, 9.2. HR-ESI-MS calculated for $C_{18}H_{31}BrO_4N_2Na$ $(M+Na)^+$ 441.1359, found 441.1360.

Dimethyl (3*R*,4*R*,5*S*)-4-acetamido-5-[(*tert*-butoxycarbonyl)-amino]-3-(1-ethylpropoxy)-1-cyclohexene-1-phosphonate (15)

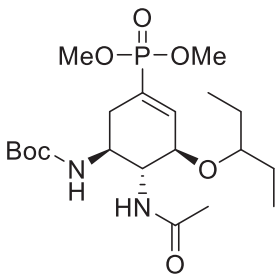

To a solution of the vinyl bromide **14** (0.18 g, 0.39 mmol) in toluene (10 mL) was added tetrakis(triphenylphosphine)palladium (0.07 g, 0.06 mmol), triethylamine (0.21 mL, 1.54 mmol) and dimethyl phosphite (0.14 mL, 1.54 mmol). The reaction mixture was stirred at 80 °C for 90 min. The reaction was quenched with a saturated solution of NH_4Cl (6 mL) and diluted with DCM (30 mL). The organic phase was washed with a saturated solution of NH_4Cl (6 mL) and brine (2x5 mL), dried over $MgSO_4$ and concentrated. The residue was purified by flash column chromatography (eluent EtOAc gradient to EtOAc/MeOH 6:1) to afford the phosphonate **15** (0.16 g, 86% yield).

TLC (EtOAc/MeOH 6:1) R_f = 0.42. ^{1}H NMR (300 MHz, $CDCl_3$) δ 6.59 (d, *J* = 21.8 Hz, 1H), 6.02 (d, *J* = 8.8 Hz, 1H), 5.17 (d, *J* = 9.0 Hz, 1H), 4.11 – 3.99 (m, 1H), 3.94 (s, 1H), 3.77 (d, *J* = 11.9 Hz, 1H), 3.72 (d, *J* = 2.4 Hz, 3H), 3.69 (d, *J* = 2.4 Hz, 3H), 3.39 – 3.27 (m, 1H), 2.67 – 2.49 (m, 1H), 2.28 – 2.11 (m, 1H), 1.97 (s, 3H), 1.56 – 1.44 (m, 4H), 1.40 (s, 9H), 0.86 (td, *J* = 7.4, 5.1 Hz, 6H). ^{13}C NMR (75 MHz, $CDCl_3$) δ 171.2, 156.3, 141.9 (d, *J* = 6.8 Hz), 129.3 (d, *J* = 180.4 Hz), 81.8, 79.8, 76.0 (d, *J* = 20.2Hz), 54.1, 52.8 (d), 52.7 (d), 49.8 (d), 30.7 (d), 28.2, 25.9, 25.6, 23.1, 9.7, 9.3. HR-ESI-MS calculated for $C_{20}H_{37}O_7NaN_2P$ $(M+Na)^+$ 471.2231, found 471.2232.

Methyl (3*R*,4*R*,5*S*)-4-acetamido-5-[(*tert*-butoxycarbonyl)-amino]-3-(1-ethylpropoxy)-1-cyclohexene-1-phosphonate (16)

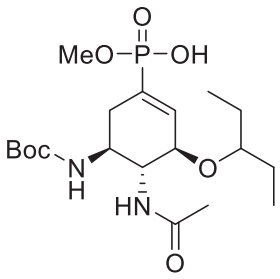

An aqueous solution of NaOH (0.5M; 2.8 mL) was added to a stirred solution of the dimethoxyphosphonate **15** (0.31 g, 0.698 mmol) in 1,4-dioxane (2.8 mL). The reaction mixture was stirred for 18 h at room temperature. The pH was adjusted to neutral by addition of Amberlite IR 120 hydrogen form. Amberlite was removed by filtration and the filtrate was

concentrated under reduced pressure. The residue was purified by flash column chromatography (eluent EtOAc/MeOH gradient 6:1 to 1:2) to furnish phosphonic acid **16** (0.27 g, 91% yield) as a white solid.

TLC (DCM/MeOH 2:1), R_f = 0.2. ^{1}H NMR (600 MHz, D_2O) δ 6.32 (d, *J* = 19.7 Hz, 1H), 4.25 (d, *J* = 8.6 Hz, 1H), 3.83 (t, *J* = 10.0 Hz, 1H), 3.75 (s, 1H), 3.52 (d, *J* = 10.7 Hz, 3H), 2.45 – 2.43 (m, 2H), 2.24 (s, 3H), 1.57 (dd, *J* = 13.6, 6.7 Hz, 4H), 1.51 – 1.34 (m, 9H), 0.88 (dt, *J* = 34.7, 7.3 Hz, 6H).^{13}C NMR (151 MHz, D_2O) δ 174.2, 157.6, 137.0, 131.6, 130.5, 84.2, 80.9, 76.9, 76.7, 55.6, 51.6, 51.6, 49.3, 49.2, 31.1, 27.6, 25.6, 25.3, 22.2, 8.6, 8.5. ^{31}P NMR (121 MHz, D_2O) δ 15.27. HR-ESI-MS calculated for $C_{19}H_{36}O_7N_2P$ $(M+H)^+$ 435.2255, found 435.2256.

(6-Azidohexyl) (3*R*,4*R*,5*S*)-4-acetylamino-5-[(*tert*-butoxycarbonyl)-amino]-3-(1-ethylpropoxy)-1-cyclohexene-1-phosphonic acid (17)

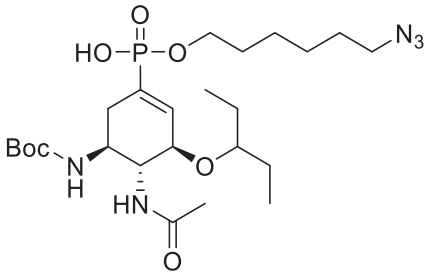

Methyl (3*R*,4*R*,5*S*)-4-acetamido-5-[(tert-butoxycarbonyl)-amino]-3-(1-ethylpropoxy)-1-cyclohexene-1-phosphonate **16** (100 mg, 0.23 mmol) was dissolved in DMF (1.5 mL) followed by addition of DIPEA (0.16 mL, 0.92 mmol), 1-azido-6-bromohexane (120 mg, 0.57 mmol) and sodium iodide (5 mg, 0.034 mmol). The reaction was then purged with argon and heated to 60 ^{o}C for 48 h. The solvent was evaporated under reduced pressure and the crude mixture purified by flash chromatography (from EtOAc to EtOAc/MeOH 80:20) to yield the alkylated phosphonic acid **17** (72 mg, 56%).

^{1}H NMR (401 MHz, Methanol-*d4*) δ 6.36 (d, *J* = 19.0 Hz, 1H), 4.15 – 4.00 (m, 1H), 3.88 – 3.78 (m, 1H), 3.77 (t, *J* = 6.4 Hz, 1H), 3.70 (dd, *J* = 10.0, 4.4 Hz, 1H), 3.55 – 3.44 (m, 1H), 3.41 (t, *J* = 5.4 Hz, 1H), 3.28 (d, *J* = 6.8 Hz, 2H), 2.62 (d, *J* = 17.1 Hz, 1H), 2.22 (t, *J* = 14.2 Hz, 1H), 1.97 (s, 3H), 1.61 (m, 3H), 1.50 (ddd, *J* = 16.4, 7.6, 6.1 Hz, 4H), 1.43 (s, 12H), 1.34 (d, *J* = 6.6 Hz,

2H), 0.89 (dt, *J* = 15.1, 7.4 Hz, 6H). ^{13}C NMR (101 MHz, Methanol-*d4*) δ 172.4, 156.6, 136.0, 132.6 (d, J = 211.8 Hz), 82.1, 78.8, 76.5, 64.2, 55.2, 54.5, 51.0, 30.4, 28.5 (x3), 27.4, 26.2, 26.0, 25.4, 25.2, 21.7, 18.0, 8.6, 8.3. ^{31}P NMR (162 MHz, Methanol-*d4*) δ 13.12. HR-ESI-MS calculated for $C_{24}H_{43}O_7N_5P$ = 544.2906, found 544.2906.

Ethyl (3*R*,4*R*,5*S*)-4-acetamido-5-[N^2,N^3-bis(*tert*-butoxycarbonyl)guanidino]-3-(1-ethylpropoxy)-1-cyclohexene-1-carboxylate

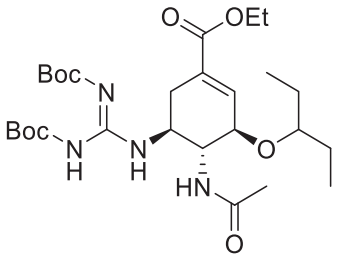

Mercury(II) chloride (0.11 g, 0.40 mmol) was added portionwise to a solution of oseltamivir base **6** (0.10 g, 0.32 mmol), *N,N′*−di-(*tert*-butoxycarbonyl)thiourea (0.11 g, 0.40 mmol) and triethylamine (0.11 mL, 0.80 mmol) in DMF (15 mL) at 0 °C. The reaction mixture was stirred for 24 h at room temperature. The mixture was diluted with EtOAc (10 mL), filtered through a pad of Celite and concentrated under reduced pressure. The residue was diluted with water (30 mL) and extracted with EtOAc (3x10 mL). The combined organic phase was washed with water, brine, dried over Na_2SO_4, filtered and evaporated. The residue was purified by flash column chromatography (eluent Hexanes/EtOAc, 2:1) to afford the Boc-protected guanidine derivative **7** (0.16 g, 89%).

TLC (Hexanes/EtOAc 1:1) R_f = 0.4. ^{1}H NMR (300 MHz, $CDCl_3$) δ 11.33 (s, 1H), 8.57 (d, *J* = 8.1 Hz, 1H), 6.76 (s, 1H), 6.16 (d, *J* = 8.9 Hz, 1H), 4.43 – 4.23 (m, 1H), 4.20 – 4.01 (m, 3H), 3.96 (d, *J* = 7.7 Hz, 1H), 3.36 – 3.21 (m, 1H), 2.72 (dd, *J* = 17.6, 5.3 Hz, 1H), 2.42 – 2.23 (m, 1H), 1.85 (s, 3H), 1.55 – 1.49 (m, *J* = 8.4, 4.7 Hz, 22H), 1.22 (dd, *J* = 12.6, 5.5 Hz, 3H), 0.82 (dt, *J* = 10.3, 7.4 Hz, 6H). ^{13}C NMR (101 MHz, $CDCl_3$) δ 170.3, 166.0, 163.3, 157.0, 152.7, 138.1,

128.7, 83.6, 82.8, 79.6, 76.3, 61.1, 54.5, 48.2, 30.6, 28.41, 28.2, 26.2, 25.9, 23.4, 14.3, 9.7, 9.4. HR-ESI-MS calculated for $C_{27}H_{47}O_8N_4$ $(M+H)^+$ 555.3388, found 555.3389.

(3*R*,4*R*,5*S*)-4-Acetamido-5-[N^2,N^3-bis(*tert*-butoxycarbonyl)guanidino]-3-(1-ethylpropoxy)-1-cyclohexene-1-carboxylic acid

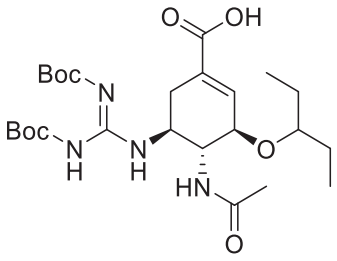

An aqueous solution of NaOH (0.5 M; 0.55 mL) was added to a solution of ester (0.15 g, 0.27 mmol) in 1,4-dioxane (0.55 mL). The reaction mixture was stirred overnight at room temperature. The pH was adjusted to neutral by addition of Amberlite IR 120 hydrogen form. Amberlite was removed by filtration and the filtrate was concentrated under reduced pressure. The residue was purified by flash column chromatography (Toluene/EtOAc/AcOH 1:1:0.5%) to afford the free acid (0.07 g, 48%).

TLC (Toluene/EtOAc/AcOH 1:1:0.5%) R_f = 0.2. ^{1}H NMR (300 MHz, $CDCl_3$) δ 8.64 (d, J = 8.1 Hz, 1H), 6.82 (s, 1H), 6.23 (d, J = 8.9 Hz, 1H), 4.39 (dd, J = 8.3, 6.0 Hz, 1H), 4.26 – 4.16 (m, 2H), 4.16 – 4.08 (m, 1H), 4.06 – 3.98 (m, 1H), 3.41 – 3.29 (m, 1H), 2.78 (dd, J = 17.6, 5.3 Hz, 1H), 2.47 – 2.32 (m, 1H), 1.91 (s, 3H), 1.61 – 1.41 (m, 22H), 1.27 (dt, J = 10.9, 7.1 Hz, 4H), 0.89 (dt, J = 10.3, 7.4 Hz, 6H). ^{13}C NMR (75 MHz, CD_3OD) δ 173.6, 169.3, 164.4, 157.7, 153.7, 138.7, 130.4, 84.6, 84.0, 80.5, 76.6, 54.6, 50.0, 31.4, 28.5, 28.2, 27.3, 26.9, 22.7, 9.9, 9.7. HR-ESI-MS calculated for $C_{25}H_{43}O_8N_4$ $(M+H)^+$ 527.3075, found 527.3076.

Dimethyl (3*R*,4*R*,5*S*)-4-acetamido-5-[*N*2,*N*3-bis(*tert*-butoxycarbonyl)guanidino]-3-(1-ethylpropoxy)-1-cyclohexene-1-phosphonate

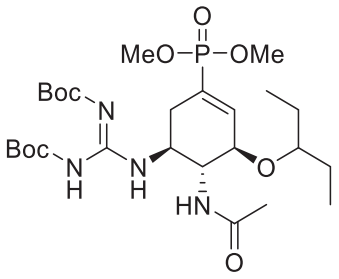

The Boc-protected phosphonate **16** (0.12 g, 0.259 mmol) was treated with trifluoroacetic acid (100%, 1 mL) for 1 h and then the trifluoroacetic acid was removed by evaporation under reduced pressure. The residue was dissolved in acetonitrile (1.5 mL) and triethylamine (0.18 mL, 1.29 mmol) was added dropwise followed by the addition of *N,N'*-di-Boc-1*H*-pyrazole-1-carboxamidine (0.08 g, 0.26 mmol). The reaction mixture was stirred for 18 h at room temperature and then was evaporated to dryness. The residue was purified by flash column chromatography (eluent EtOAc gradient to EtOAc/MeOH 6:1) to afford the guanidine phosphonate (0.07 g, 47% yield).

^{1}H NMR (300 MHz, $CDCl_3$) δ 11.39 (s, 1H), 8.60 (d, J = 7.3 Hz, 1H), 6.64 (d, J = 22.5 Hz, 1H), 6.35 (d, J = 9.2 Hz, 1H), 4.41 (d, J = 8.2 Hz, 1H), 4.23 – 4.04 (m, 1H), 3.99 (s, 1H), 3.73 (s, 3H), 3.70 (s, 3H), 3.39 – 3.27 (m, 1H), 2.72 – 2.58 (m, 1H), 2.36 – 2.22 (m, 1H), 1.92 (s, 3H), 1.58 – 1.41 (m, 22H), 0.88 (dd, J = 16.2, 7.4 Hz, 6H). ^{13}C NMR (75 MHz, $CDCl_3$) δ 170.6, 163.2, 157.0, 152.7, 143.2, 143.1, 132.2, 132.1, 126.6, 124.1, 83.7, 82.8, 79.8, 76.4, 76.1, 54.3, 52.8, 52.7, 52.6, 52.6, 48.4, 48.2, 30.9, 30.8, 28.3, 28.1, 26.0, 25.7, 23.3, 9.6, 9.3. HR-ESI-MS calculated for $C_{26}H_{48}O_9N_4P$ $(M+H)^+$ 591.3153, found 591.3153.

Ethyl (3*R*,4*R*,5*S*)-4-acetamido-5-[*N*-[dimethyl aspartyl]methyl]-3-(1-ethylpropoxy)-1-cyclohexene-1-carboxylate (21)

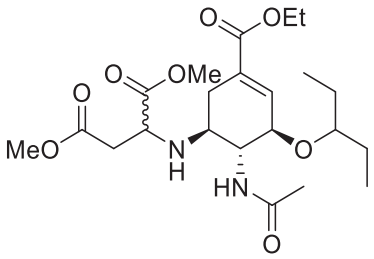

Dimethyl maleate (0.57 g, 4.0 mmol) was added to a stirred solution of oseltamivir free base **5** (0.22 g, 0.73 mmol) in methanol (3 mL) and the mixture was refluxed overnight. The solvent was evaporated under reduced pressure and the residue was purified by flash chromatography (DCM/MeOH 90:10) to yield the mixture of diastereomers **21** (0.25 g, 75%).

^{1}H NMR (300 MHz, $CDCl_3$) δ 6.68 (s, 1H), 6.03 (d, *J* = 7.5 Hz, 1H), 4.26 (d, *J* = 8.3 Hz, 1H), 4.19 – 4.01 (m, 2H), 3.64 (s, 3H), 3.67 – 3.63 (m, 1H), 3.60 (s, 3H), 3.51 – 3.36 (m, 1H), 3.35 – 3.20 (m, 1H), 3.08 (dt, *J* = 10.1, 5.0 Hz, 1H), 2.96 – 2.86 (m, 1H), 2.72 – 2.52 (m, 3H), 2.10 – 1.95 (m, 1H), 1.92 (s, 3H), 1.42 (ddt, *J* = 7.4, 5.7, 1.9 Hz, 4H), 1.26 – 1.13 (m, 3H), 0.90 – 0.75 (m, 6H). ^{13}C NMR (75 MHz, $CDCl_3$) of major diastereomer δ 174.2, 171.4, 170.9, 166.3, 137.7, 129.0, 81.7, 74.4, 60.7, 57.4, 56.1, 53.4, 52.3, 51.8, 37.8, 31.5, 26.2, 25.6, 23.6, 14.2, 9.5, 9.3. ^{13}C NMR (75 MHz, $CDCl_3$) of minor diastereomer δ 174.8, 171.3, 171.0, 166.5, 137.8, 129.1, 82.0, 75.9, 60.9, 55.9, 55.2, 53.8, 52.4, 52.0, 38.7, 31.7, 26.2, 25.7, 23.8, 14.3, 9.7, 9.4. HR-ESI-MS calculated for $C_{22}H_{36}N_2O_8Na$ $(M+Na)^+$ 479.2364, found 479.2364.

Ethyl (3*R*,4*R*,5*S*)-4-Acetamido-5-{2-[2-(2-methoxyethoxy)ethoxy]acetamido}-3-(1-ethylpropoxy)-1-cyclohexene-1-carboxylate (22)

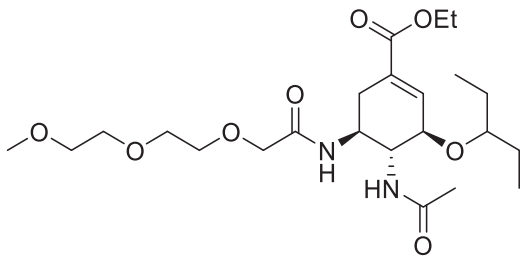

To a solution of 2-(1H-benzotriazole-1-yl)-1,1,3,3-tetramethyluronium tetrafluoroborate (0.28 g, 0.87 mmol) and 2-[2-(2-methoxyethoxy)ethoxy]acetic acid (0.13 g, 0.72 mmol) in DMF (3 mL) was added triethylamine (0.5 ml, 3.6 mmol). The reaction mixture was stirred for 5 min at room temperature followed by addition of Oseltamivir phosphate **5** (0.15 g, 0.36 mmol) and the reaction was stirred for an additional for 16 h. The reaction mixture was quenched by addition of water (10 mL) and $NaHCO_3$ saturated solution (5 mL) until the pH was slightly basic. The aqueous solution was extracted with DCM and the combined organic phases were washed with water and brine, dried over Na_2SO_4, and evaporated to dryness under reduced pressure. Purification of the crude residue by flash column chromatography (eluent DCM/MeOH 90:10) furnished the amide **22** (0.16 g, 93%).

^{1}H NMR (401 MHz, $CDCl_3$) δ 7.33 (d, *J* = 8.6 Hz, 1H), 6.82 – 6.74 (m, 1H), 6.06 (d, *J* = 8.8 Hz, 1H), 4.19 (qd, *J* = 7.1, 1.0 Hz, 3H), 4.13 – 4.06 (m, 1H), 4.04 – 3.99 (m, 1H), 3.69 – 3.61 (m, 8H), 3.59 – 3.52 (m, 2H), 3.37 - 3.31 (m, 1H), 3.35 (s, 3H), 2.85 – 2.69 (m, 1H), 2.37 (dd, *J* = 17.7, 9.8 Hz, 1H), 1.92 (s, 3H), 1.56 – 1.43 (m, 4H), 1.27 (t, *J* = 7.1 Hz, 3H), 0.87 (dt, *J* = 10.4, 7.4 Hz, 6H). ^{13}C NMR (101 MHz, $CDCl_3$) δ 170.8, 170.7, 166.1, 137.9, 129.3, 82.4, 75.7, 72.0, 71.1, 70.7, 70.4, 70.4, 61.0, 59.1, 54.5, 47.5, 30.6, 26.3, 25.8, 23.4, 14.3, 9.7, 9.4. HR-ESI-MS calculated for $C_{23}H_{40}O_8N_2$ $(M+H)^+$ 473.2865, found 473.2857.

Ethyl (3*R*,4*R*,5*S*)-4-acetamido-5-[(1-ethoxy-1-oxopropan-2-yl)amino]-3-(1-ethylpropoxy)-1-cyclohexene-1-carboxylate.

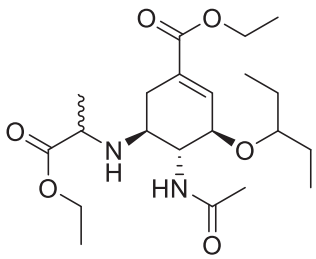

To a solution of oseltamivir phosphate **5** (0.2 g, 0.49 mmol) and ethyl 2-bromopropionate (0.11 g, 0.58 mmol) in DMF (3 mL) was added $NaHCO_3$ (0.25 g, 2.9 mmol) portionwise. The reaction mixture was stirred at 80 ºC overnight. The mixture was then quenched by the addition of water (5 mL) and extracted with EtOAc (3x 10 mL). The combined organic extracts was washed with water (2x 5 mL) and brine (3 mL), dried over anhydrous $MgSO_4$ and evaporated to dryness. The resulting residue was purified by flash chromatography (EtOAc) to yield 70 mg of the A diastereomer and 77 mg of the B diastereomer, (73 % combined yield).

A diastereomer, less polar (*S*) **(18)**

^{1}H NMR (300 MHz, $CDCl_3$) δ 6.82 – 6.70 (m, 1H), 5.66 (d, *J* = 7.9 Hz, 1H), 4.29 (ddd, *J* = 5.9, 2.9, 1.5 Hz, 1H), 4.17 (tt, *J* = 8.1, 7.1 Hz, 4H), 3.55 (dt, *J* = 9.7, 7.8 Hz, 1H), 3.46 (q, *J* = 7.0 Hz, 1H), 3.33 (q, *J* = 5.7 Hz, 1H), 3.15 (ddd, *J* = 9.8, 8.8, 5.3 Hz, 1H), 2.75 – 2.60 (m, 1H), 2.18 (ddt, *J* = 11.7, 5.5, 2.8 Hz, 1H), 2.13 – 2.02 (m, 1H), 1.99 (s, 3H), 1.57 – 1.40 (m, 4H), 1.32 – 1.19 (m, 9H), 0.88 (t, *J* = 7.4 Hz, 6H). ^{13}C NMR (75 MHz, $CDCl_3$) δ 176.0, 170.7, 166.5, 137.4, 129.5, 81.9, 74.3, 60.9 (2x O**C**$H_2$$CH_3$), 57.0, 55.1, 52.9, 31.5, 26.3, 25.9, 23.8, 19.4, 14.3 (2x OCH_2**C**H_3), 9.6, 9.5.

B diastereomer, more polar (*R*) **(19)**

^{1}H NMR (300 MHz, $CDCl_3$) δ 6.73 (t, *J* = 2.5 Hz, 1H), 5.80 (d, *J* = 6.6 Hz, 1H), 4.15 (dtd, *J* = 8.6, 7.0, 3.3 Hz, 4H), 4.07 – 3.99 (m, 1H), 3.77 (dt, *J* = 10.7, 8.7 Hz, 1H), 3.49 – 3.38 (m, 1H), 3.35 – 3.24 (m, 1H), 2.83 – 2.70 (m, 1H), 2.70 – 2.60 (m, 1H), 2.09 (q, *J* = 5.2, 4.8 Hz, 2H), 2.03 (s, 3H), 1.56 – 1.38 (m, 4H), 1.25 (td, *J* = 6.8, 4.3 Hz, 9H), 0.95 – 0.76 (m, 6H). ^{13}C NMR (75 MHz, $CDCl_3$) δ 176.4, 170.8, 166.4, 137.7, 129.0, 81.8, 75.8, 60.8 (2x O**C**H_2CH_3), 55.4, 53.8, 53.5, 31.4, 26.1, 25.6, 23.7, 19.8, 14.2 (2x OCH_2**C**H_3), 9.5, 9.2.

HR-ESI-MS calculated for $C_{21}H_{36}N_2O_6Na$ $(M+Na)^+$ 435.2466, found 435.2466.

Ethyl (3*R*,4*R*,5*S*)-4-acetamido-5-[N-((*R*)-1-ethoxy-1-oxopropan-2-yl)-4-nitrobenzamido]-3-(1-ethylpropoxy)-1-cyclohexene-1-carboxylate (20)

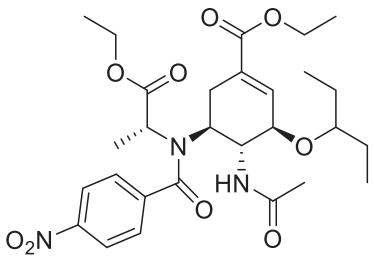

4-Nitrobenzoyl chloride (0.086 g, 0.46 mmol) was added to a solution of the B diastereomer **19** (0.16 g, 0.39 mmol) and trimethylamine (0.1 mL, 0.77 mmol) in DCM (3 mL). The reaction mixture was stirred overnight at room temperature. The reaction was quenched by the addition of water (1.5 mL) and the resulting mixture was extracted with EtOAc (3x 10mL). The combined organic extracts were washed with water, brine and were evaporated to dryness. The residue was purified by flash chromatography (Hex/EtOAc 1:2) which was followed by crystallization (EtOH) to furnish the desired compound **20** (79 mg, 36% yield).

^{1}H NMR (401 MHz, Chloroform-d_3) δ 8.26 (d, *J* = 8.7 Hz, 2H), 7.48 (d, *J* = 8.7 Hz, 2H), 7.13 (d, *J* = 6.1 Hz, 1H), 6.75 (t, *J* = 2.4 Hz, 1H), 5.10 (dd, *J* = 7.3, 3.5 Hz, 1H), 4.63 (td, *J* = 10.9, 6.2 Hz, 1H), 4.35 – 4.16 (m, 4H), 3.79 (q, *J* = 6.8 Hz, 1H), 3.25 (p, *J* = 5.7 Hz, 1H), 3.10 (ddd, *J* = 11.3, 8.5, 6.1 Hz, 1H), 2.89 – 2.77 (m, 1H), 2.56 – 2.43 (m, 1H), 1.96 (d, *J* = 6.3 Hz, 3H), 1.67 (d, *J* = 6.8 Hz, 3H), 1.55 – 1.40 (m, 4H), 1.39 – 1.27 (m, 6H), 0.95 – 0.80 (m, 6H). ^{13}C NMR (101 MHz, $CDCl_3$) δ 171.7, 171.1, 169.8, 166.0, 148.8, 141.2, 138.9, 128.3, 127.9, 126.9, 124.1, 124.0, 82.1, 71.2, 62.2, 61.3, 56.7, 55.6, 52.6, 28.4, 26.5, 25.7, 24.3, 16.3, 14.4, 14.2, 9.8, 9.3.

HR-ESI-MS calculated for $C_{28}H_{39}N_3O_9Na$ $(M+Na)^+$ 584.2578, found 584.2578.

X-ray analysis of the crystals determinates that the product obtained was the *R* diastereomer.

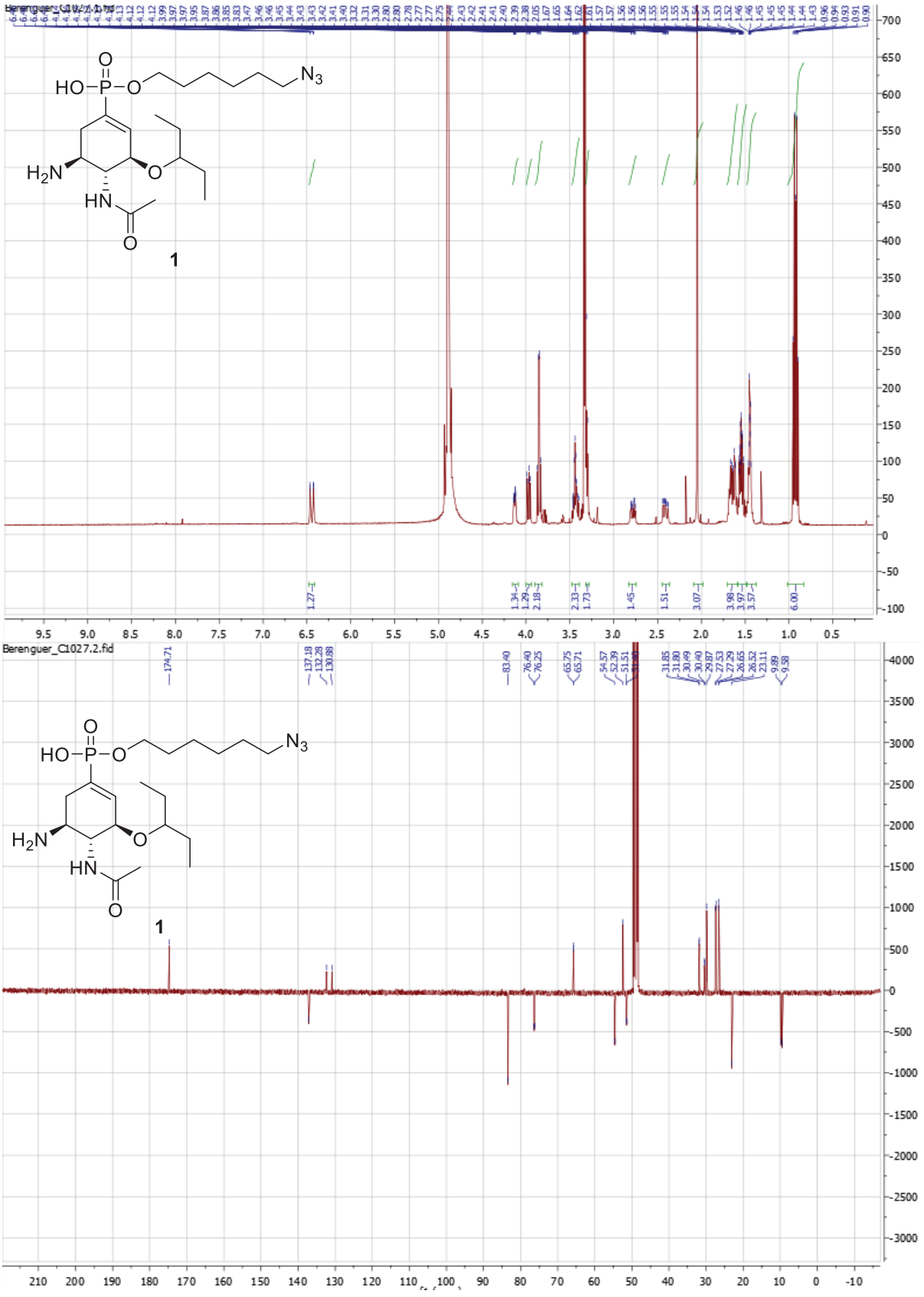
HO–P–O
N3
H2N
HN
O
1
Berengüer_C1027.2.fid

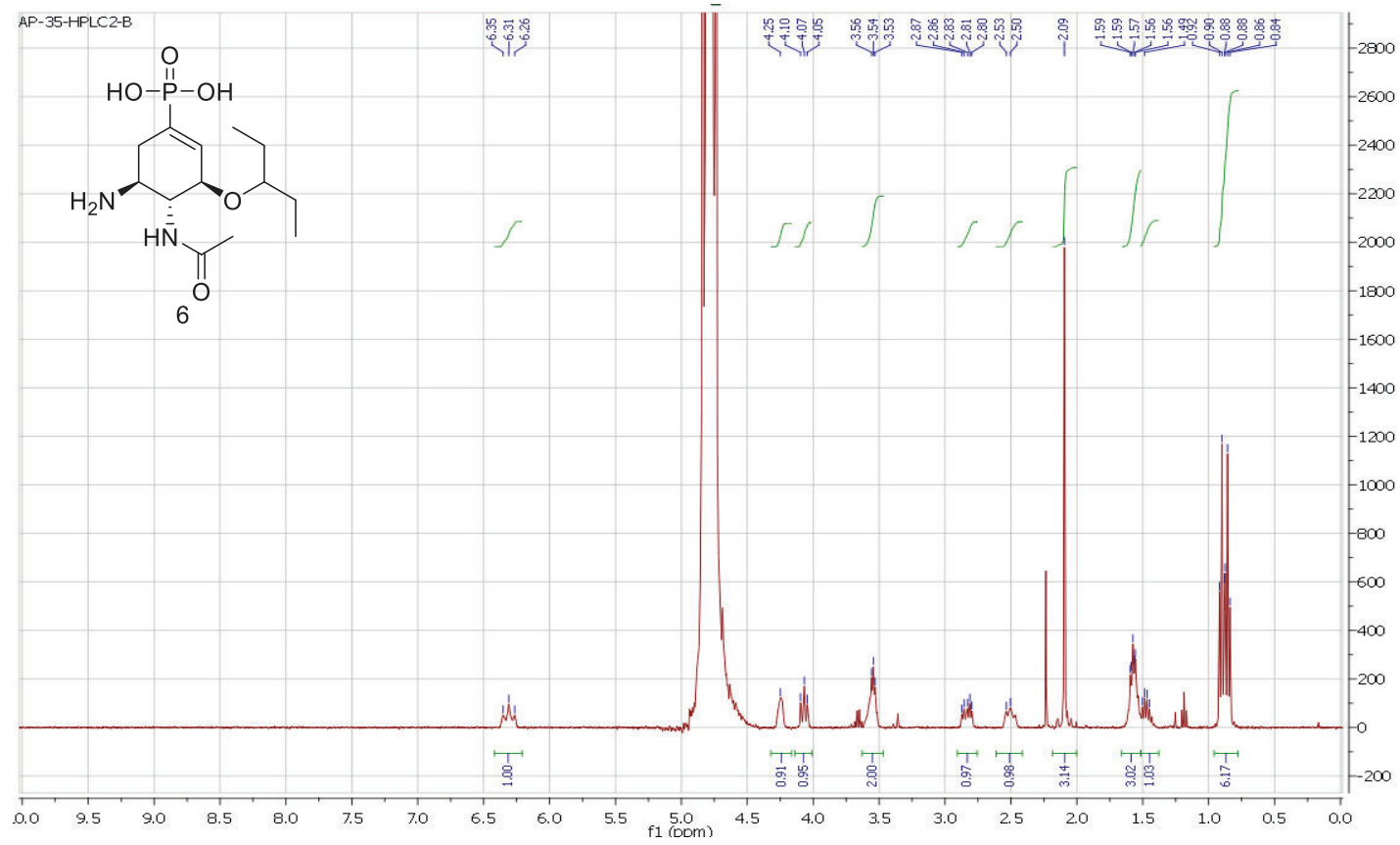
AP-35-HPLC2-B
6.35
6.31
6.26
4.25
4.10
4.07
4.05
3.56
3.54
3.53
2.87
2.86
2.83
2.81
2.80
2.53
2.50
2.09
1.59
1.59
1.57
1.56
1.56
1.49
0.92
0.90
0.88
0.88
0.86
0.84
1.00
0.91
0.95
2.00
0.97
0.98
3.14
3.02
1.03
6.17
f1 (ppm)

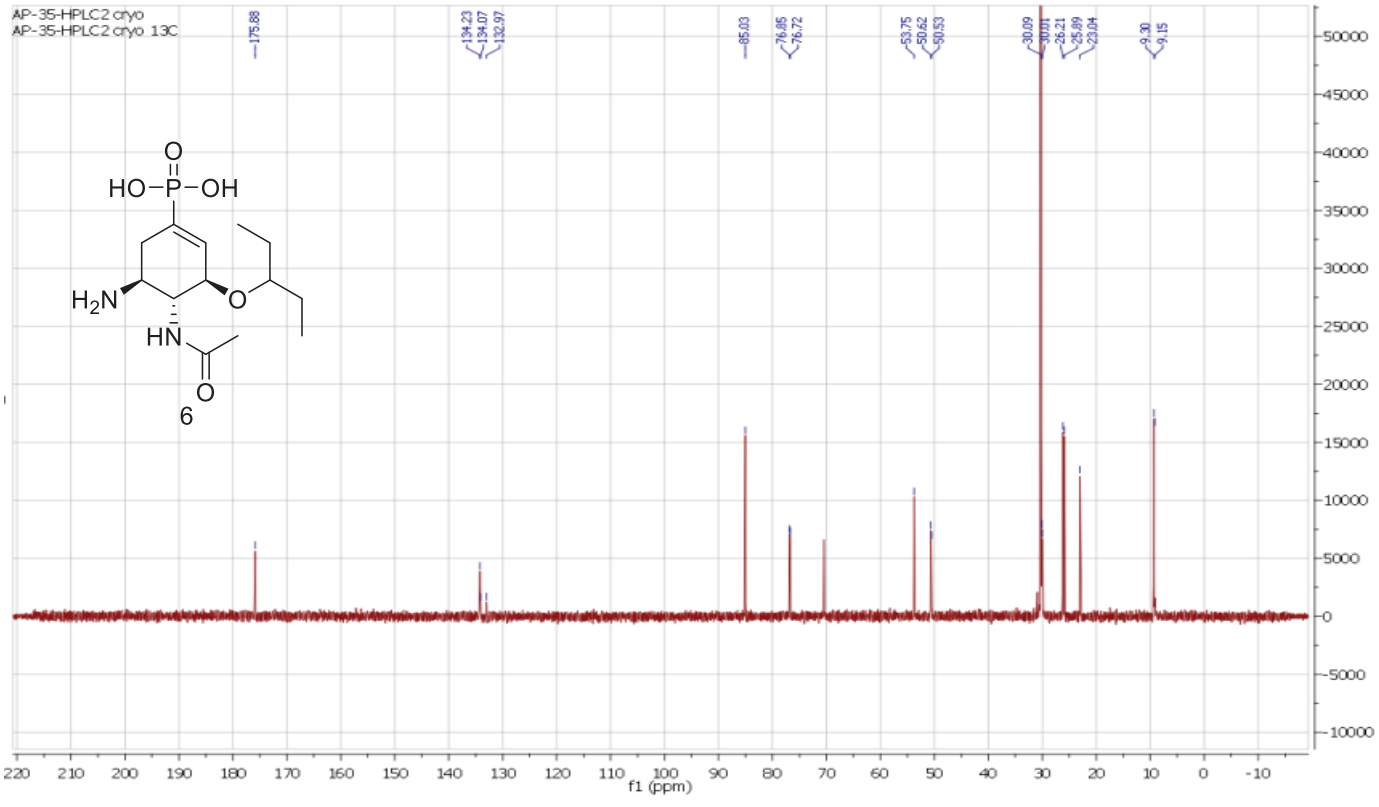
AP-35-HPLC2 cryo
AP-35-HPLC2 cryo 13C
175.88
134.23
134.07
132.97
85.03
76.85
76.72
53.75
50.62
50.53
30.09
30.01
26.21
25.89
23.04
9.30
9.15
f1 (ppm)

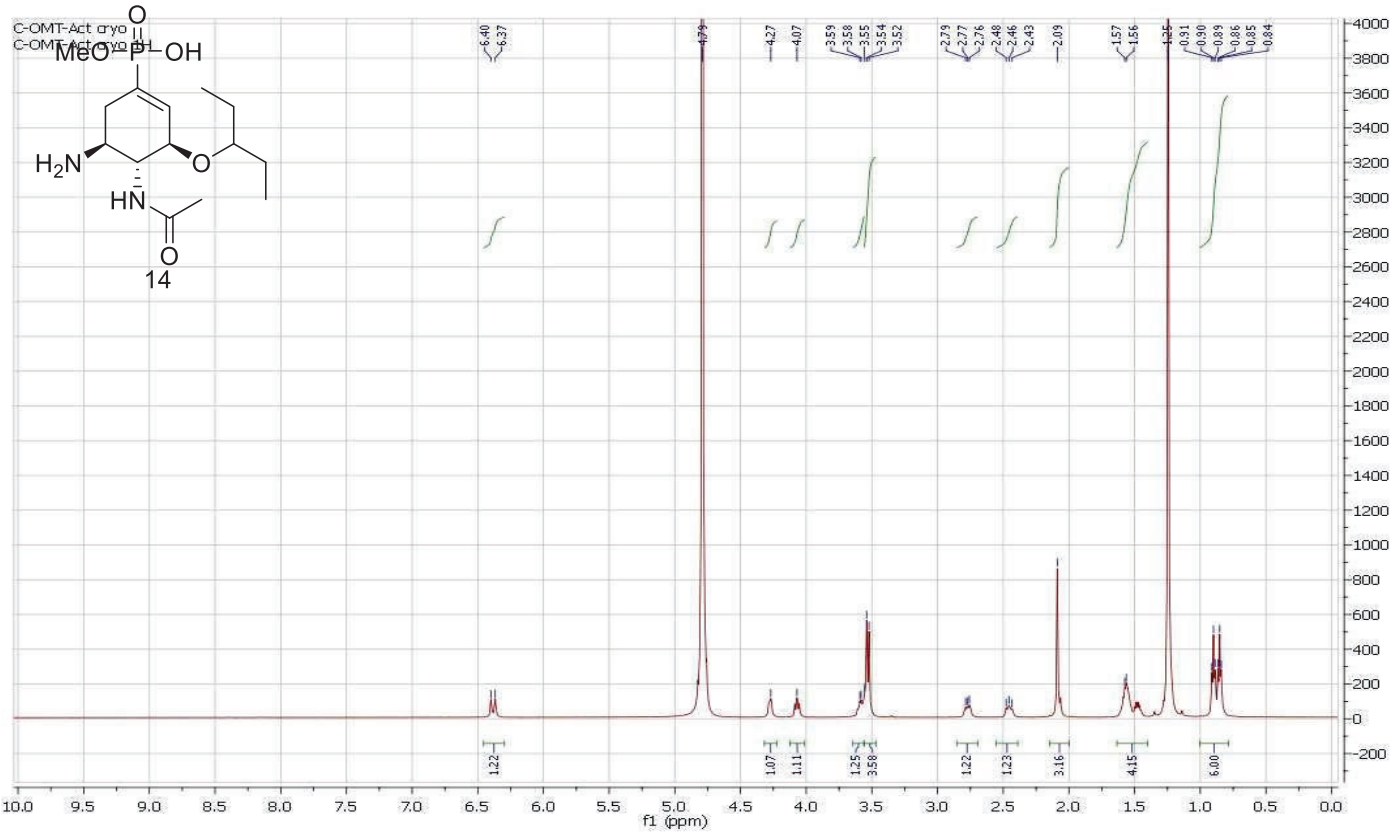
C-OMT-Act cryo
C-OMT-Act cryo 1H
MeO–P–OH
O
H2N
HN
O
O
14
f1 (ppm)

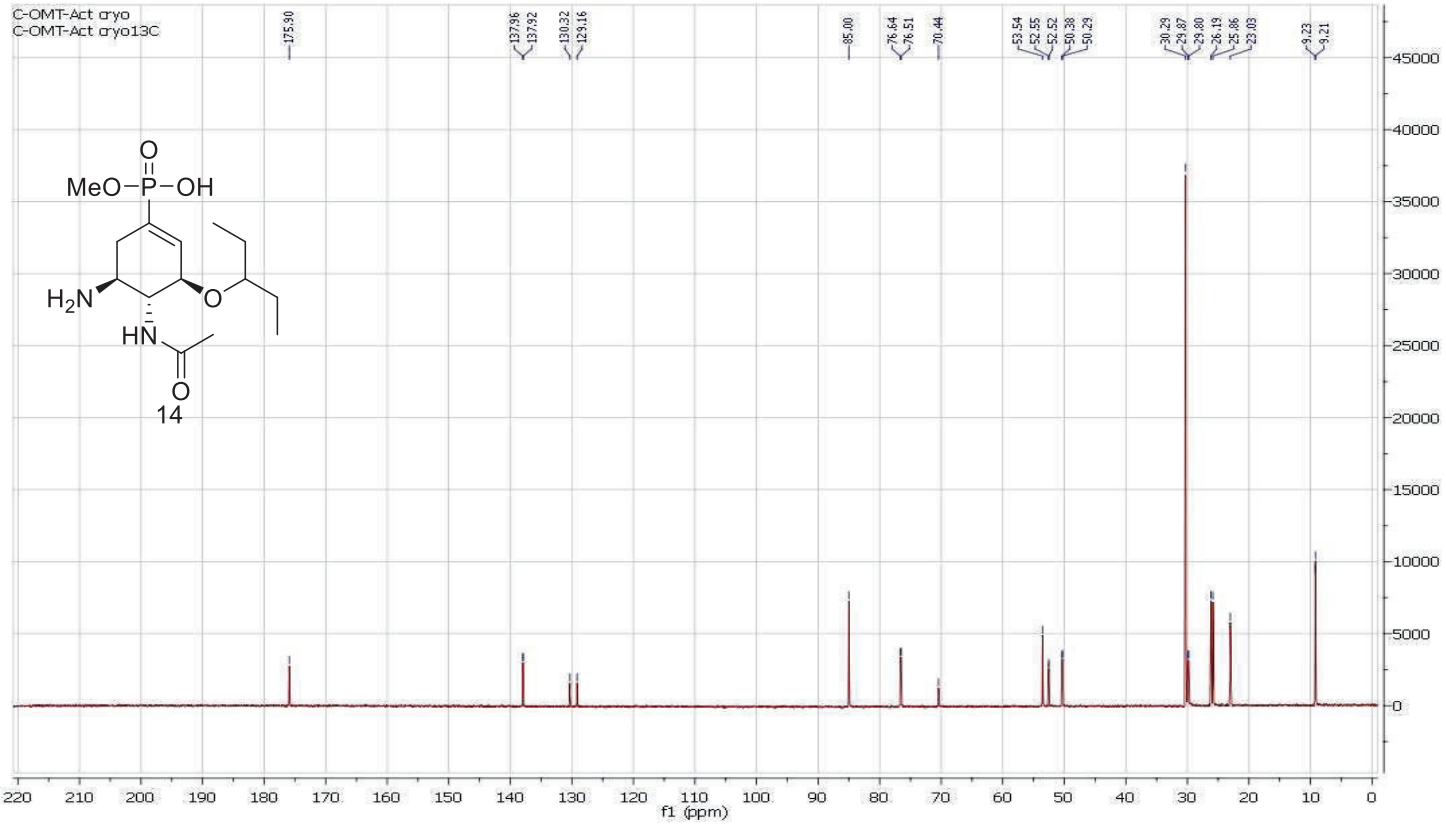
C-OMT-Act cryo
C-OMT-Act cryo13C
MeO–P–OH
O
H2N
HN
O
O
14
f1 (ppm)

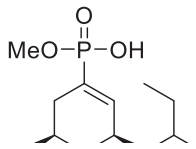
MeO–P–OH
O

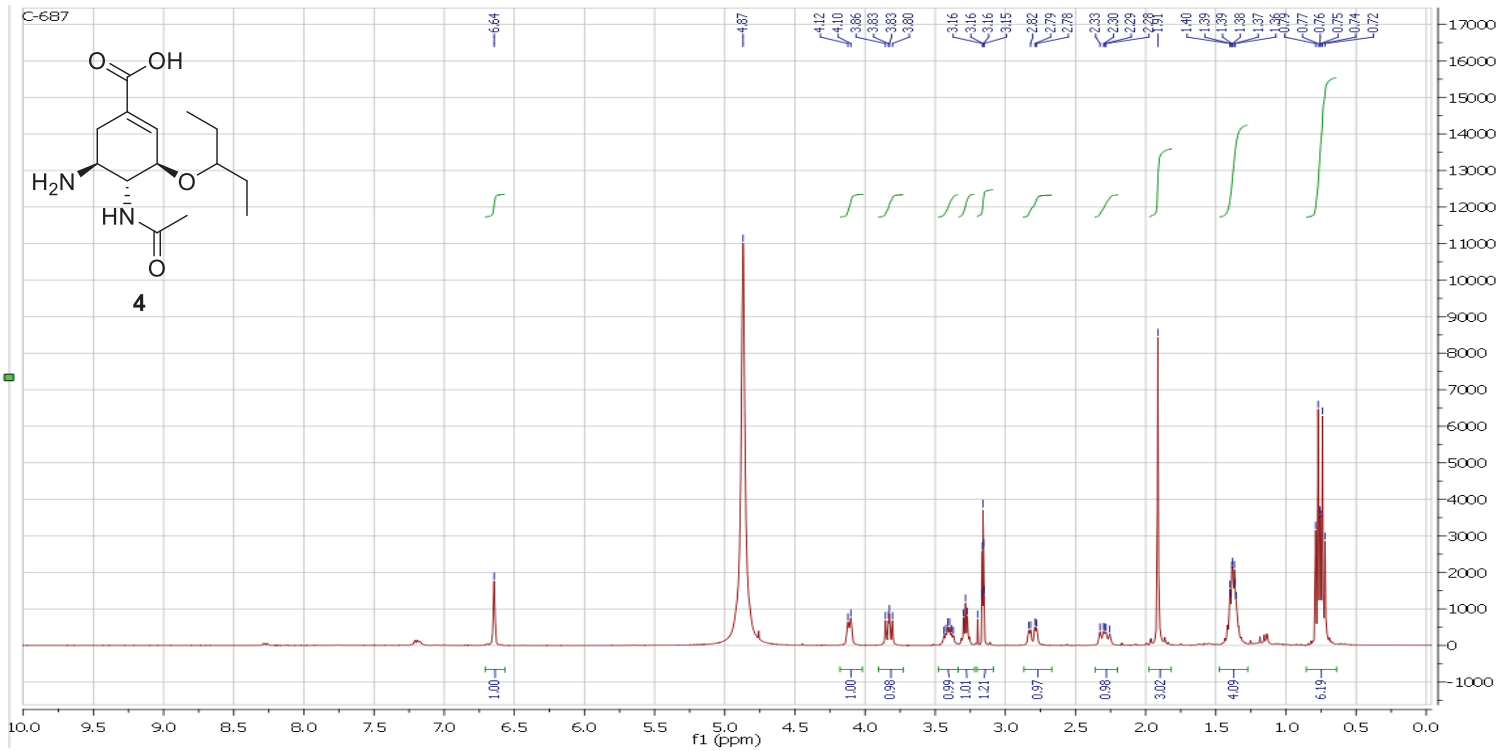
C-687
O
OH
H2N
O
HN
O
4
f1 (ppm)

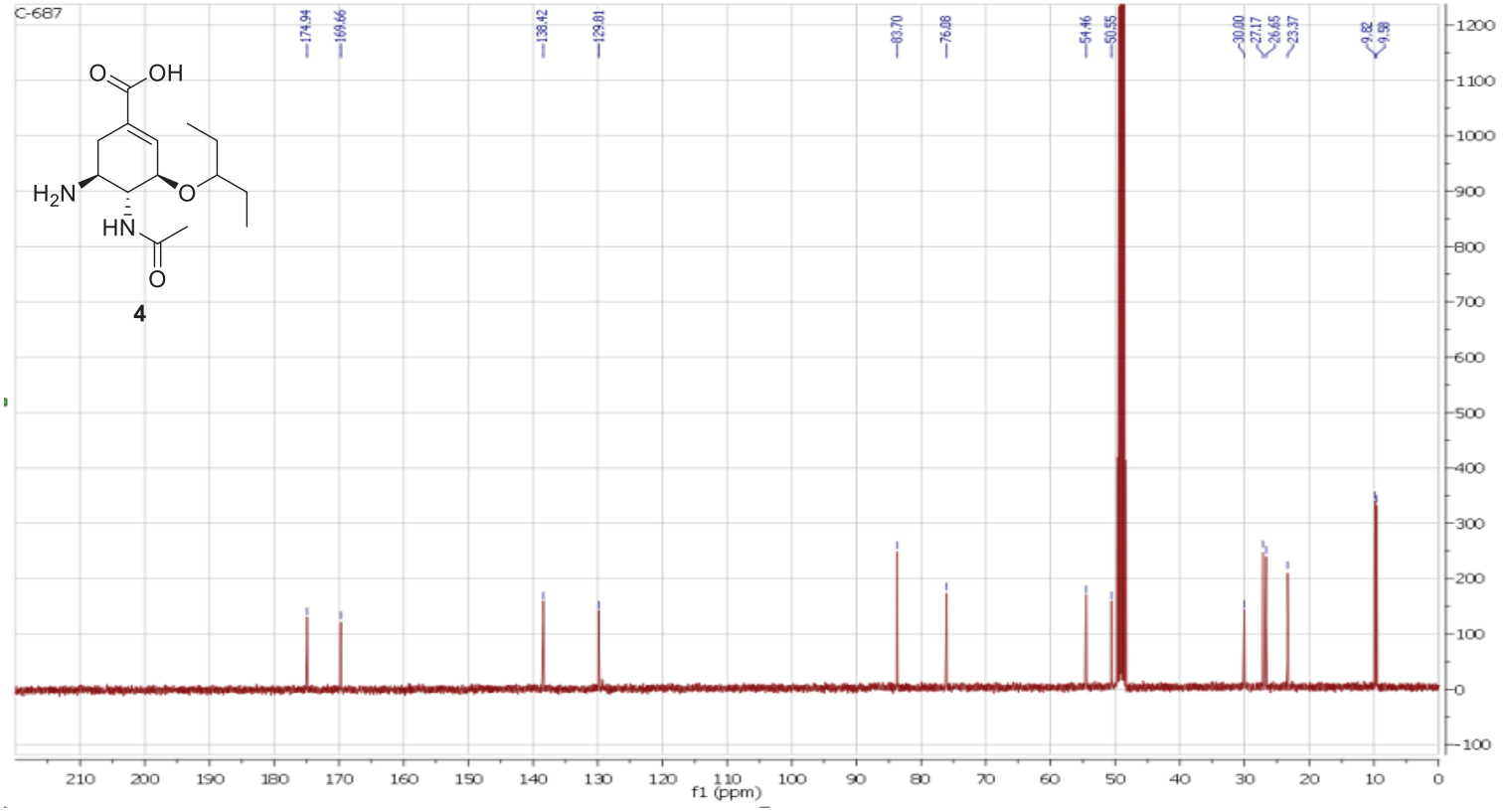
C-687
O
OH
H2N
O
HN
O
4
174.94
169.66
138.42
129.61
83.70
76.88
54.46
50.55
30.00
27.17
26.65
23.37
9.82
9.58
f1 (ppm)

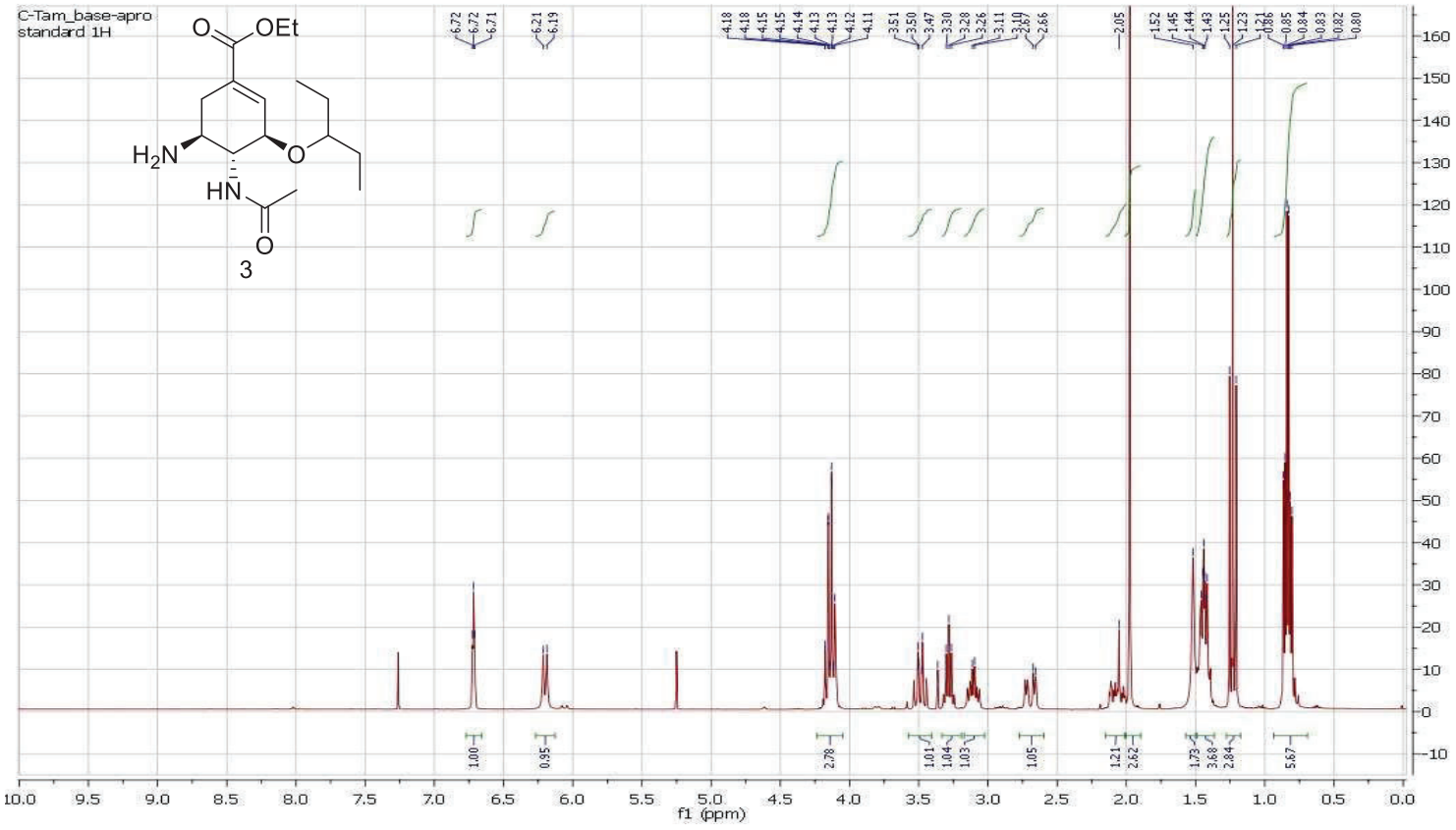
C-Tam_base-apro
standard 1H
O
OEt
H2N
O
HN
O
3
f1 (ppm)

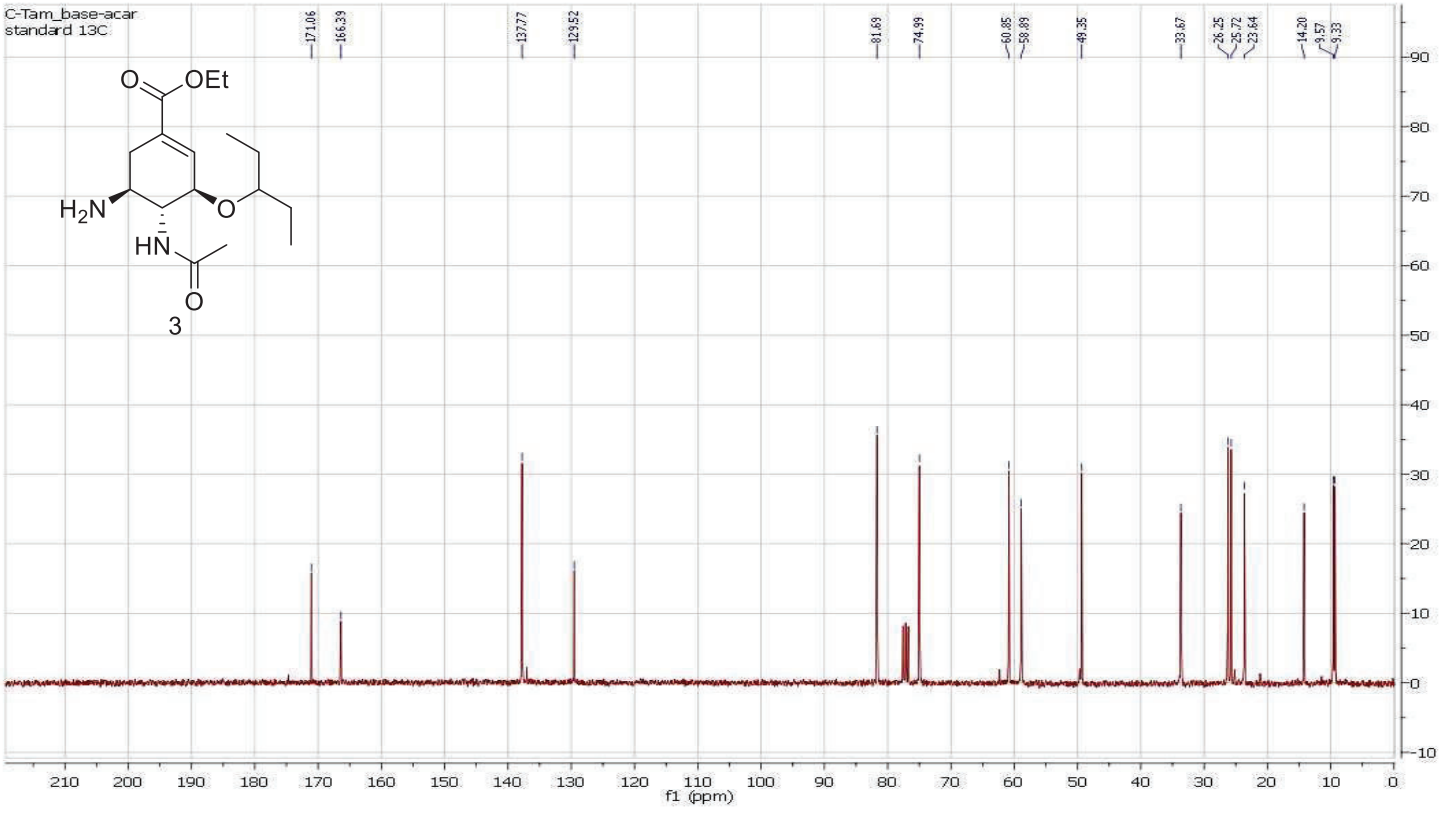
C-Tam_base-acar
standard 13C
O
OEt
H2N
O
HN
O
3
f1 (ppm)

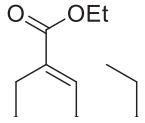
O
OEt

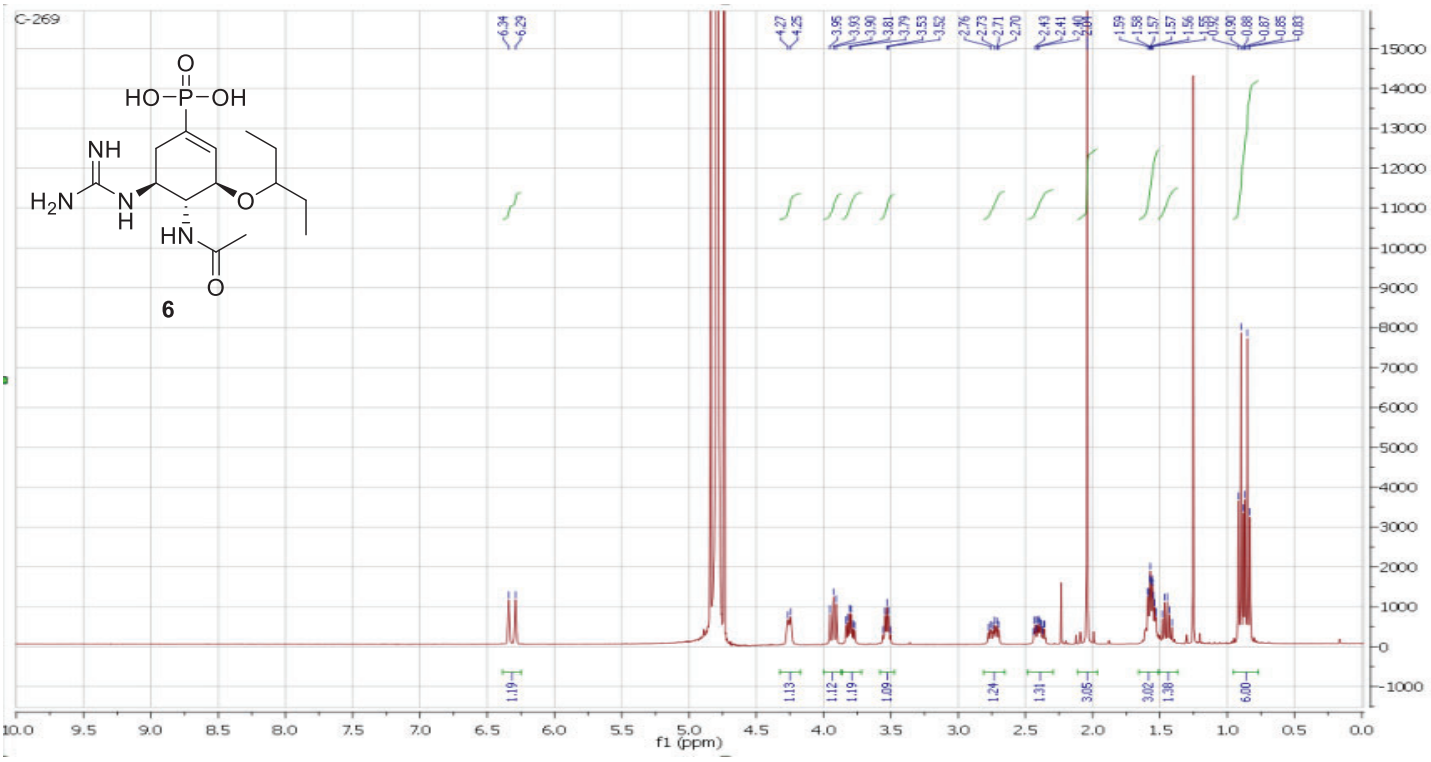
C-269
HO–P–OH
NH
H2N
N
H
O
HN
O
6
f1 (ppm)

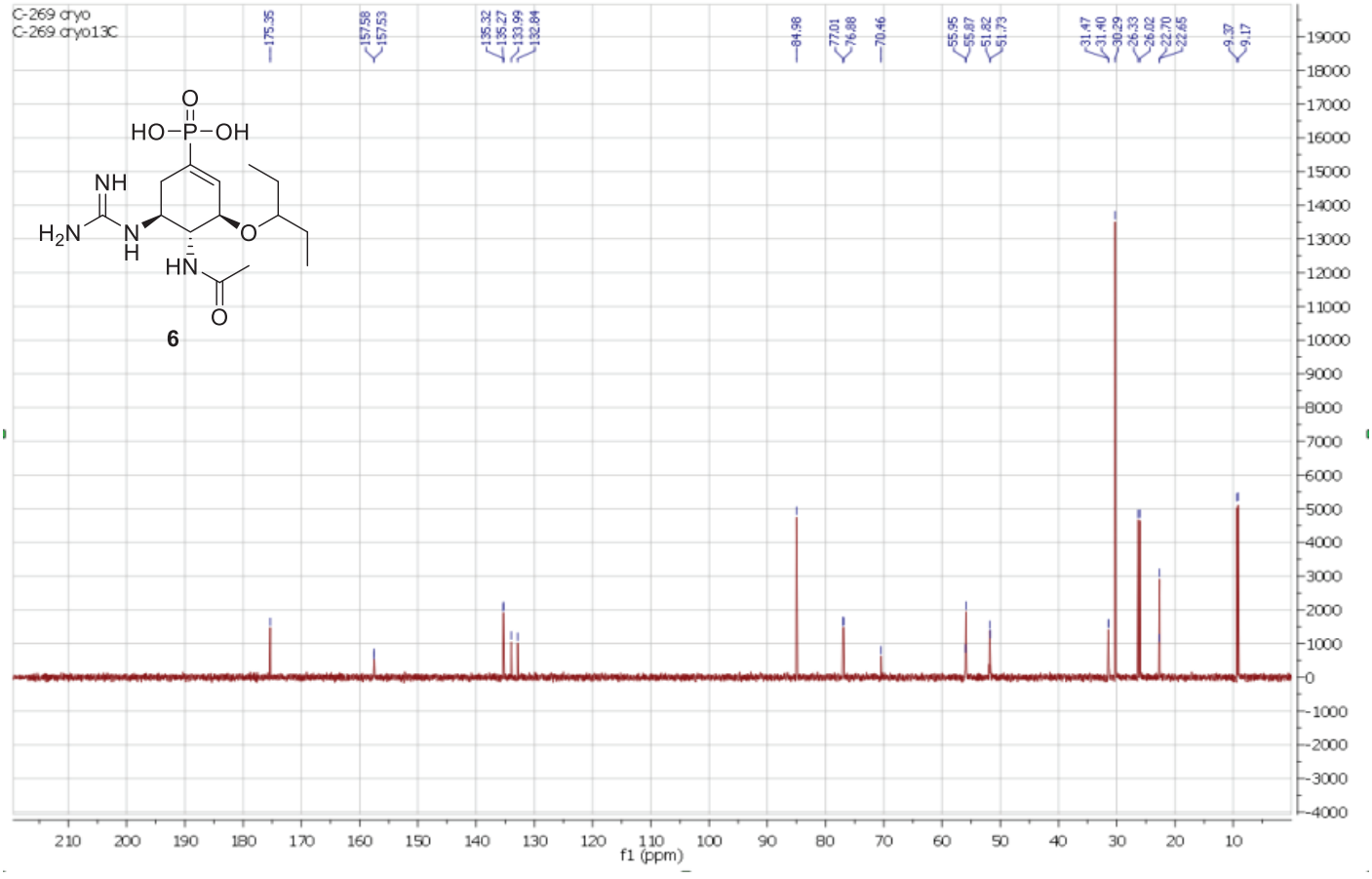
C-269 cryo
C-269 cryo13C
HO–P–OH
NH
H2N
N
H
O
HN
O
6
f1 (ppm)

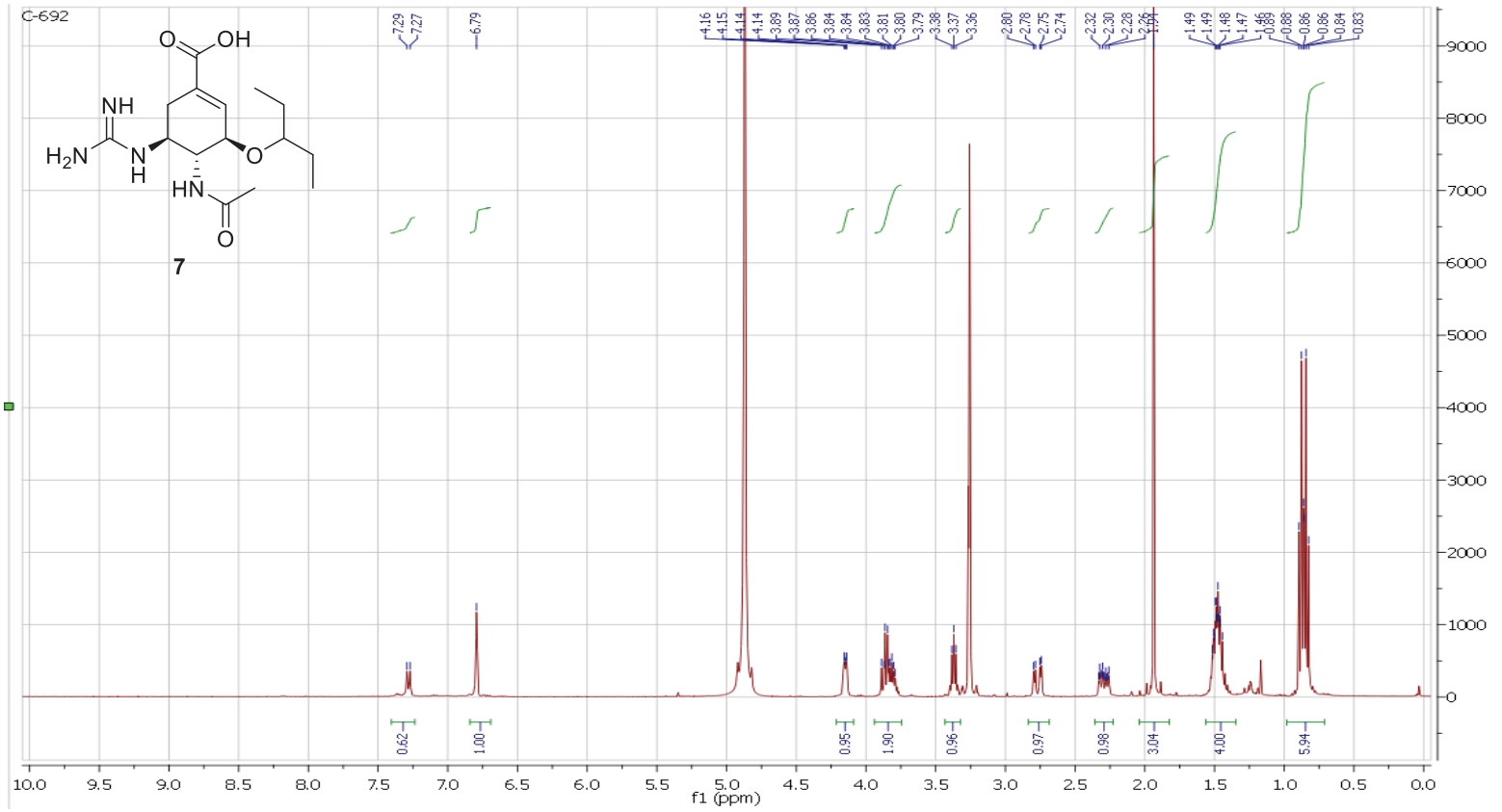
C-692
O
OH
NH
H2N
N
H
O
HN
O
7
7.29
7.27
6.79
4.16
4.15
4.14
4.14
3.89
3.87
3.86
3.84
3.84
3.83
3.81
3.80
3.79
3.38
3.37
3.36
2.80
2.78
2.75
2.74
2.32
2.30
2.28
2.26
1.91
1.49
1.49
1.48
1.47
1.46
0.88
0.88
0.86
0.86
0.84
0.83
0.62
1.00
0.95
1.90
0.96
0.97
0.98
3.04
4.00
5.94
f1 (ppm)

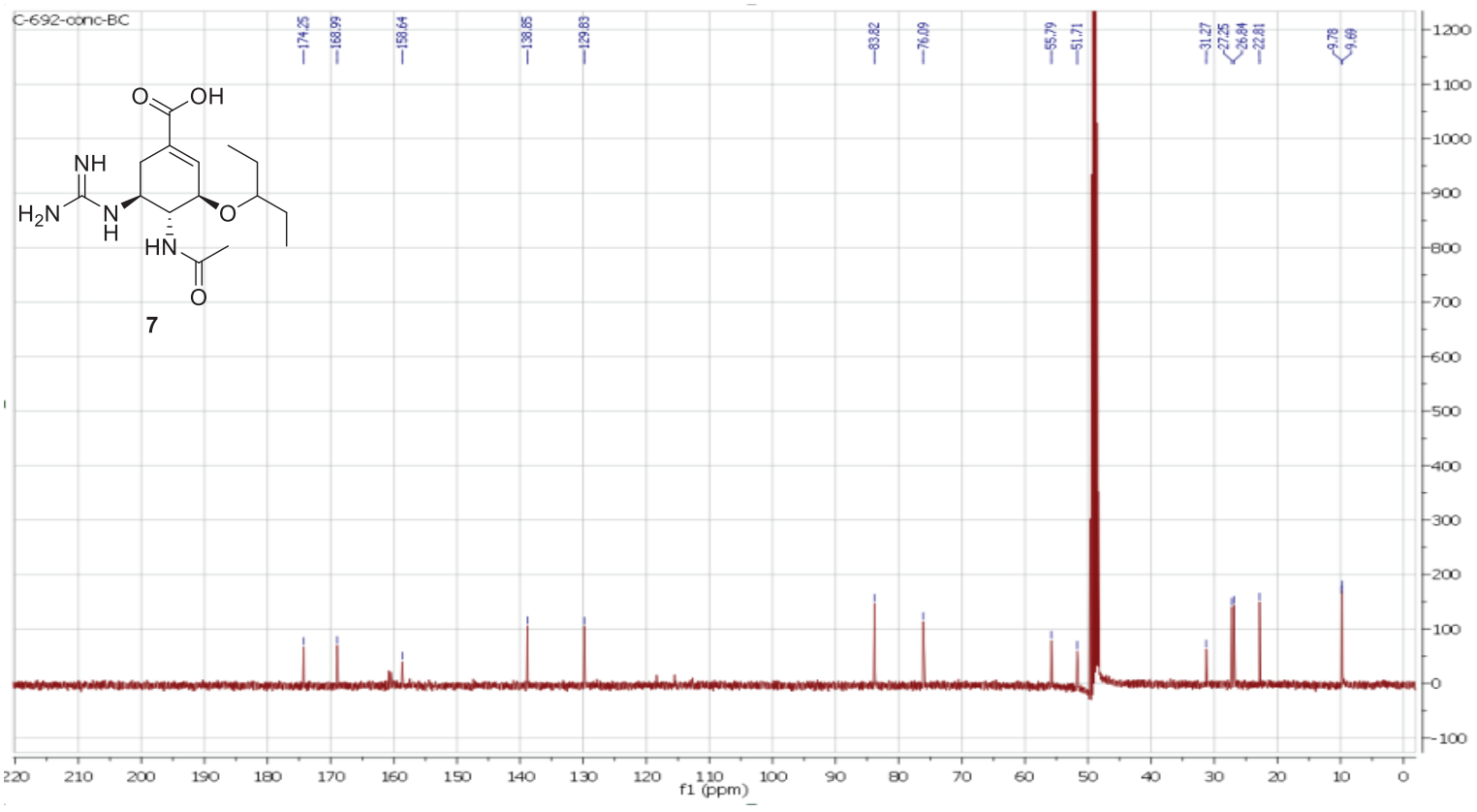
C-692-conc-BC
O
OH
NH
H2N
N
H
O
HN
O
7
174.25
168.99
158.64
138.85
129.83
83.82
76.09
55.79
51.71
31.27
27.25
26.84
22.81
9.78
9.69
f1 (ppm)

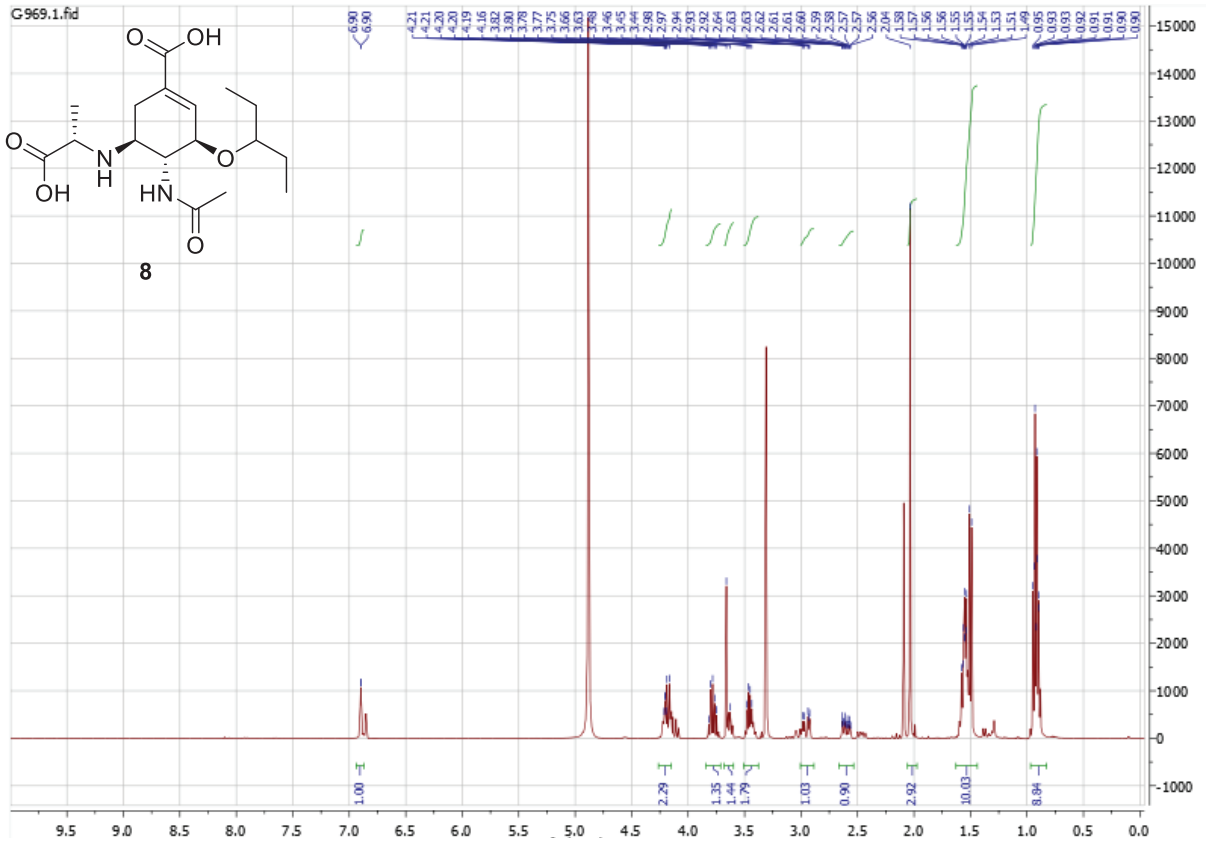
G969.1.fid
8

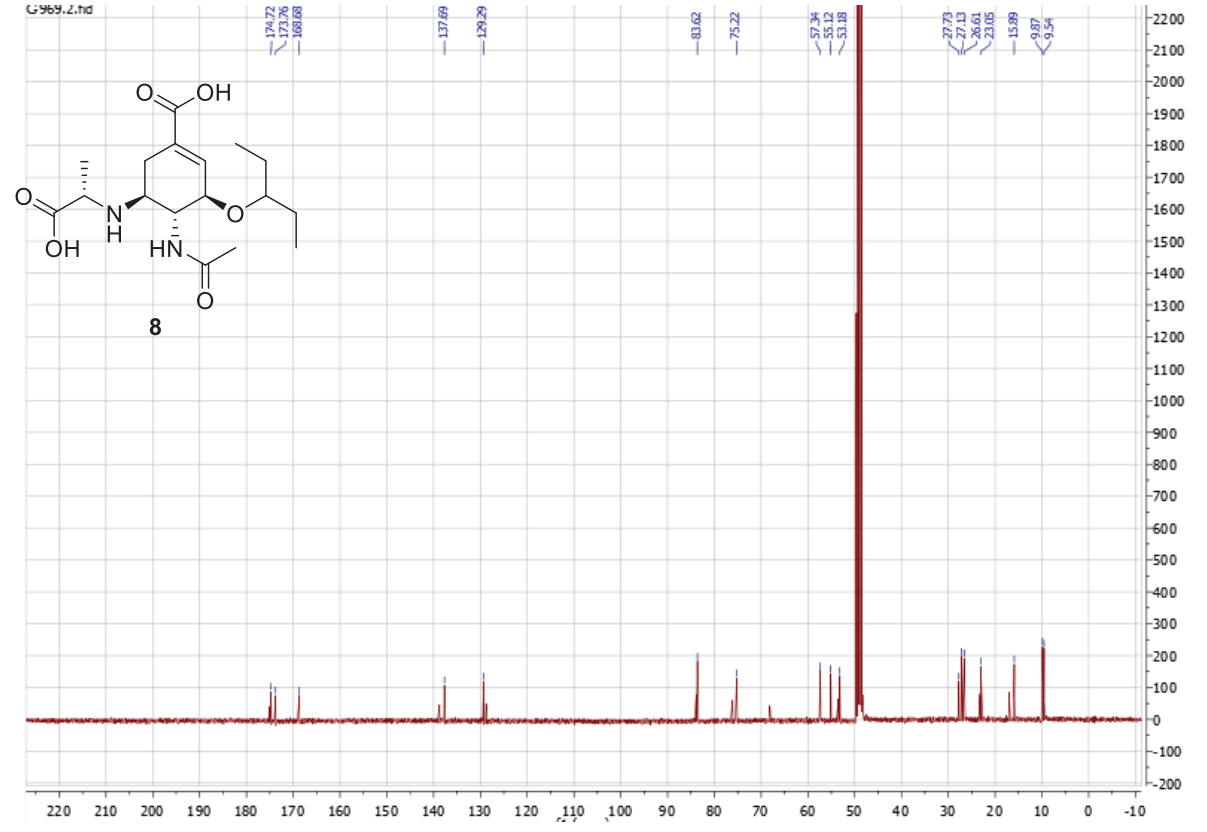
G969.2.fid
8

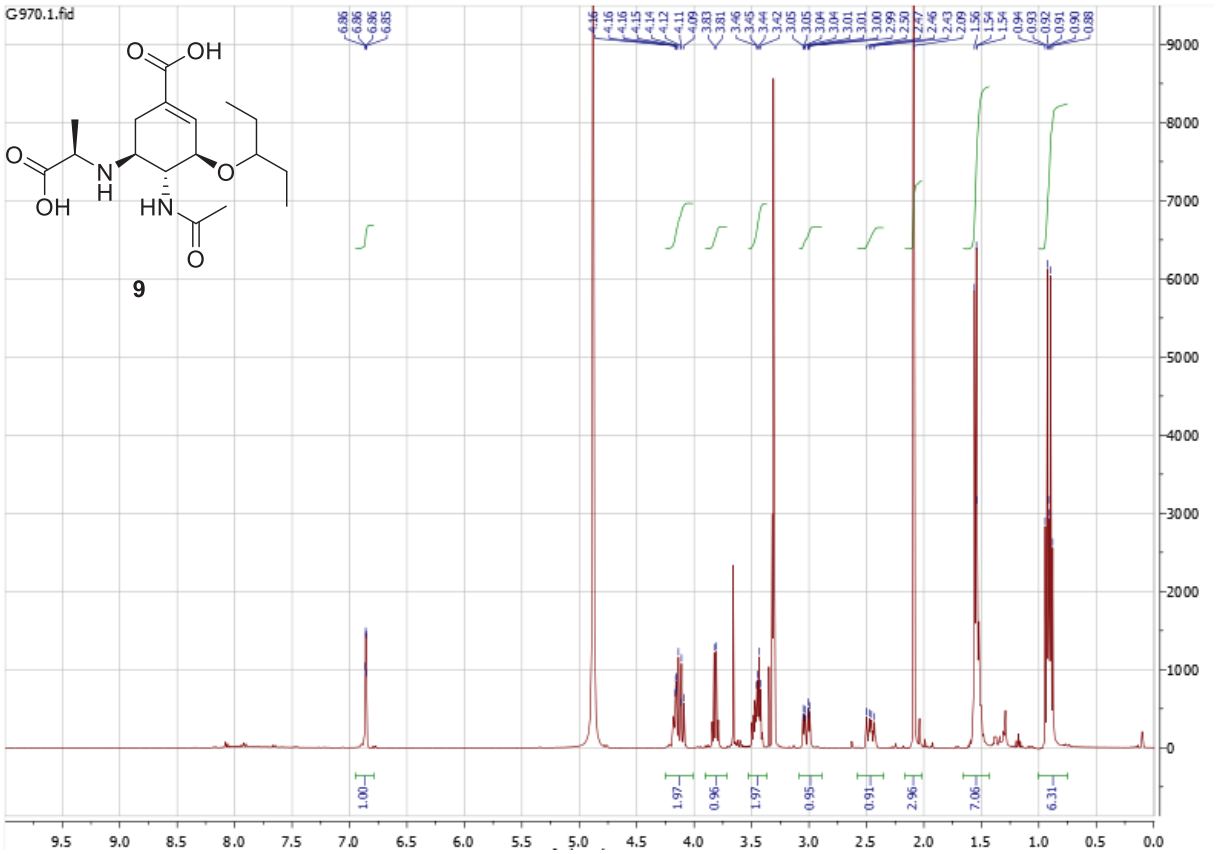
G970.1.fid
9

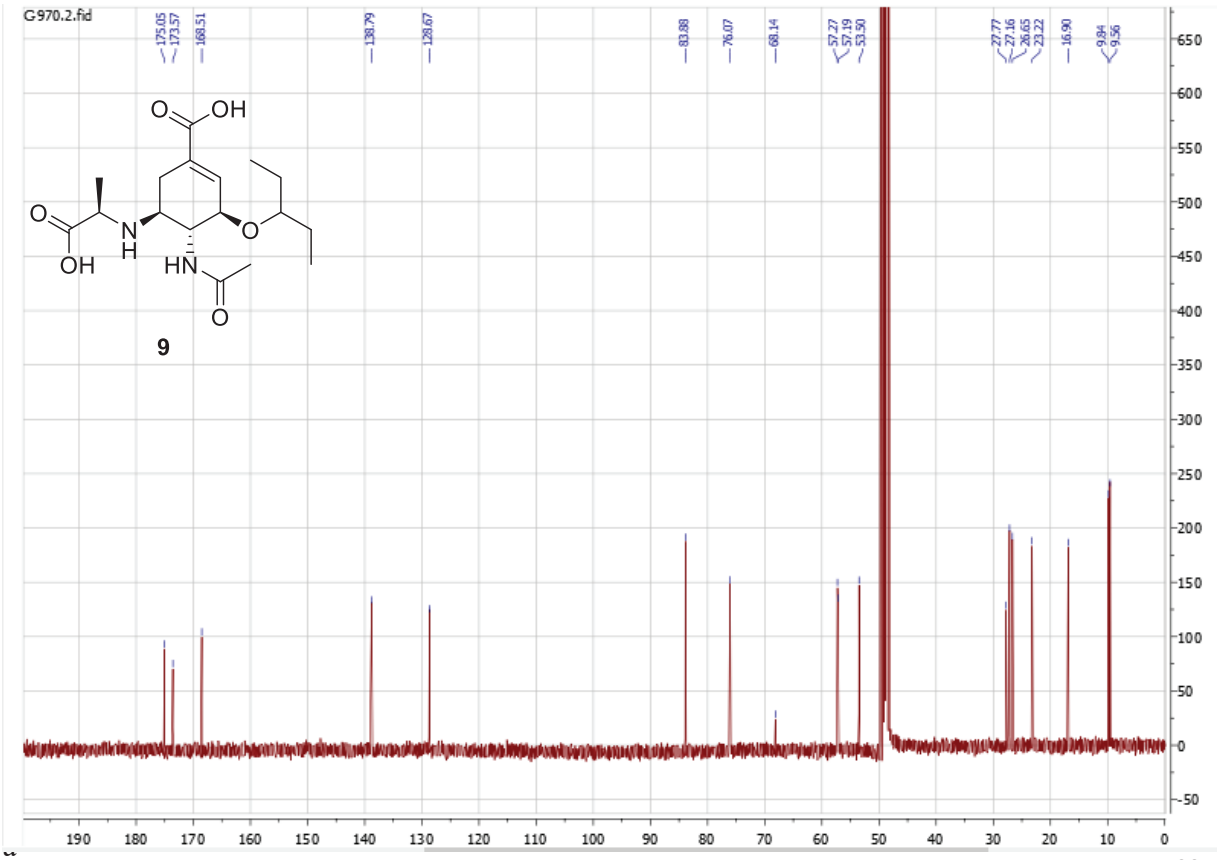
G970.2.fid
9

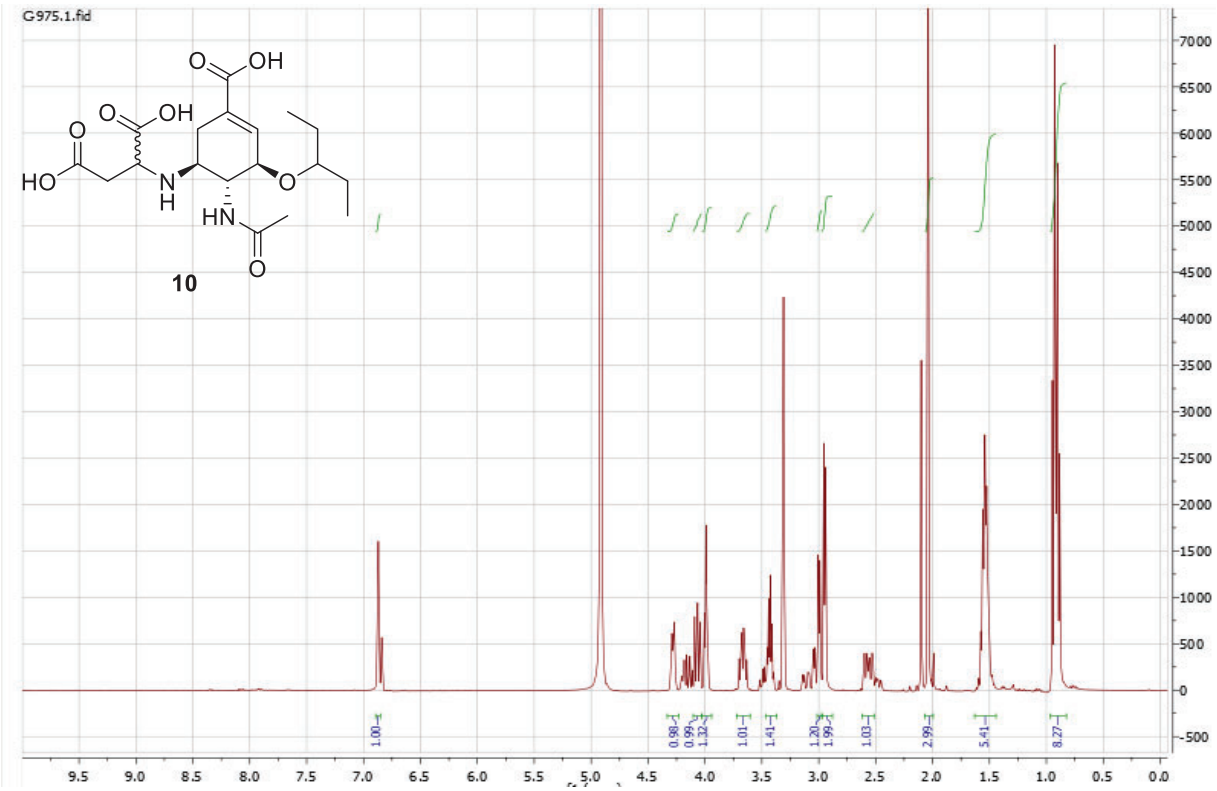
G975.1.fid
10

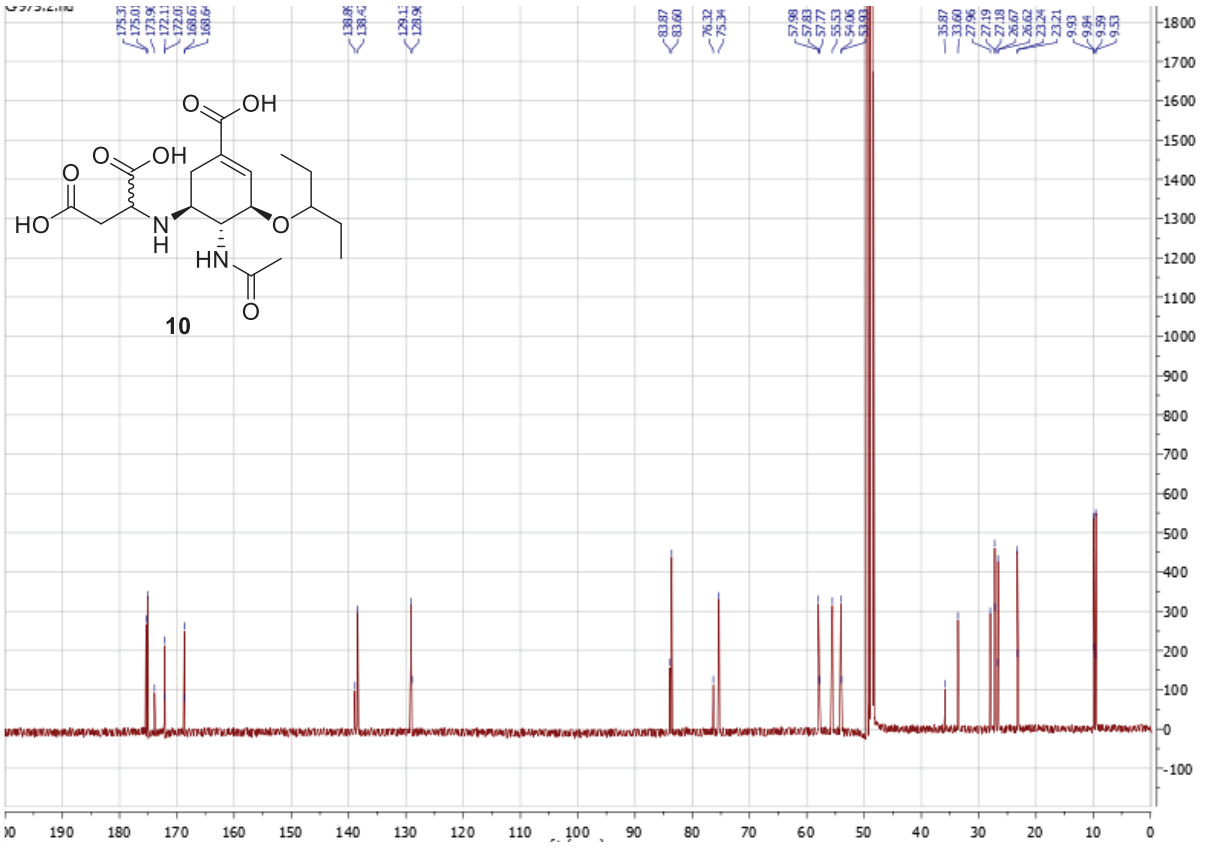
10

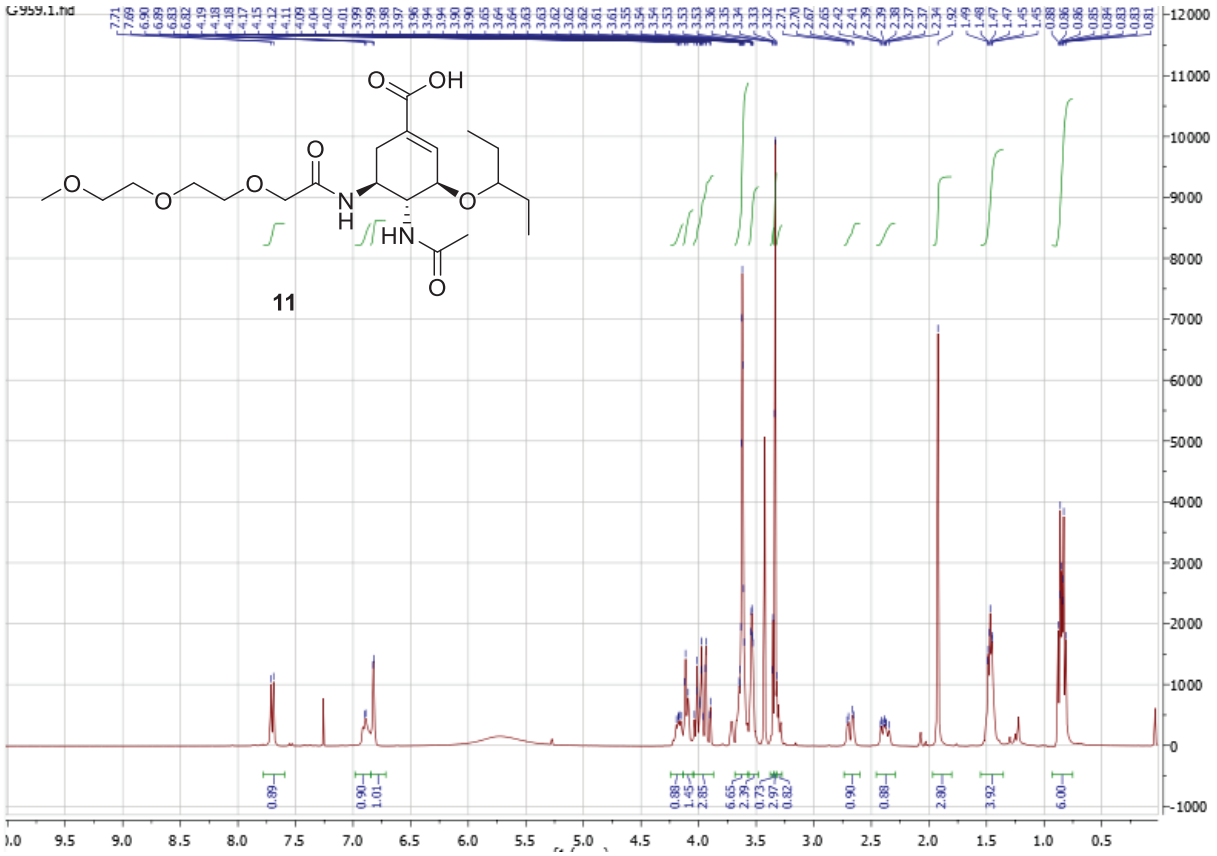

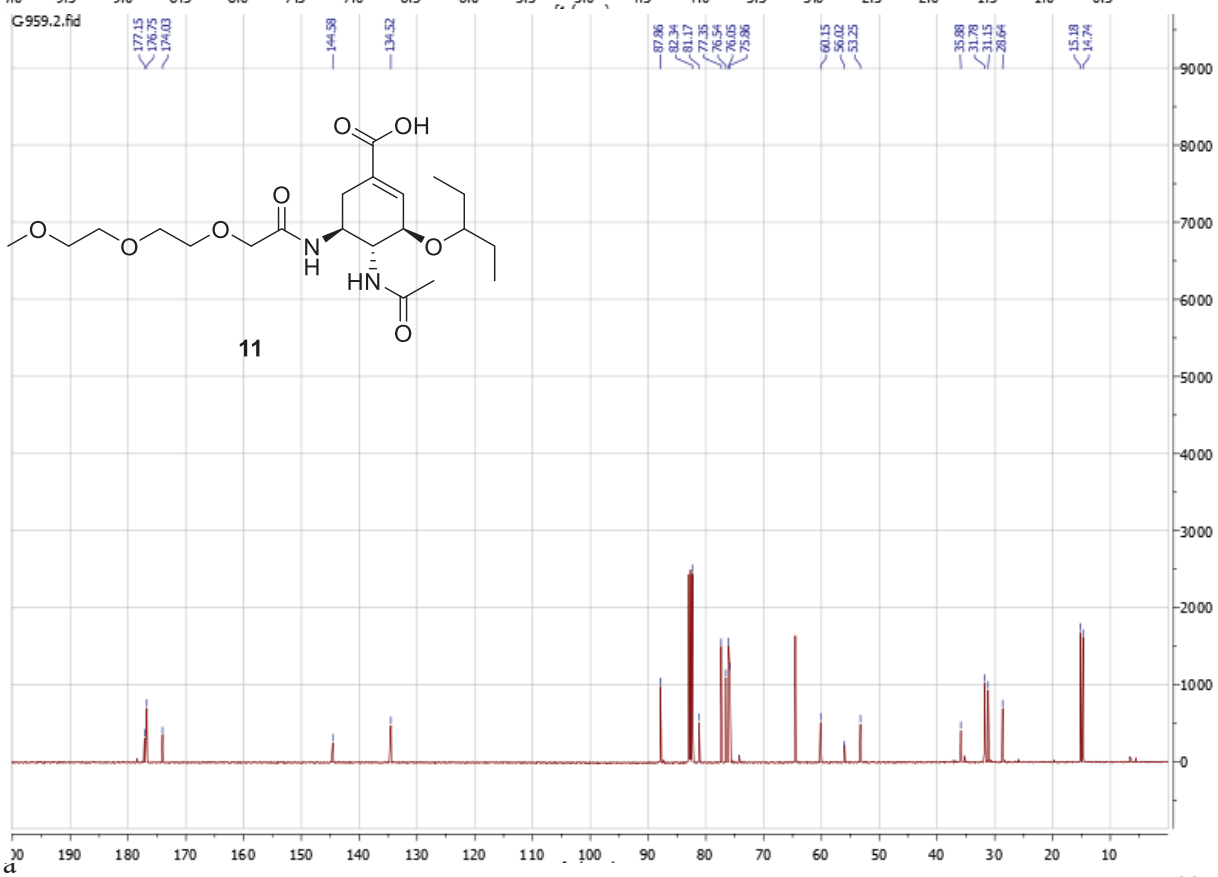

a

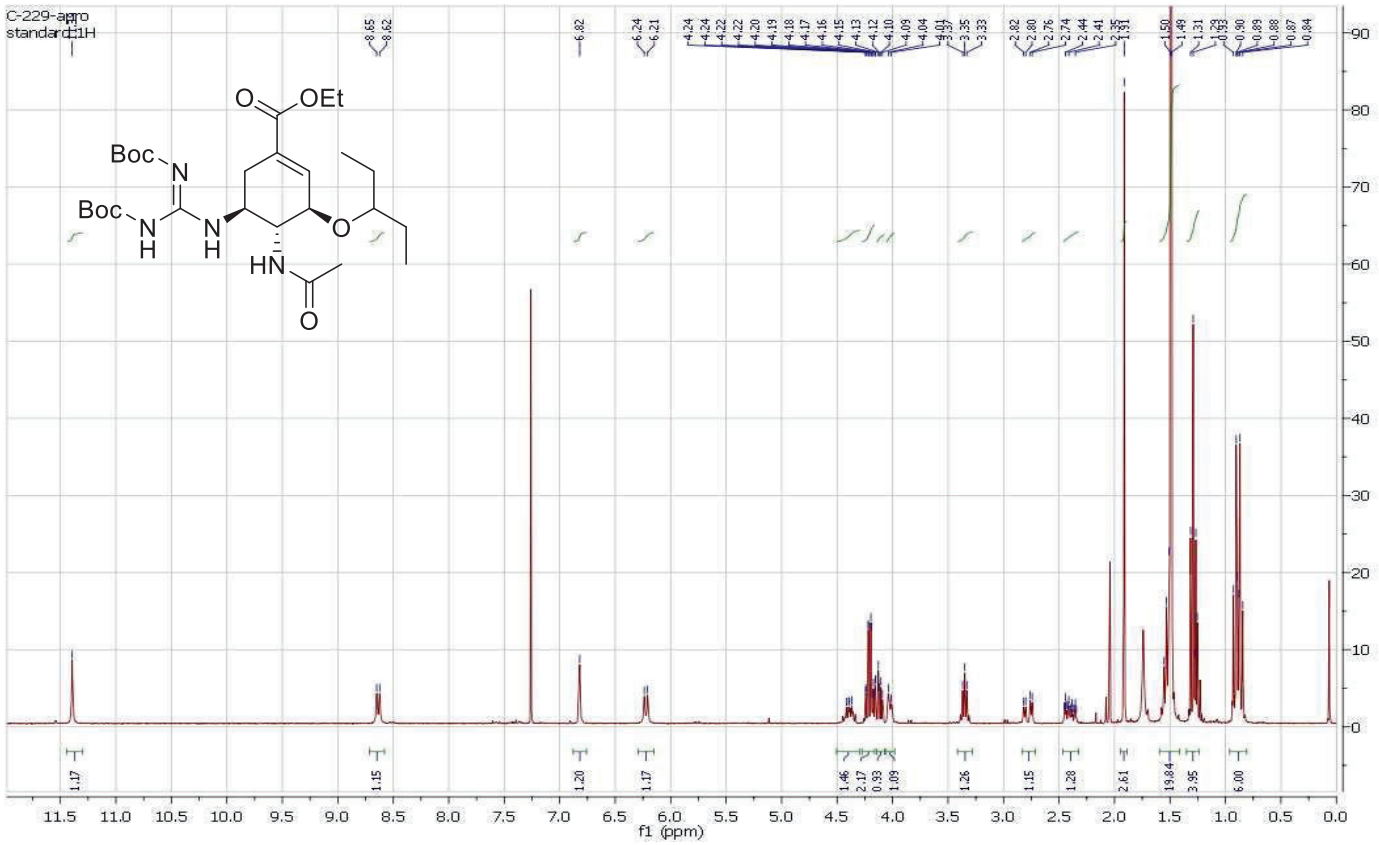
C-229-appro
standard 1H
O
OEt
Boc
N
Boc
N
H
N
H
O
HN
O
f1 (ppm)

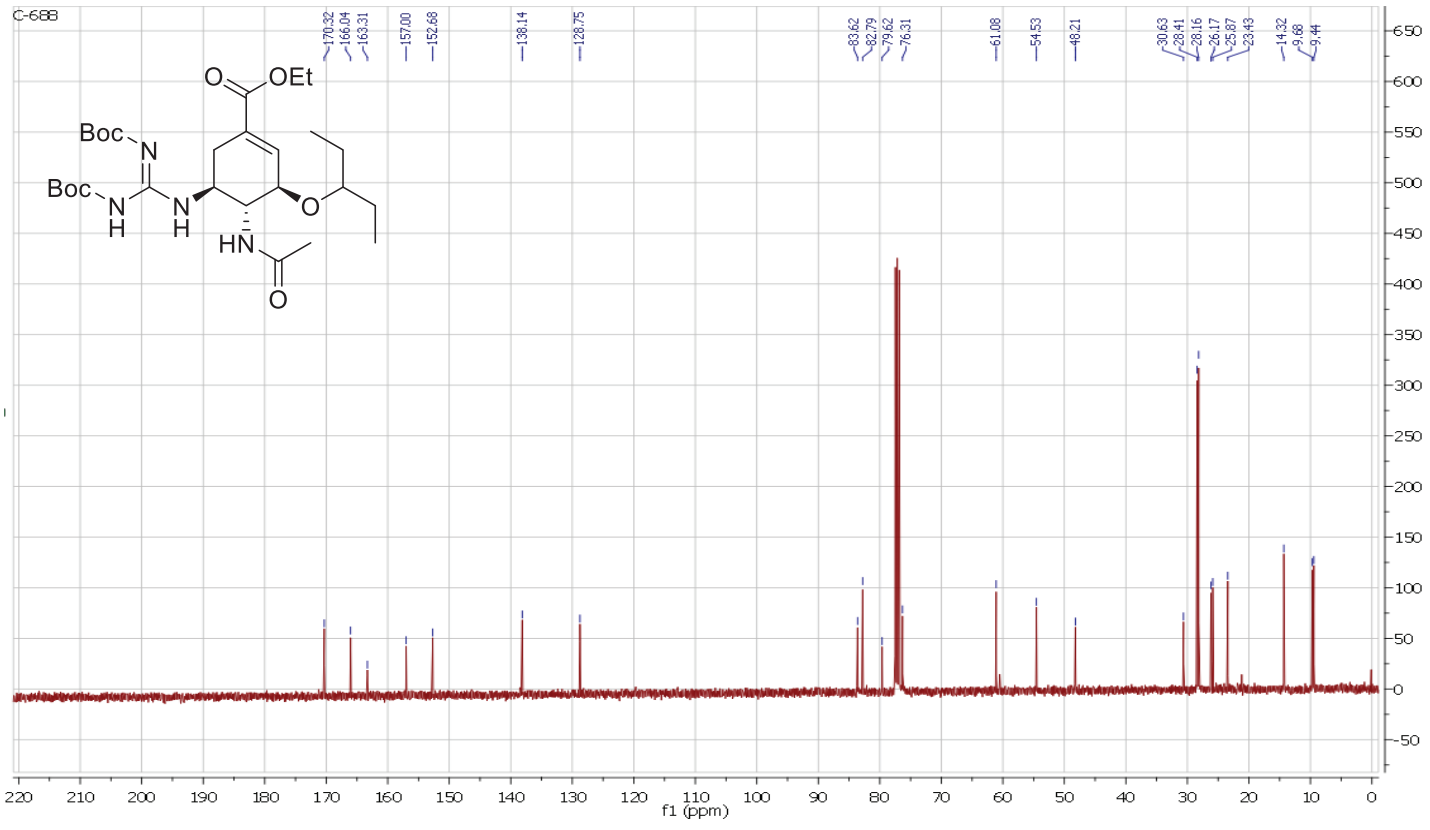
C-688
O
OEt
Boc
N
Boc
N
H
N
H
O
HN
O
f1 (ppm)

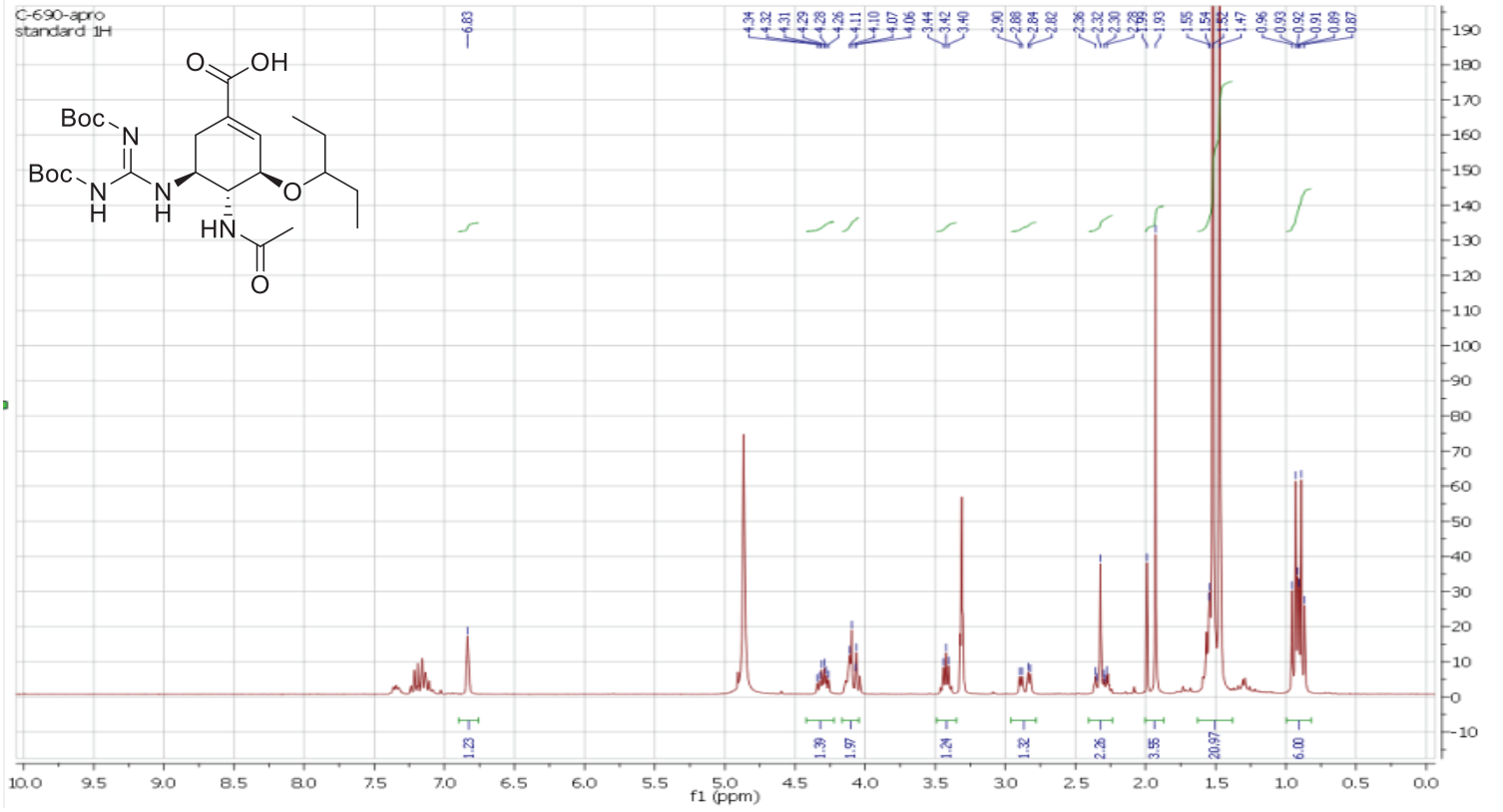
C-690-apro
standard 1H
f1 (ppm)

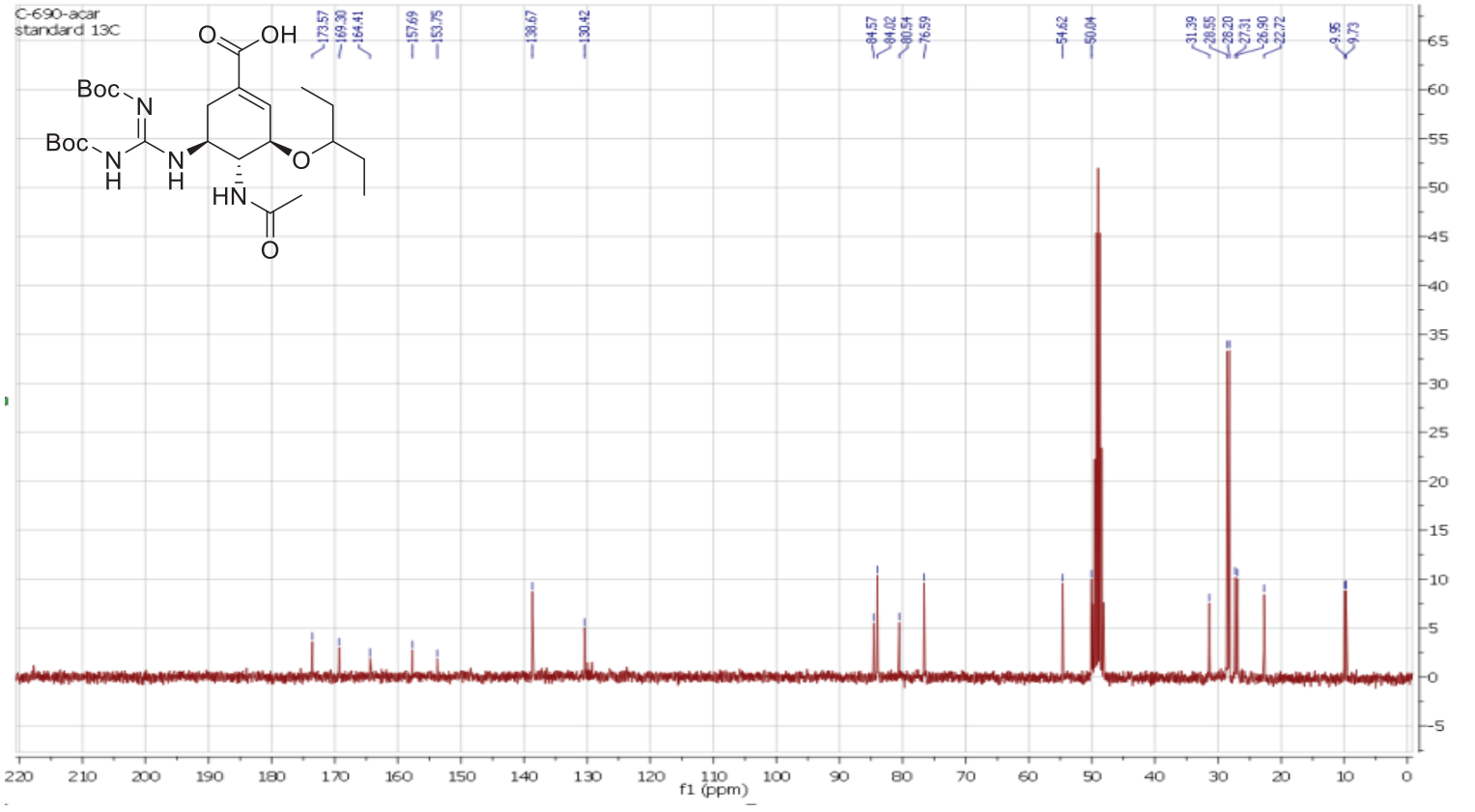
C-690-acar
standard 13C
f1 (ppm)

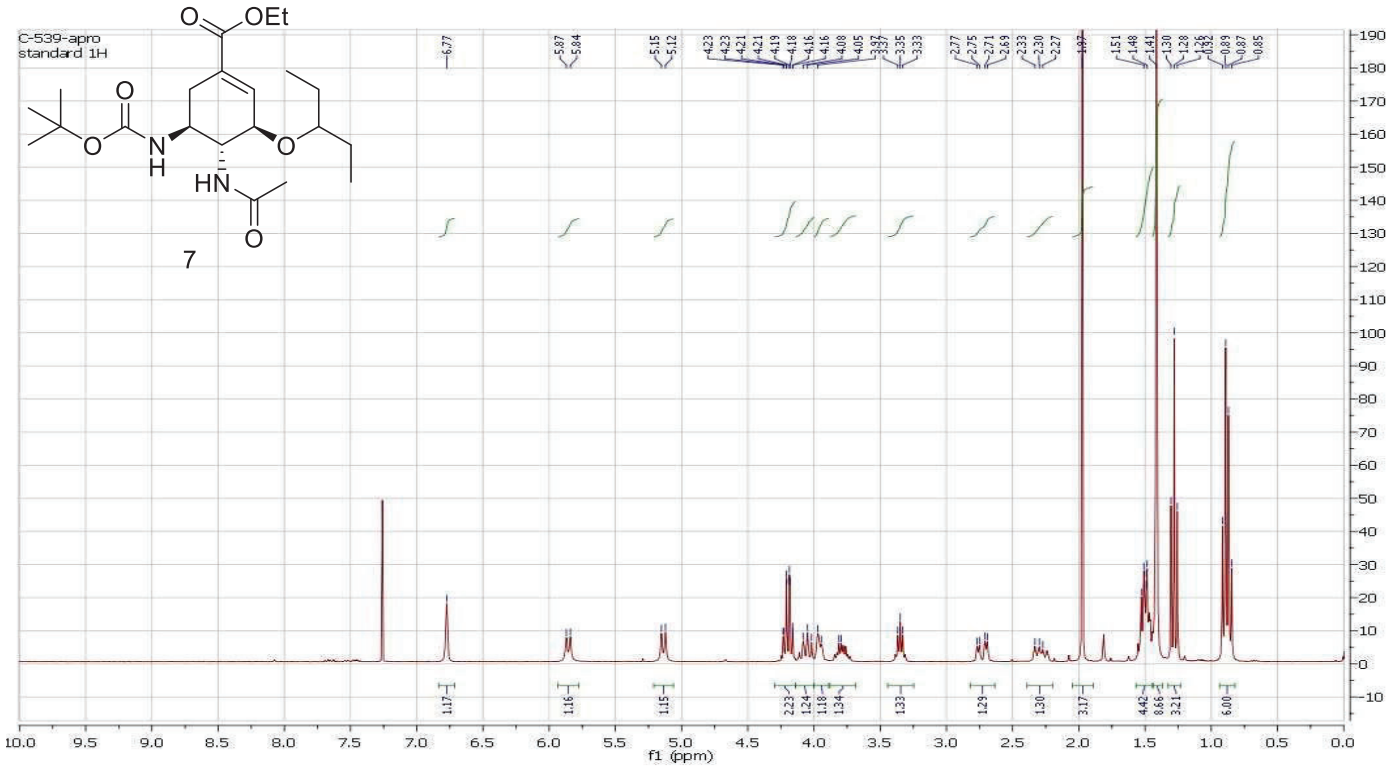
C-539-apro
standard 1H
O
OEt
O
O
N
H
O
HN
O
7
f1 (ppm)

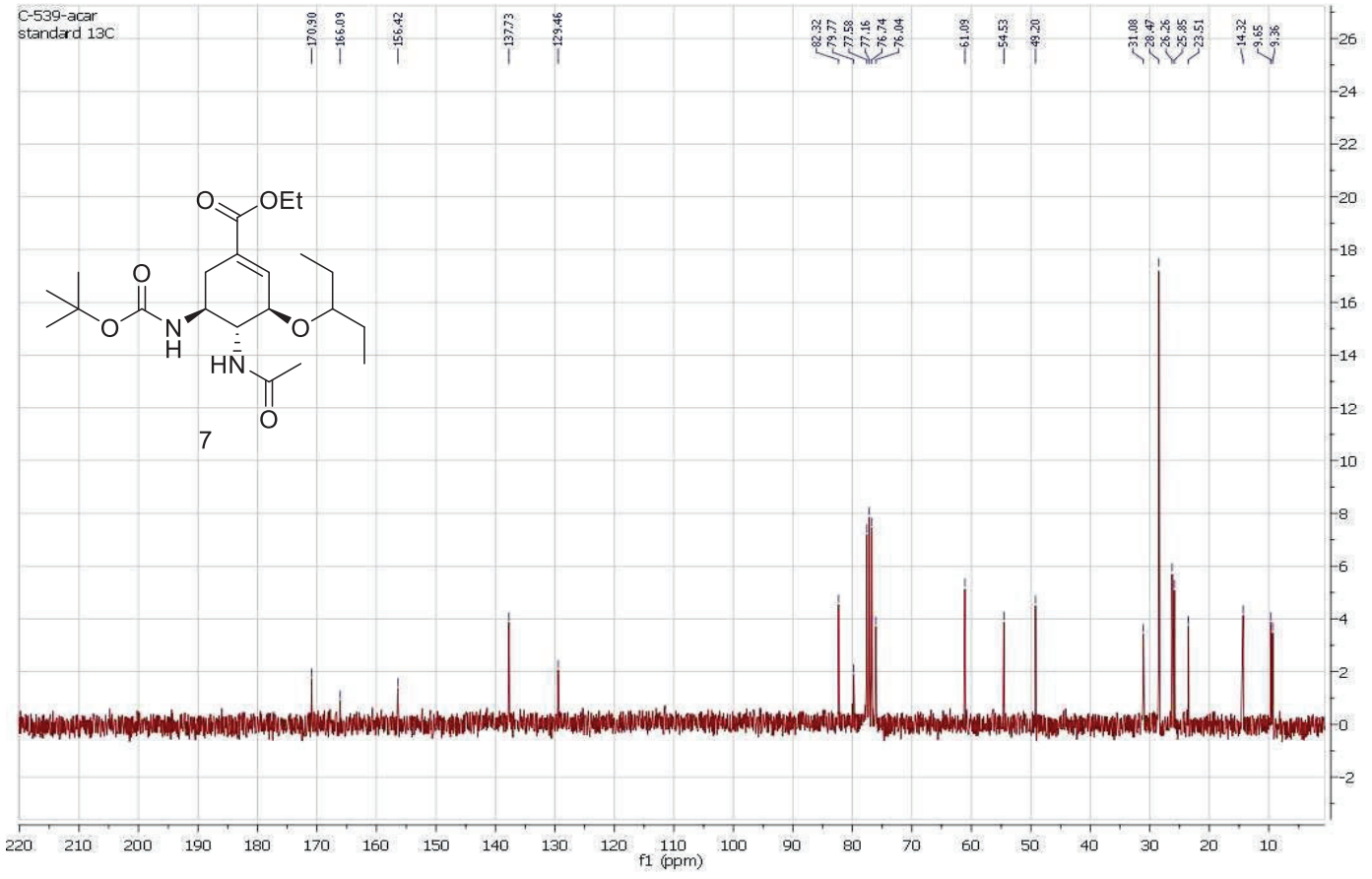
C-539-acar
standard 13C
O
OEt
O
O
N
H
O
HN
O
7
f1 (ppm)

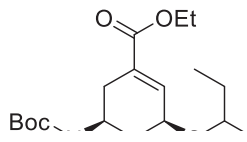
O
OEt
Boc

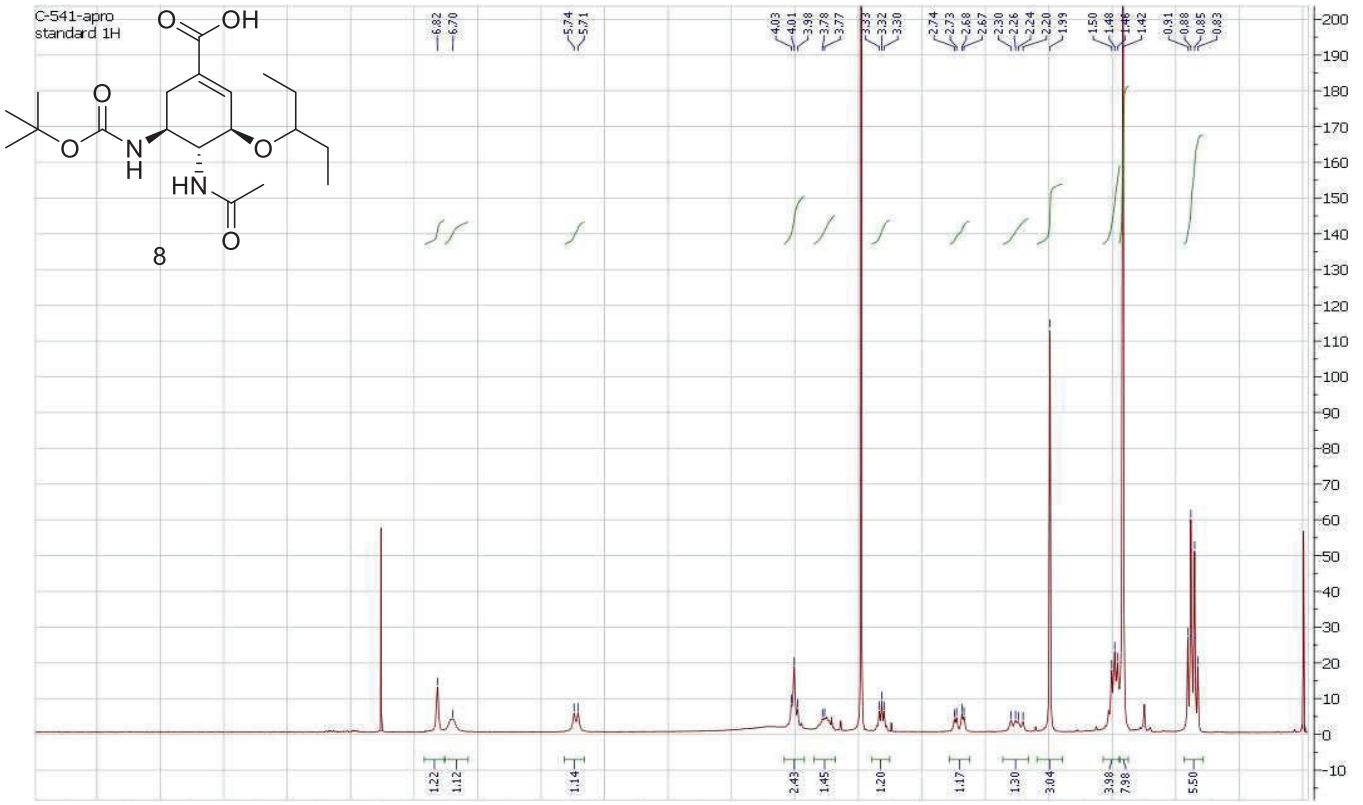
C-541-apro
standard 1H
8

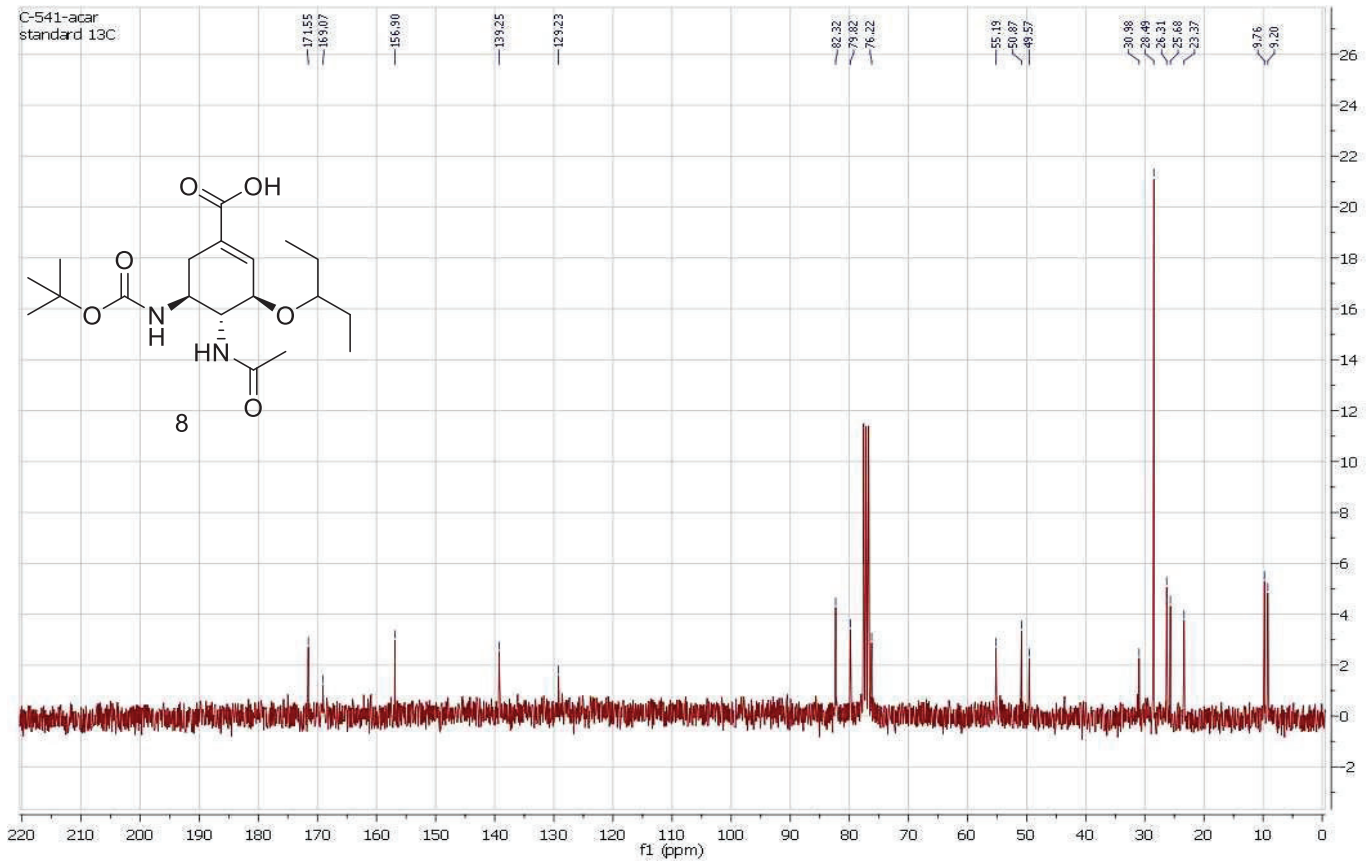
C-541-acar
standard 13C
8
f1 (ppm)

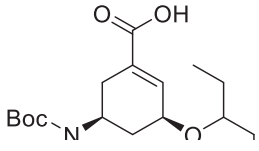
Boc

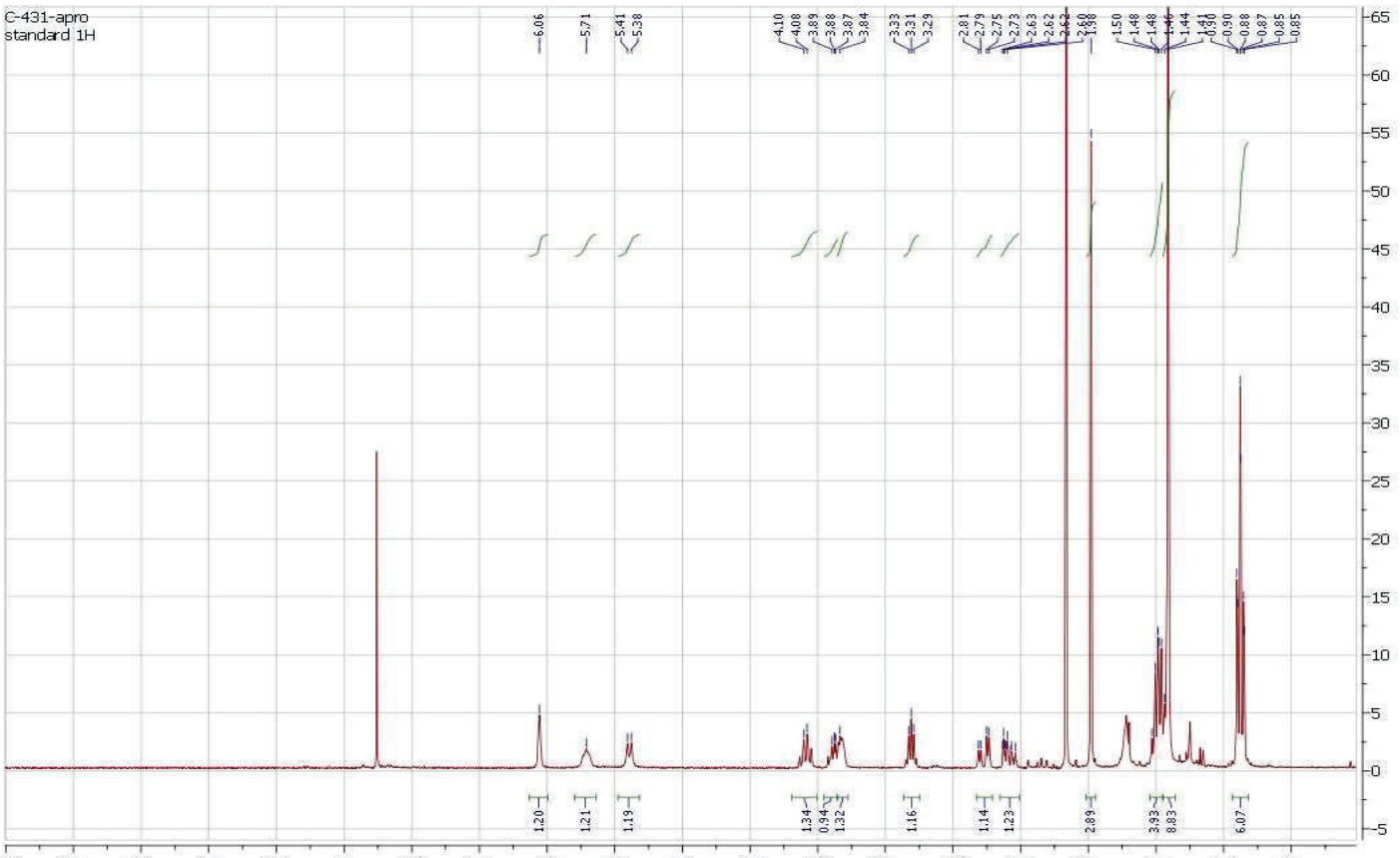
C-431-apro
standard 1H

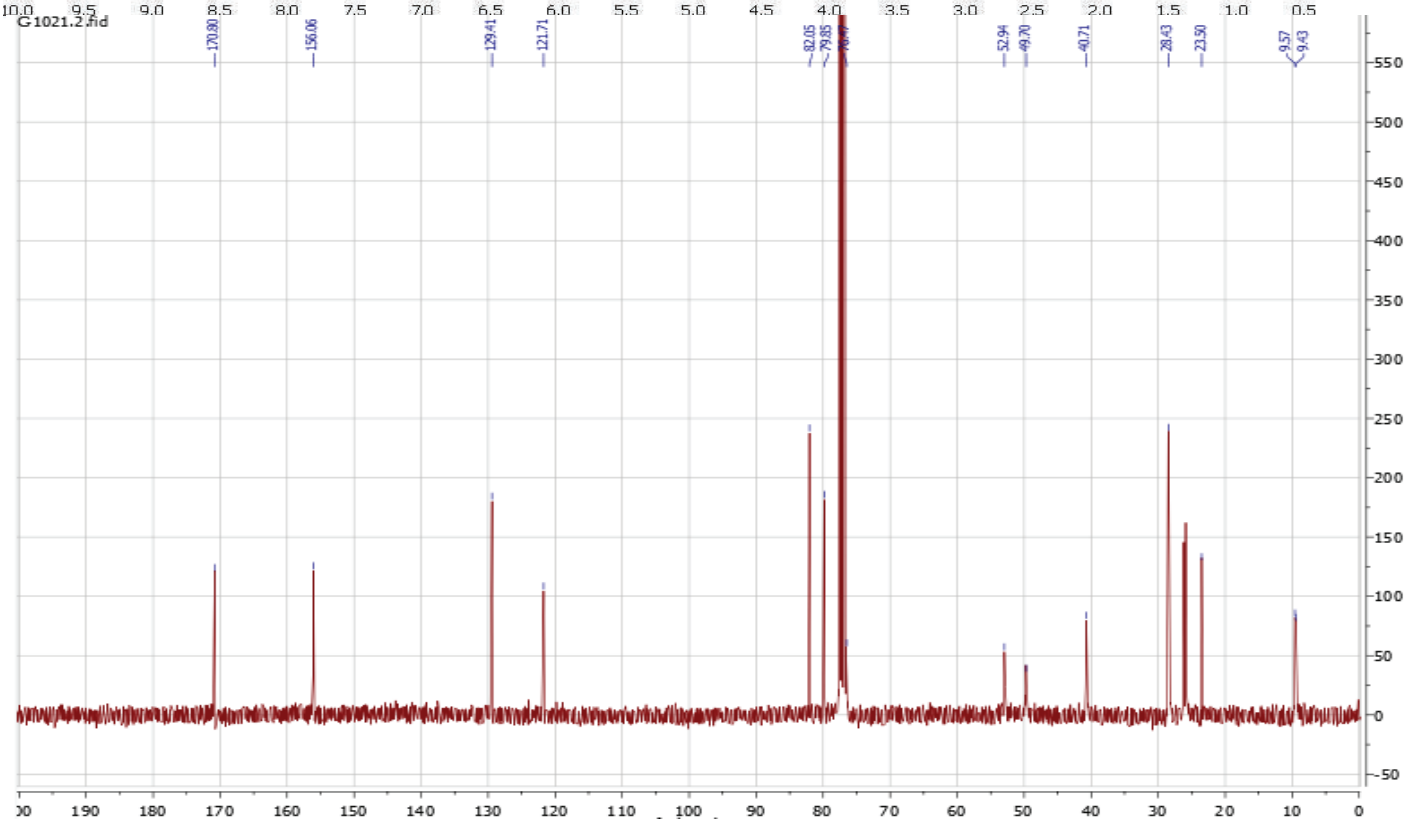
G1021.2.fid

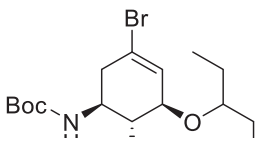
Br
Boc
N
O

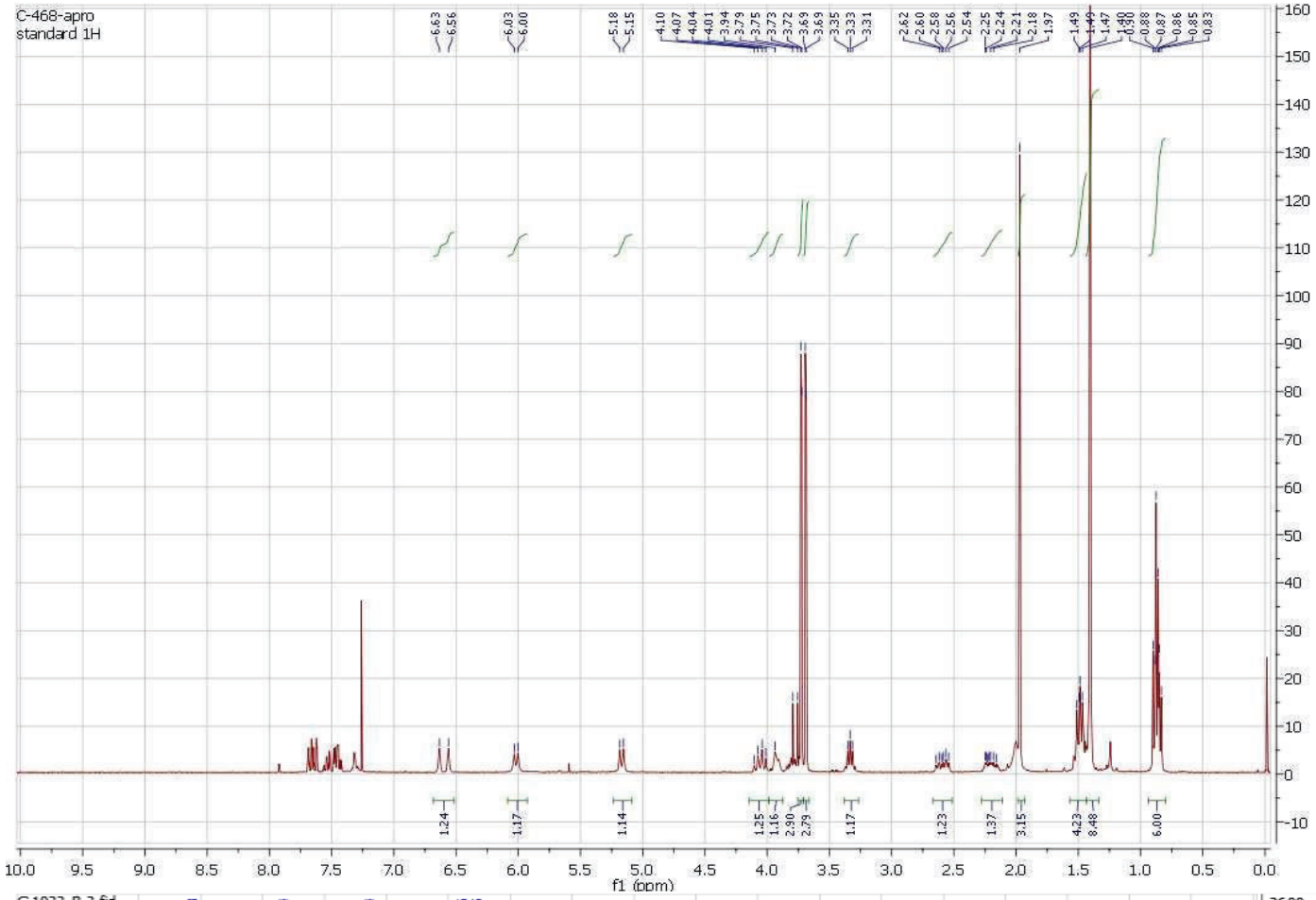
C-468-apro
standard 1H
f1 (ppm)

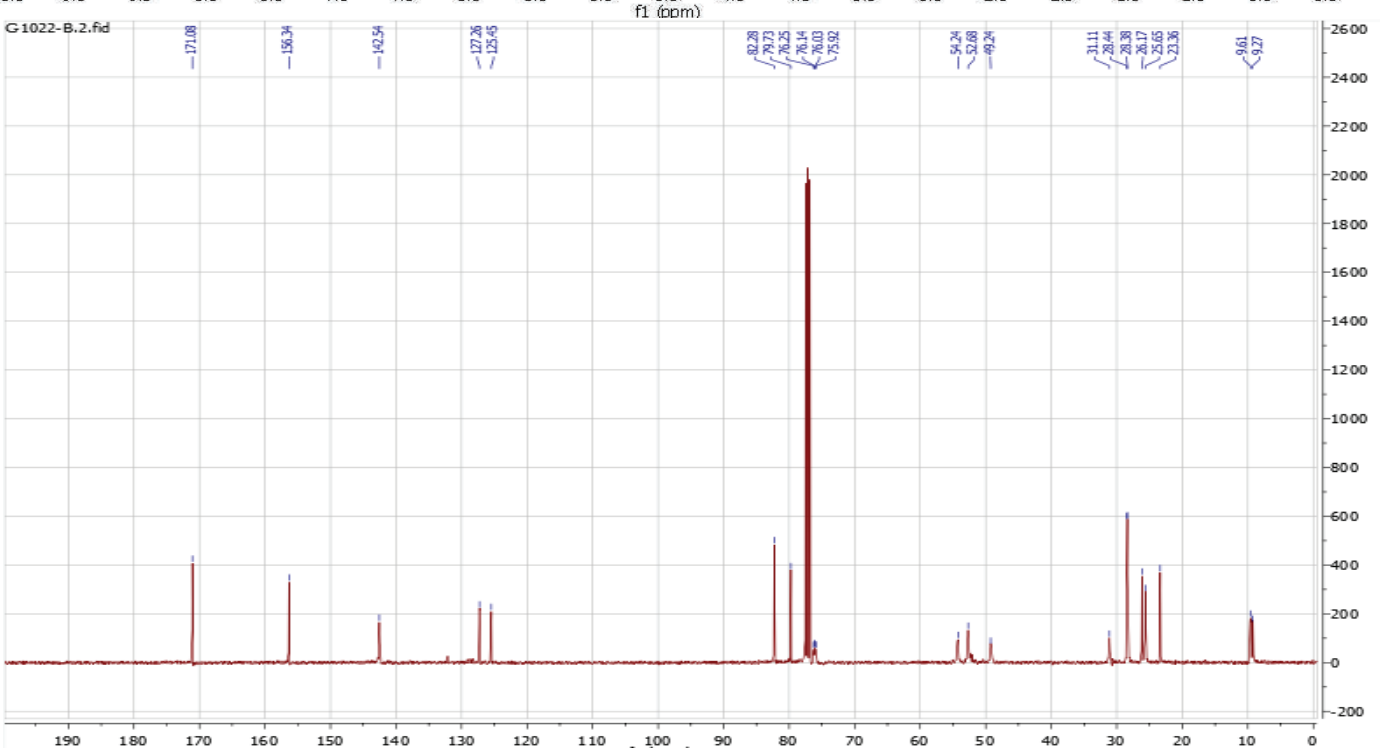
G1022-B.2.fid

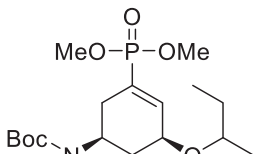
O
MeO
P
OMe
Boc

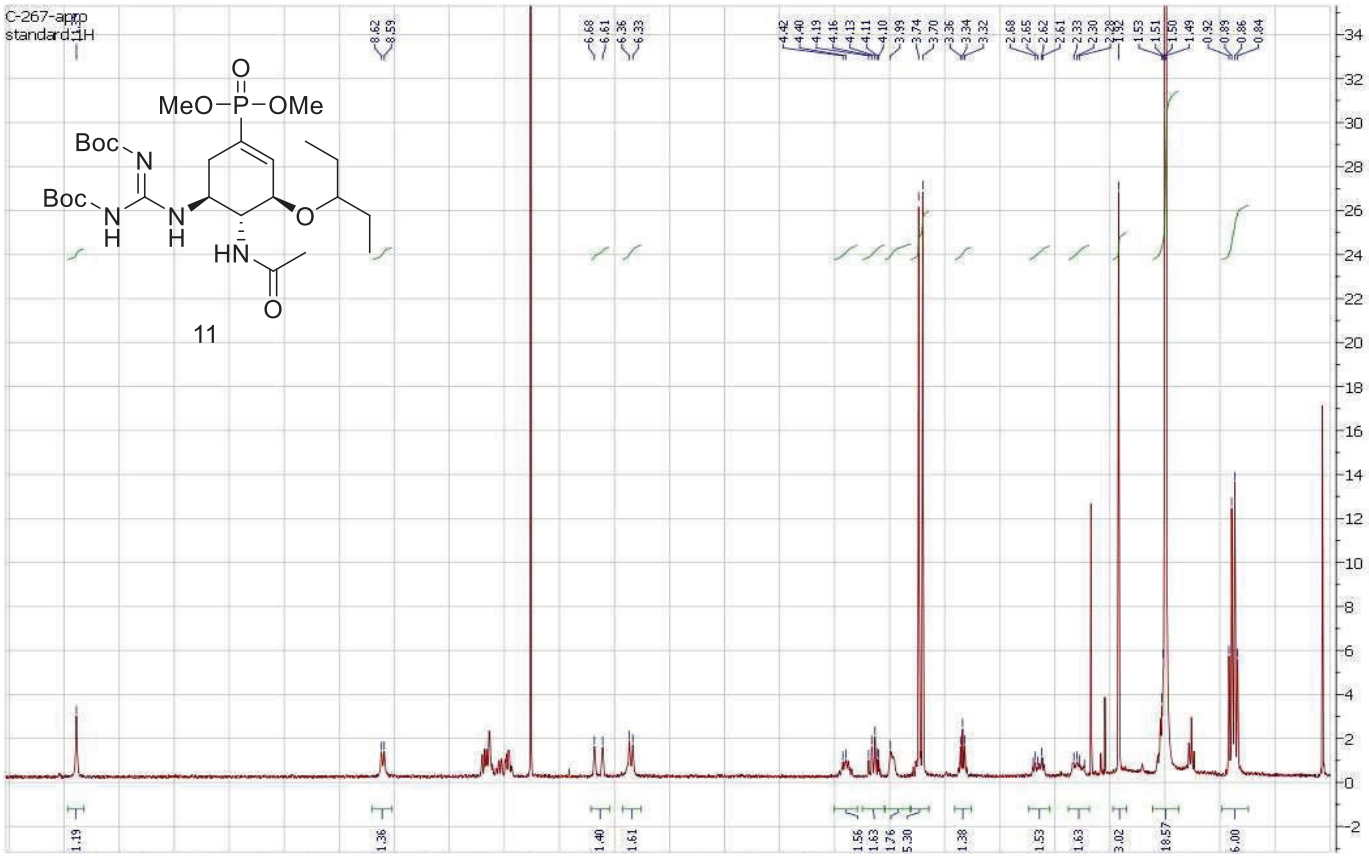
C-267-app
standard 1H
MeO–P–OMe
Boc
N
Boc
N
H
N
H
O
HN
O
11

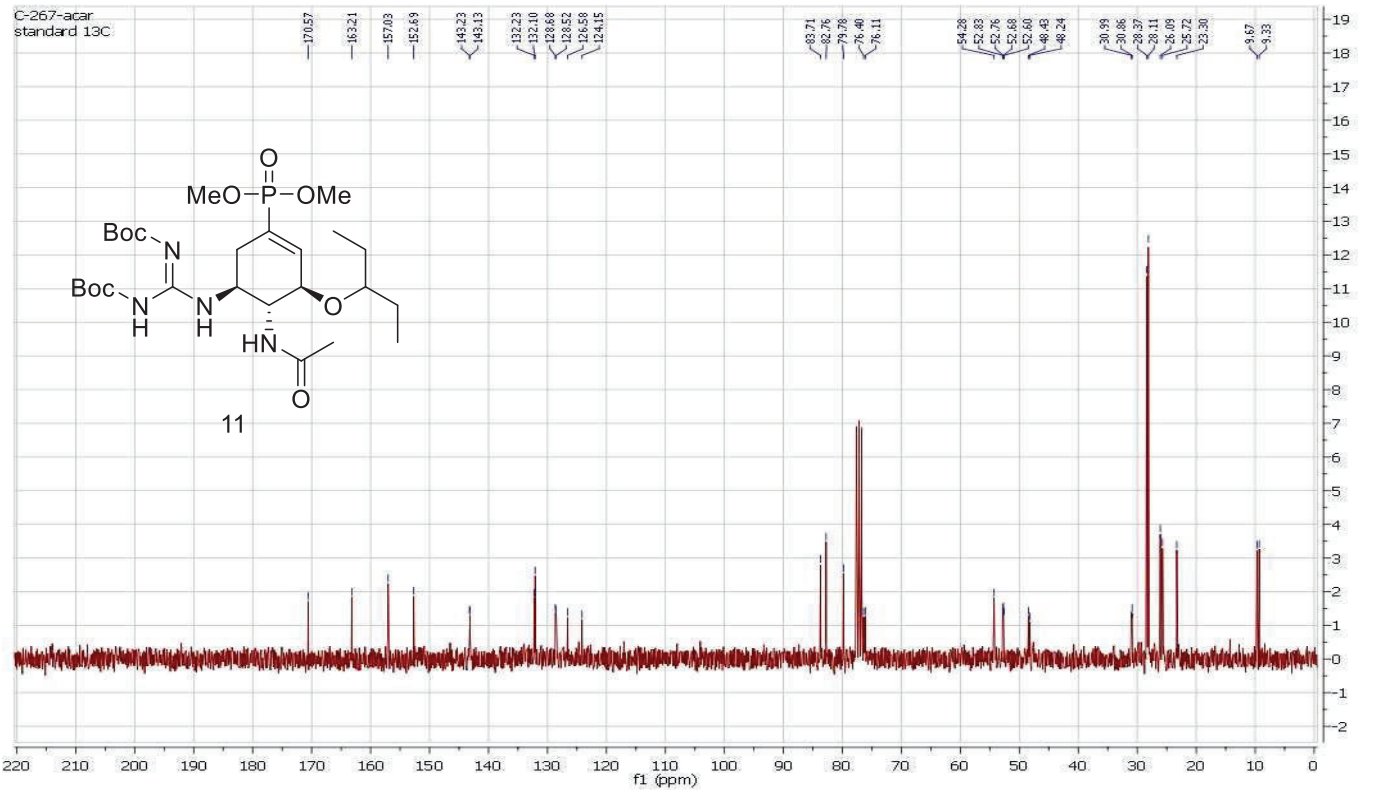
C-267-acar
standard 13C
MeO–P–OMe
Boc
N
Boc
N
H
N
H
O
HN
O
11
f1 (ppm)

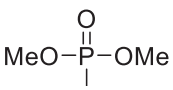
MeO–P–OMe

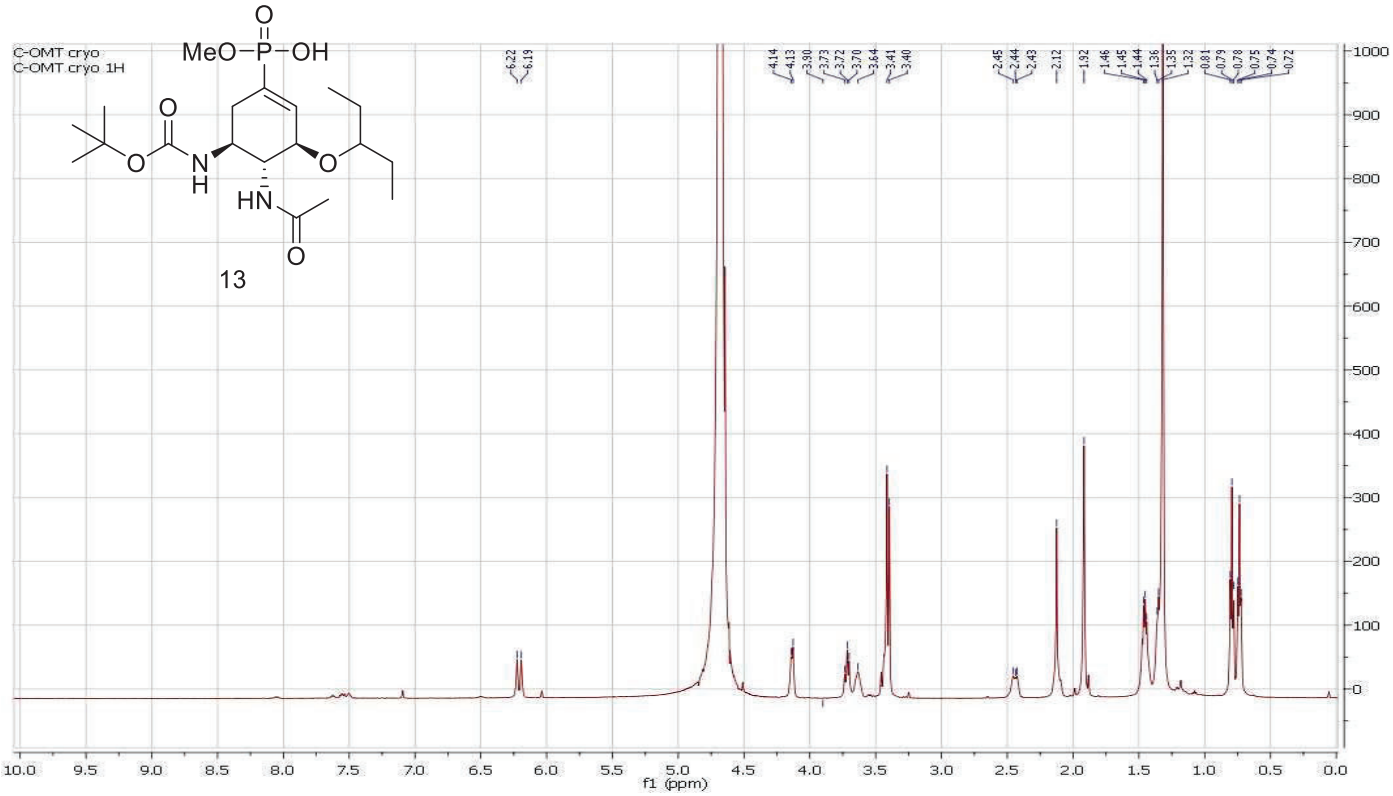
C-OMT cryo
C-OMT cryo 1H
MeO–P–OH
O
O
N
H
HN
O
O
O
13
f1 (ppm)

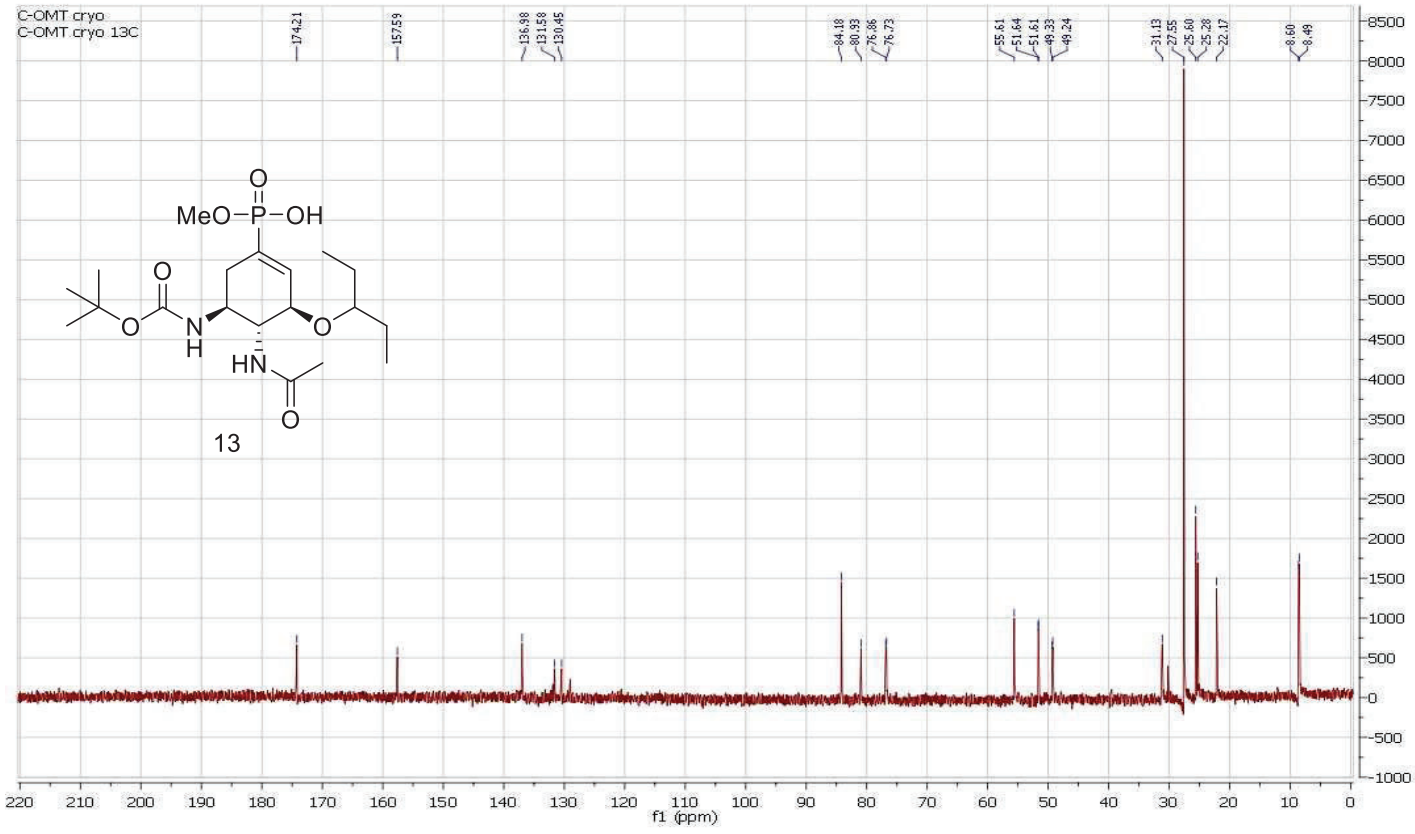
C-OMT cryo
C-OMT cryo 13C
MeO–P–OH
O
O
N
H
HN
O
O
O
13
f1 (ppm)

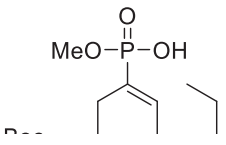
MeO–P–OH
O

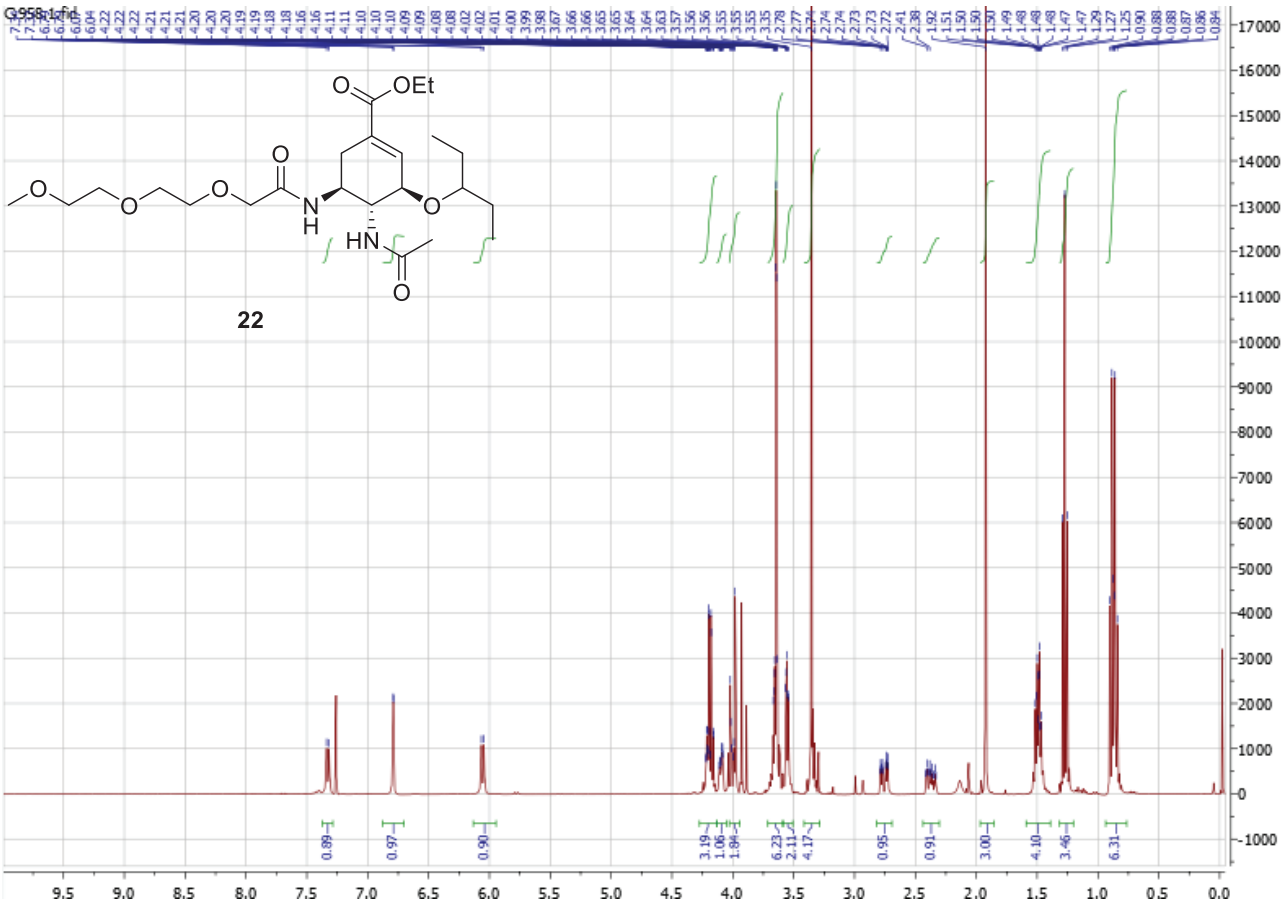
G958.1.fid
22

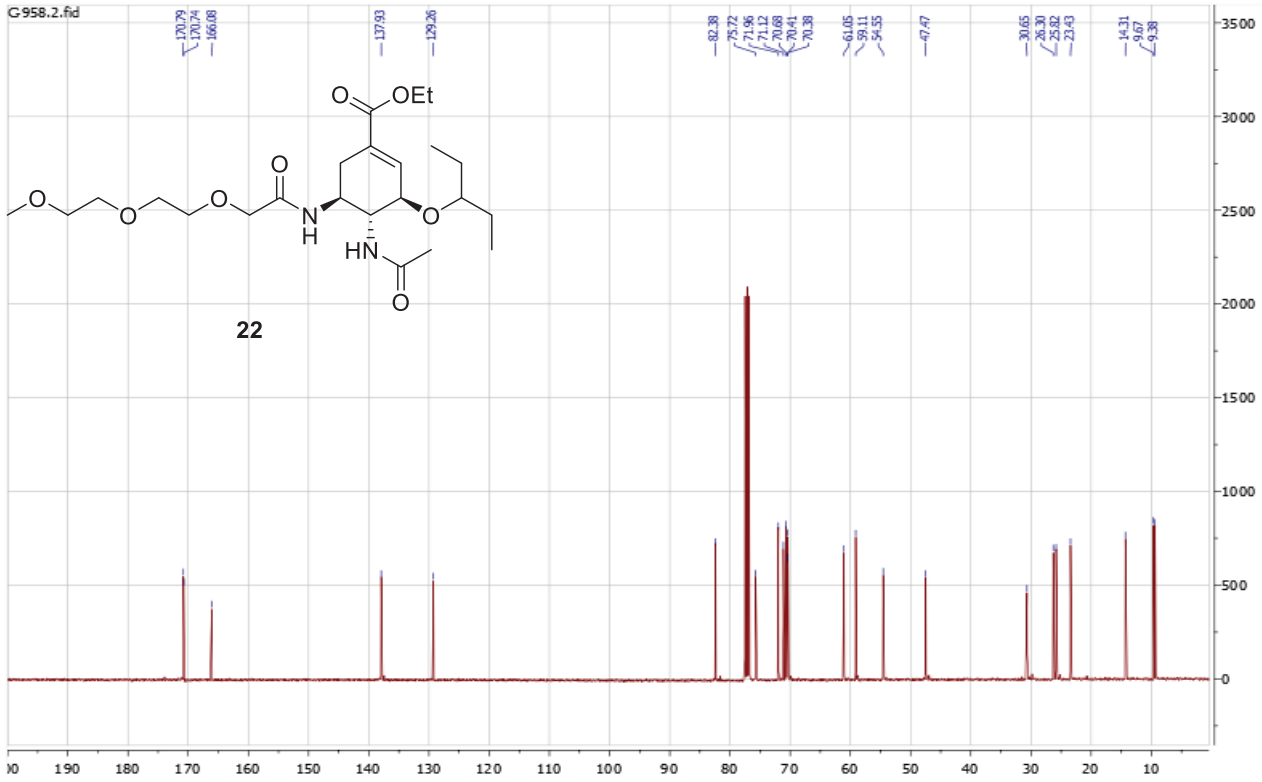
G958.2.fid
22

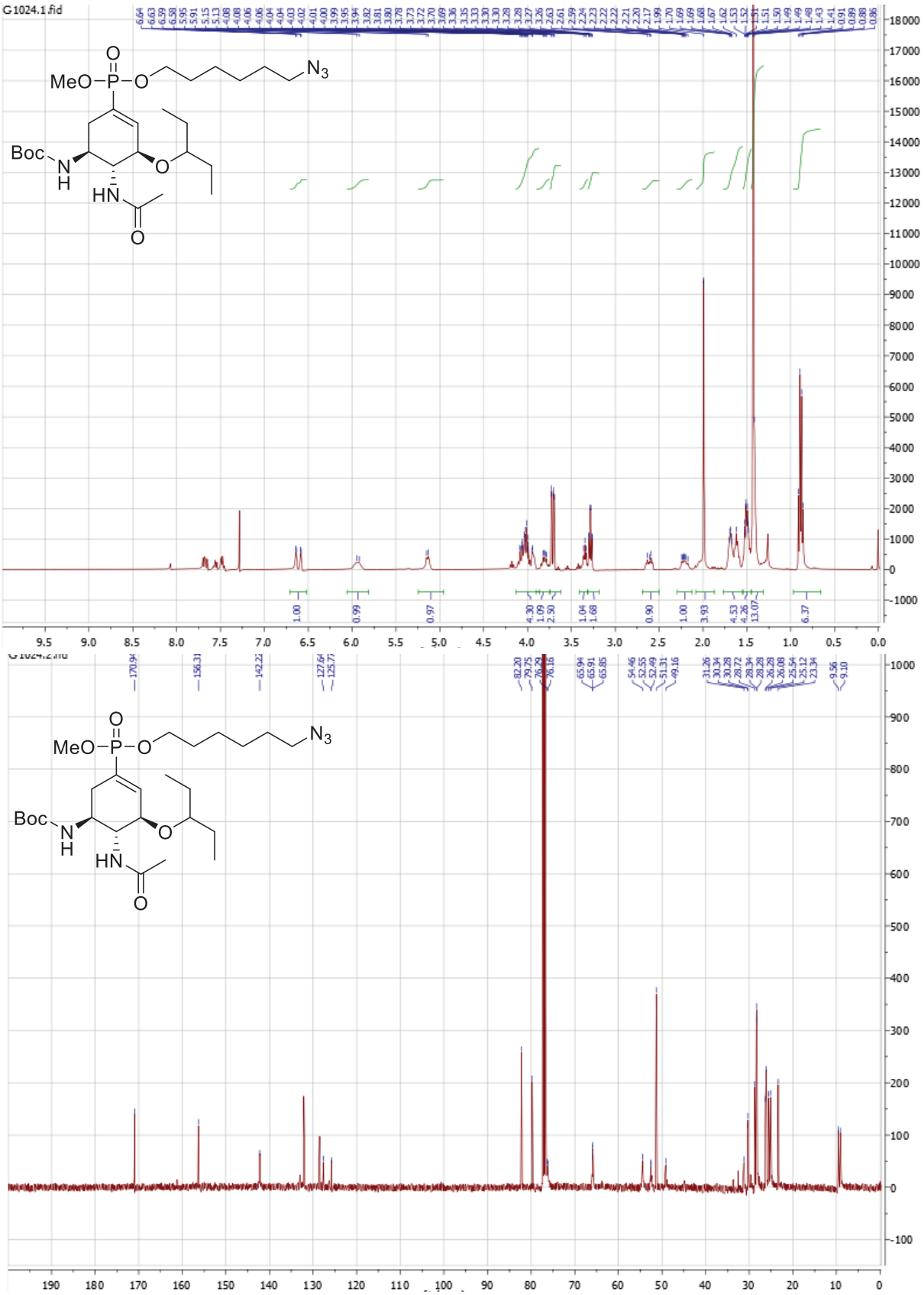

a

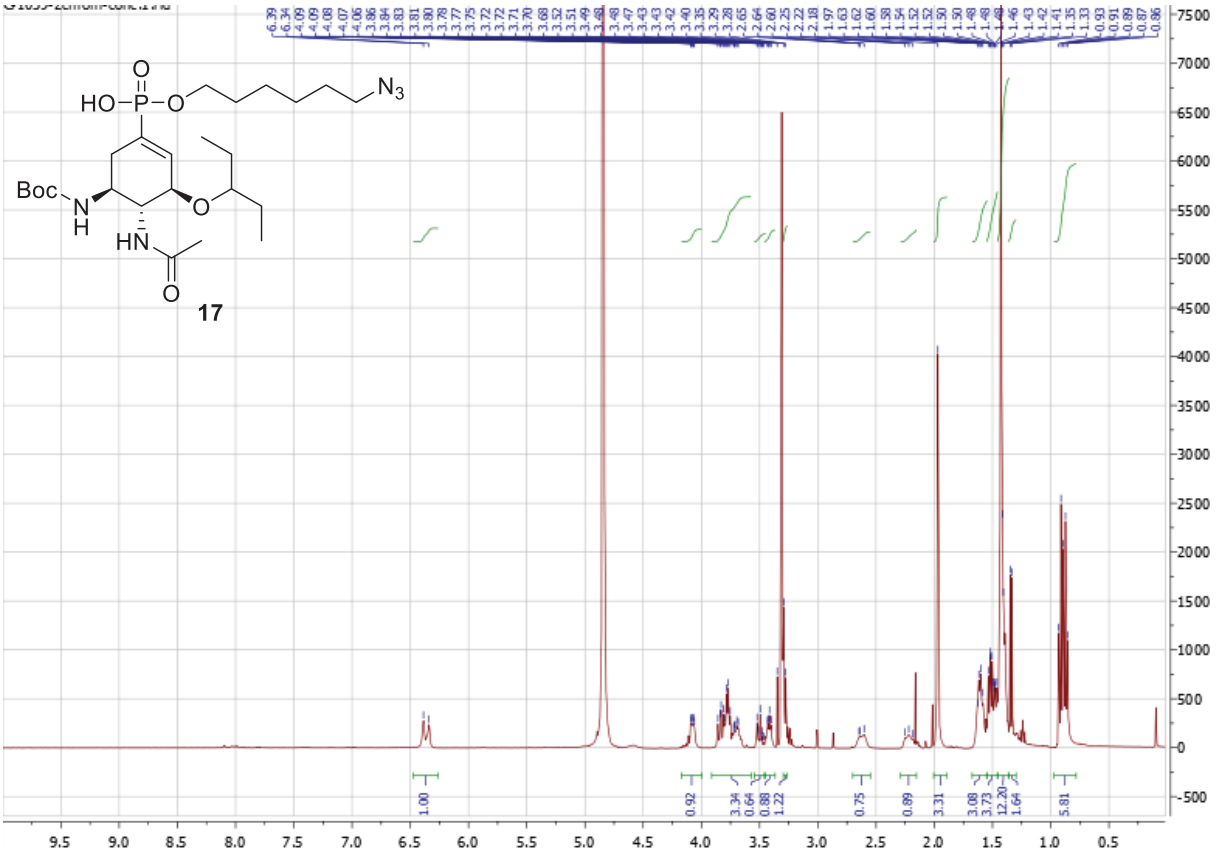
HO–P–O
N3
Boc
N
H
HN
O
17

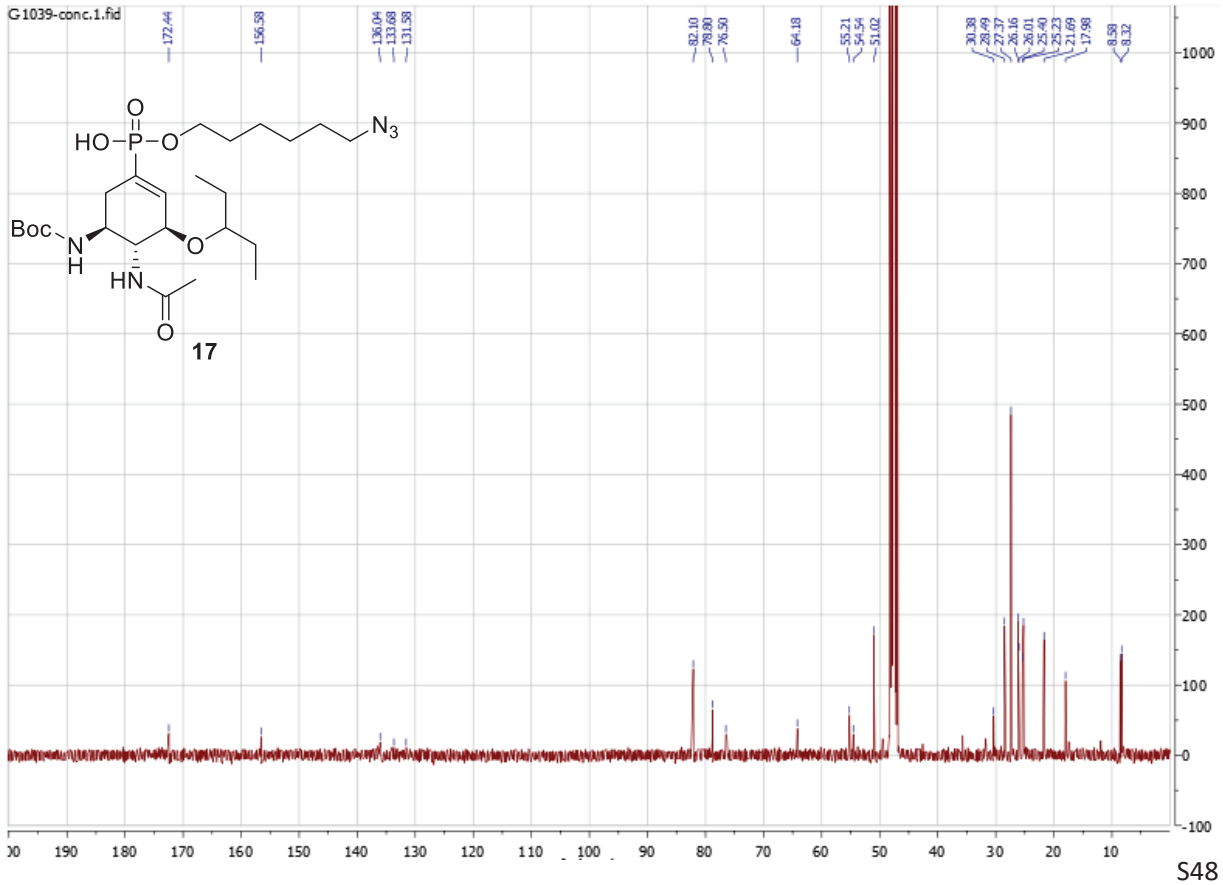
G1039-conc.1.fid
HO–P–O
N3
Boc
N
H
HN
O
17

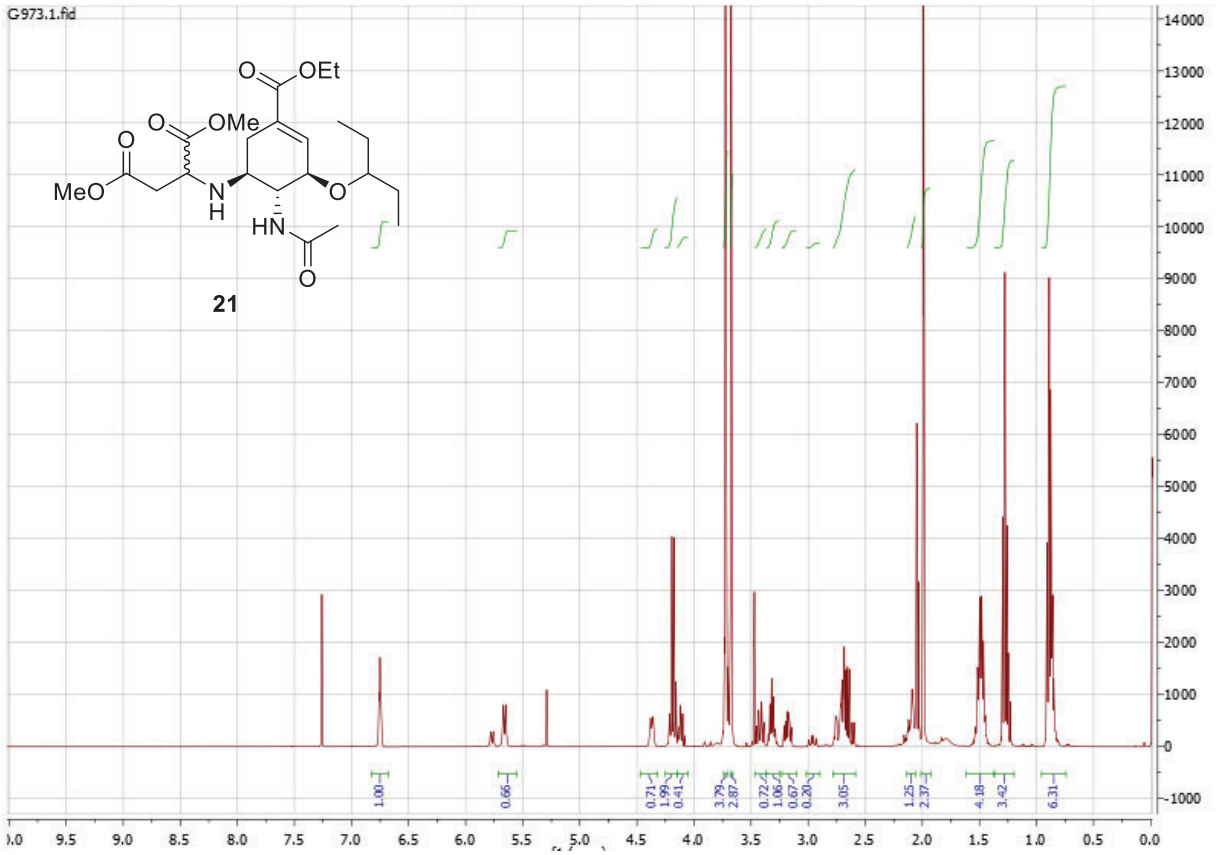
G973.1.fid
O
OEt
O
OMe
MeO
O
N
H
HN
O
O
21

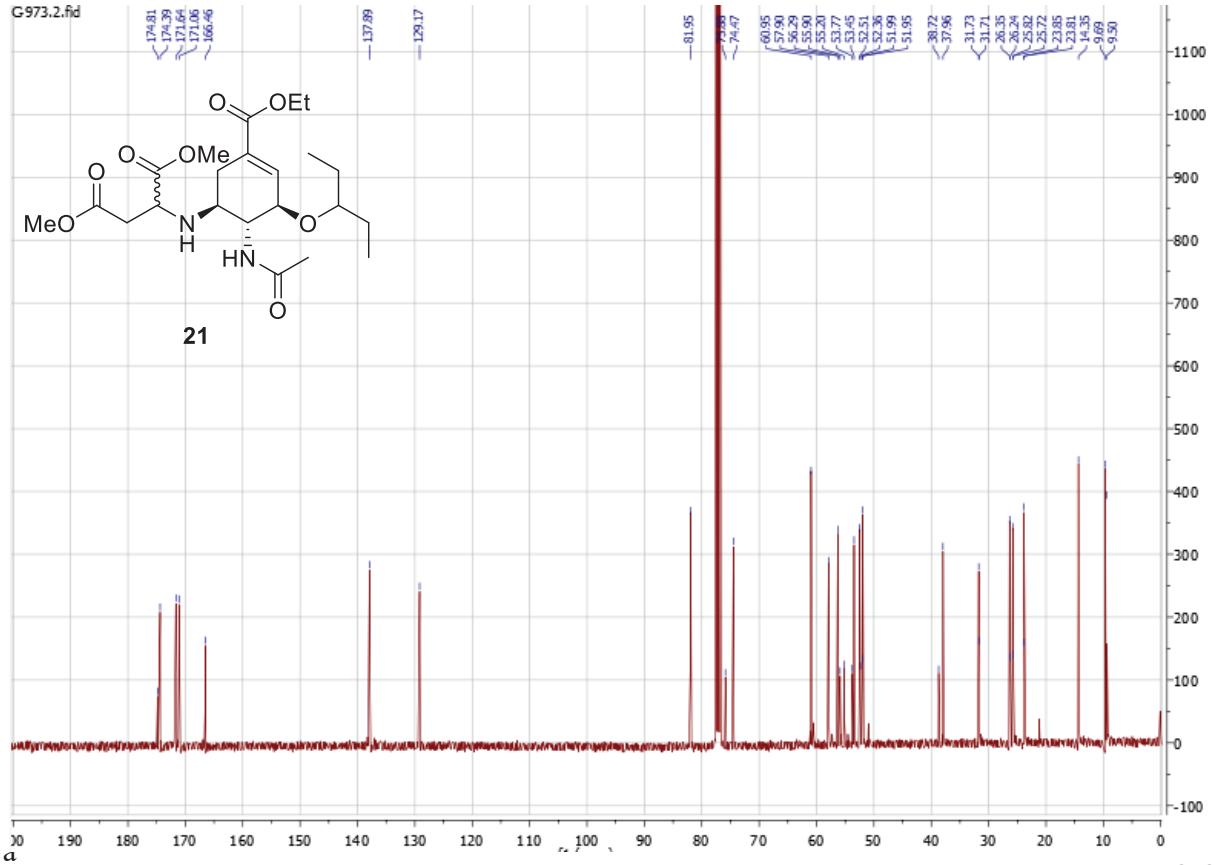
G973.2.fid
O
OEt
O
OMe
MeO
O
N
H
HN
O
O
21

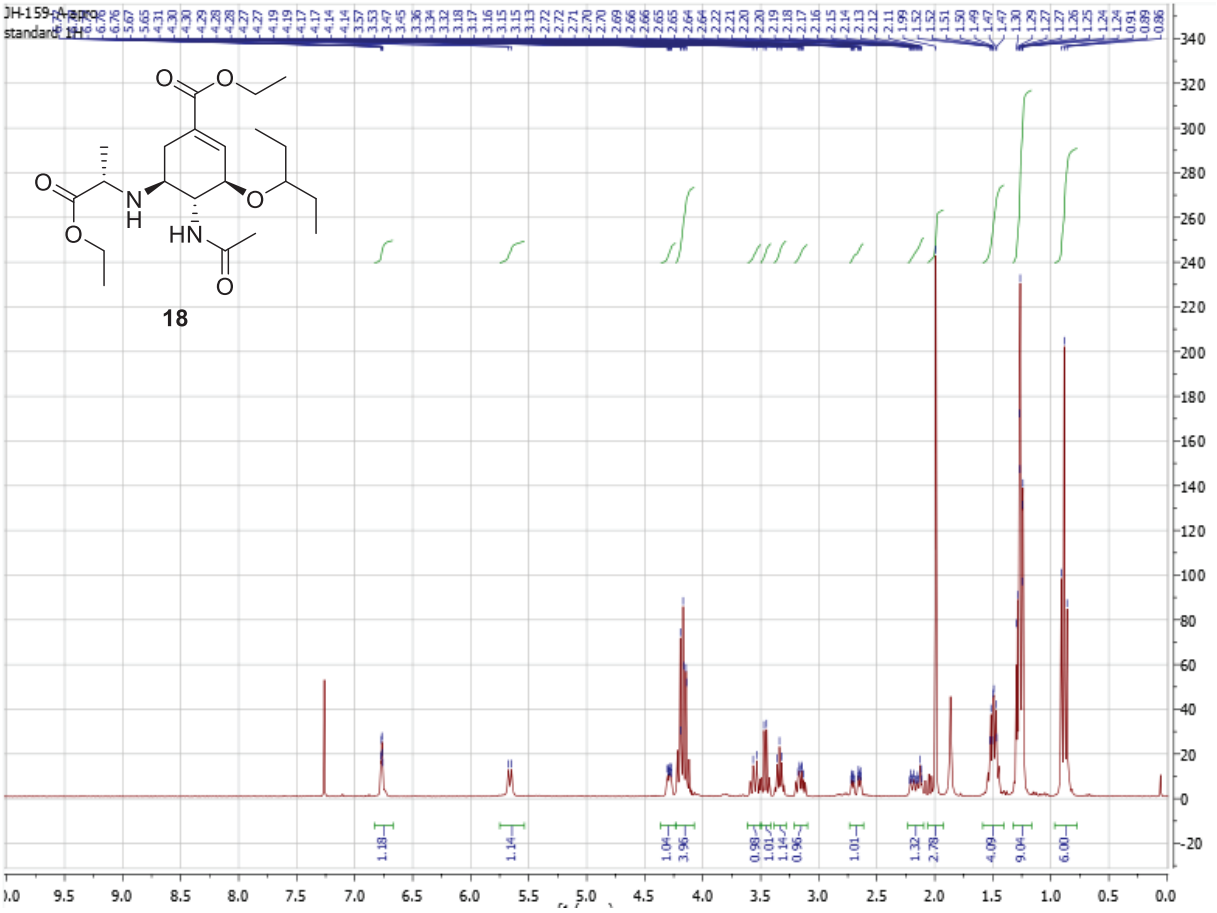
18

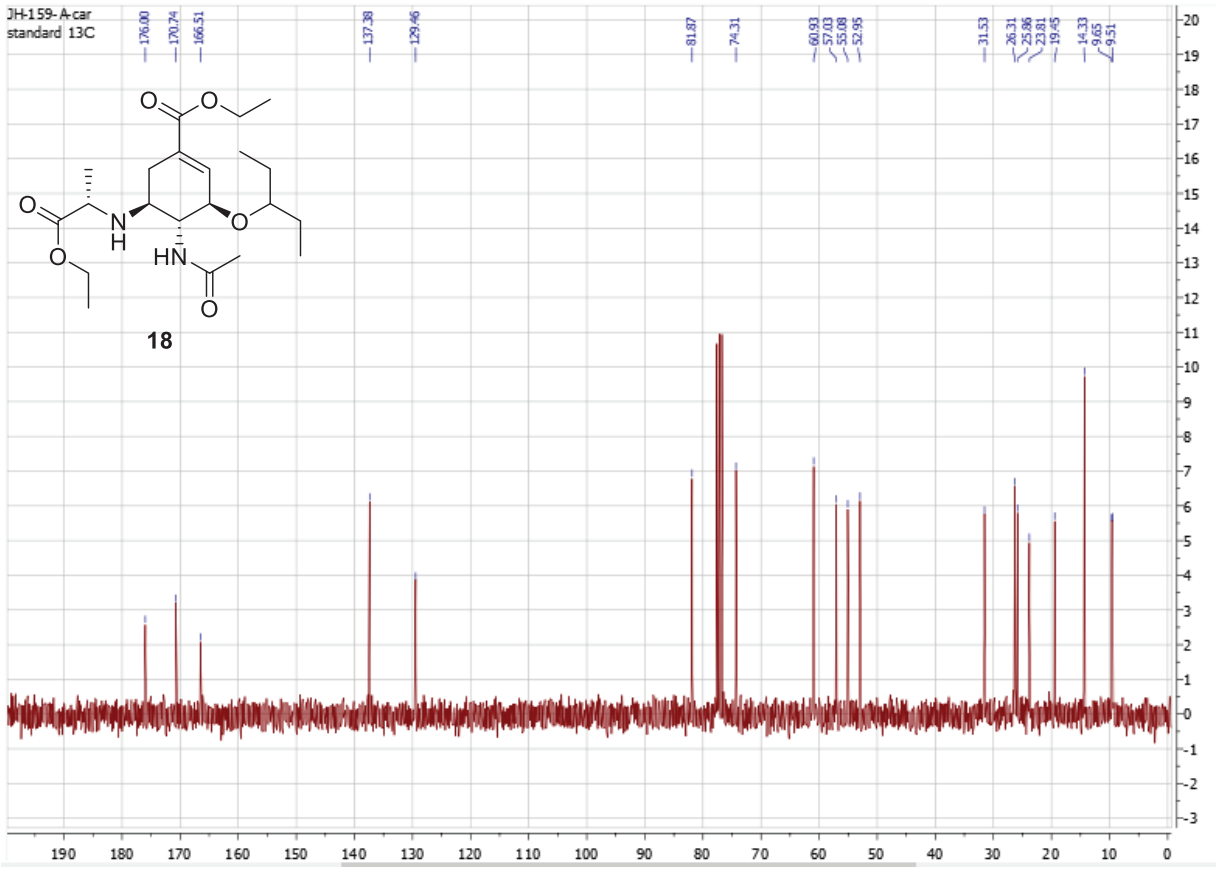
18

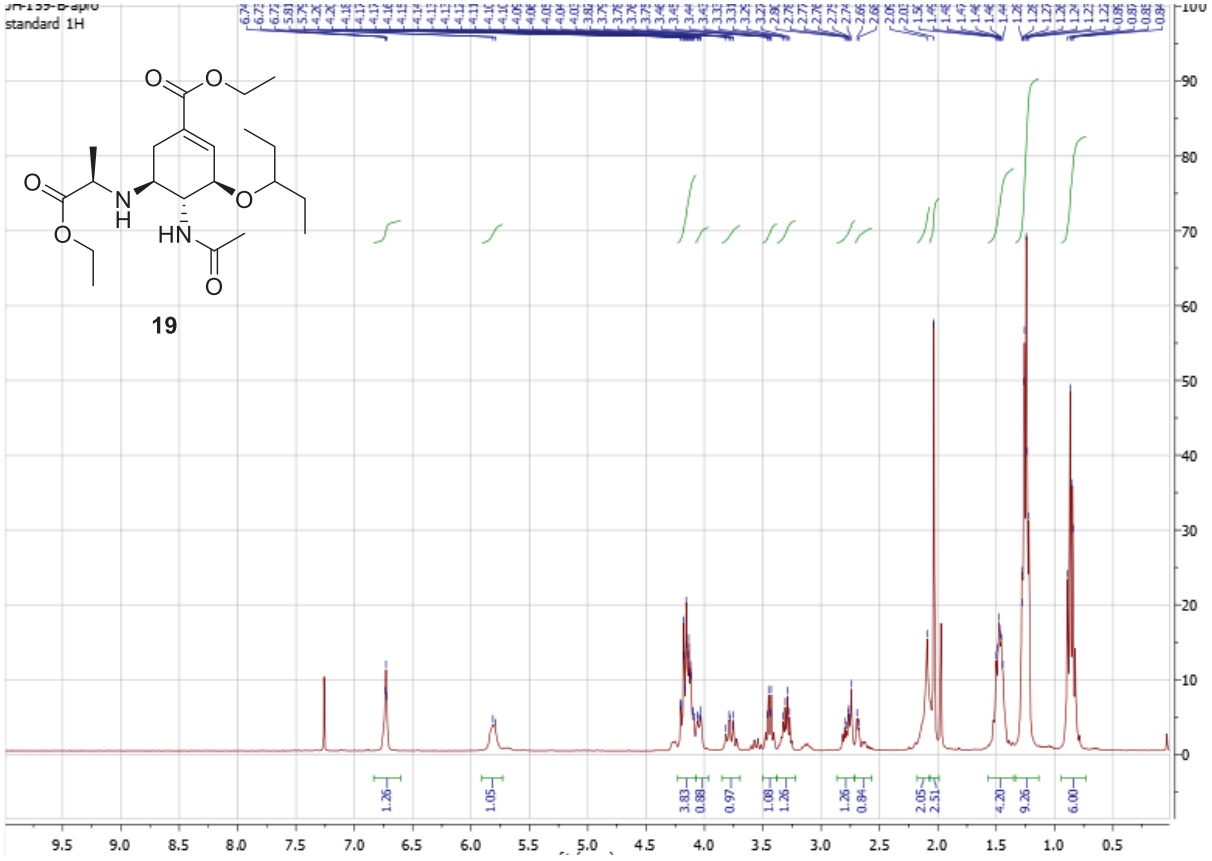
standard 1H
19

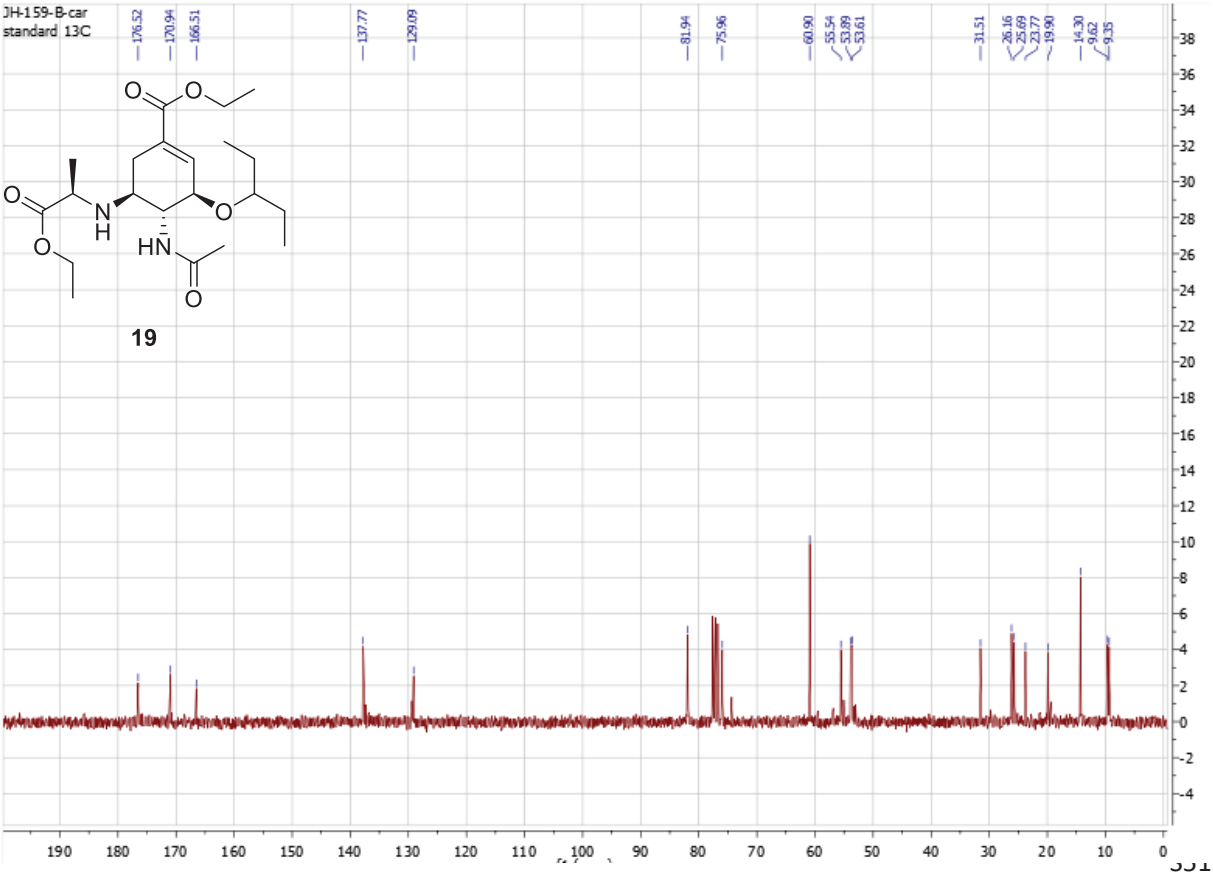
standard 13C
19

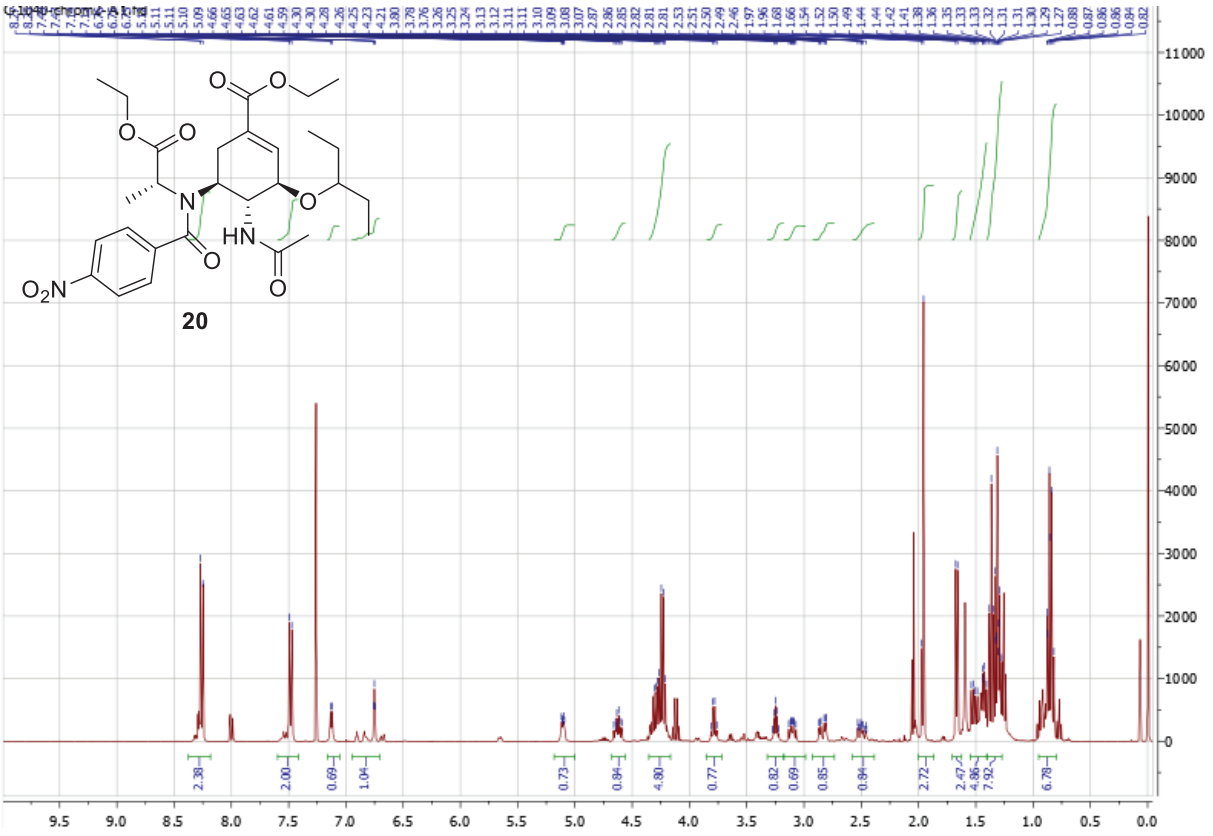
20

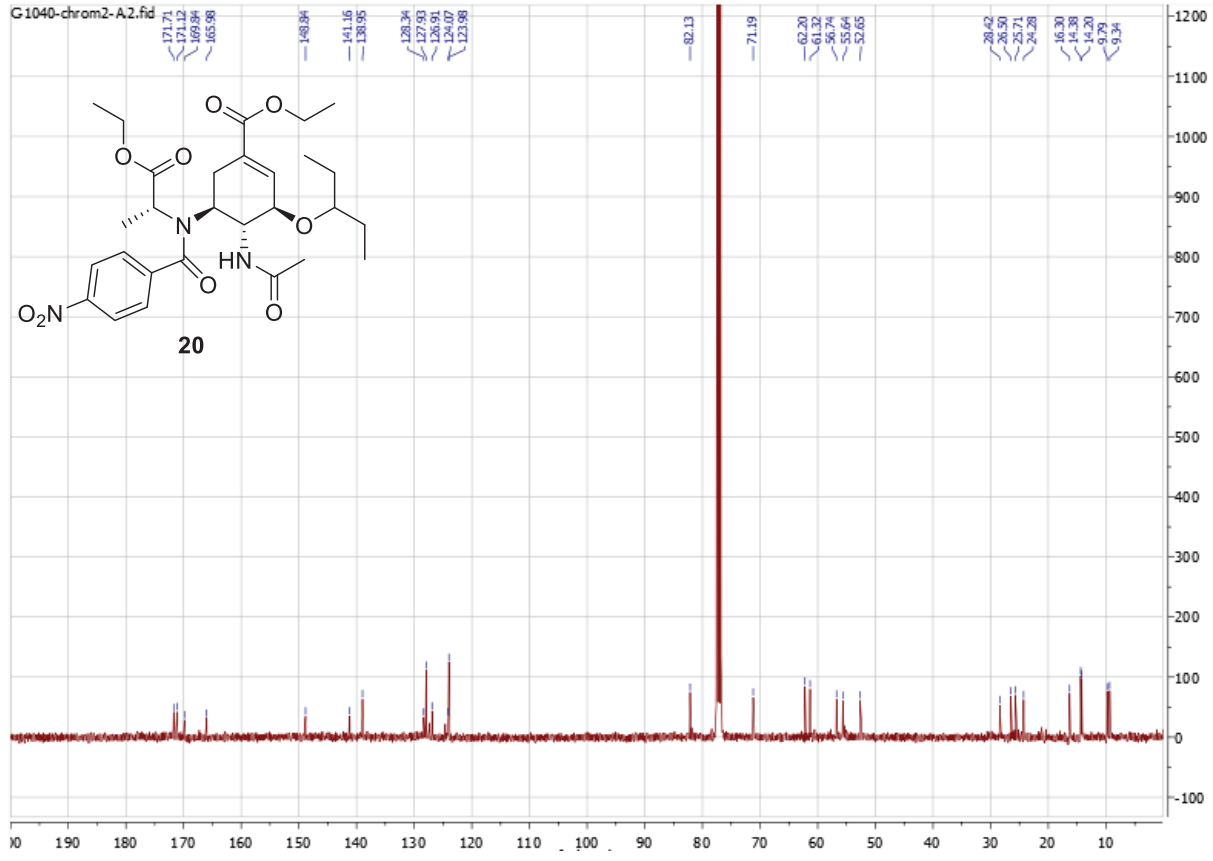
G-1040-chrom2-A2.fid
20

References

[1] Carbain, B., Collins, P. J., Callum, L., Martin, S. R., Hay, A. J., McCauley, J., and Streicher, H. (2009) Efficient Synthesis of Highly Active Phospha-Isosteres of the Influenza Neuraminidase Inhibitor Oseltamivir, *Chemmedchem 4*, 335-337.

[2] Cheng, T. J., Weinheimer, S., Tarbet, E. B., Jan, J. T., Cheng, Y. S., Shie, J. J., Chen, C. L., Chen, C. A., Hsieh, W. C., Huang, P. W., Lin, W. H., Wang, S. Y., Fang, J. M., Hu, O. Y., and Wong, C. H. (2012) Development of oseltamivir phosphonate congeners as anti-influenza agents, *J Med Chem 55*, 8657-8670.

[3] Mooney, C. A., Johnson, S. A., t Hart, P., Quarles van Ufford, L., de Haan, C. A., Moret, E. E., and Martin, N. I. (2014) Oseltamivir analogues bearing N-substituted guanidines as potent neuraminidase inhibitors, *J Med Chem 57*, 3154-3160.